Stony Brook University

Novel cyclopropenes for studying biological systems

A Thesis Presented

by

Sining Li

to

The Graduate School

in Partial Fulfillment of the

Requirements

for the Degree of

Master of Science

in

Chemistry Program

(Concentration – optional)

Stony Brook University

August 2017

Stony Brook University

The Graduate School

Sining Li

We, the thesis committee for the above candidate for the

Master of Science degree, hereby recommend

acceptance of this thesis.

Dr.Scott Laughlin
Assistant Professor, Chemistry

Dr. Kathlyn Parker
Professor, Chemistry

Dr. Isaac Carrico
Associate Professor, Chemistry

This thesis is accepted by the Graduate School

Charles Taber
Dean of the Graduate School

Abstract

Novel cyclopropenes for studying biological systems

by

Sining Li

Master of Science

in

Chemistry Program

Stony Brook University

August 2017

Click and bioorthogonal chemistry has been employed in the analysis of many biological systems, but has yet to be extended to the analysis of neural connectivity[1]. One popular bioorthogonal chemical reporter is the functionalized cyclopropene, which reacts with tetrazines through an inverse electron-demand Diels-Alder reaction[2]. Here, I describe a strategy for leveraging the cyclopropene-tetrazine ligation for analysis of neural systems and a novel photo-activatable cyclopropene for controlling reactivity in space and time. My first project employs a dopamine analog consisting of a neurotransmitter attached to a cyclopropene tag to study the dopaminergic neural circuit. I designed and synthesized three different cyclopropene-bearing dopamine analogs. These molecules will enable visualization of dopaminergic vesicles and connected neurons, when they are released into the synaptic space. My second project involves developing a new, activatable, bio-orthogonal reagent. I have synthesized a spirocyclopropene that is non-reactive when protected with a light cleavable group, but reactive towards tetrazine reagents one the group is removed by light. Ultimately, this strategy will enable controlled bioorthogonal reactivity that will permit the development of imaging tools for visualizing neural connectivity.

Table of Content

Chapter I: Novel cyclopropene-modified dopamine for analyzing dopaminergic neural systems

Introduction

The neural circuitry of the human brain is still not clearly understood. However, understanding neural circuitry of smaller brain systems, for example, the olfactory system, can provide information that can be extrapolated to more complex system to inform our understanding of neurodegenerative diseases like Parkinson's and Alzheimer's Disease.

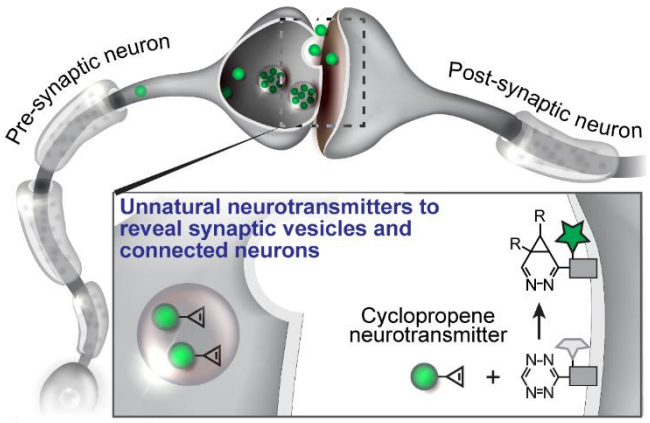

Figure 1: Strategies for visualizing neural connectivity, for example, at the neural synapse with cyclopropene-modified neurotransmitters and biorthogonal chemistries.

In the past two decades, the development of click chemistry and bioorthogonal chemistry supplies several new methods for visualizing living systems. Here, I describe a strategy for visualizing neural systems based on the cyclopropene-tetrazine ligation (Figure 1). Essentially, I have designed and synthesized reactive molecules that can react with profluorescent tetrazines in synaptic vesicles and the synaptic cleft to generate a fluorescent compound, which will enable imaging neural circuitry. These two reactive molecules are a cyclopropene-modified neurotransmitter and a pro-fluorescent lipid at the post-synaptic membrane.

Neurons never function in isolation, usually neurons are organized into circuits which process the specific kinds of information. Neural circuits varies greatly because of the different intended function. In order to figure out the neural circuits for the certain function and reveal how the

neural circuits affects disease generation, different molecular imaging methods have been developed in the past few years. Recent popular strategies for visualizing neural connectivity use protein based fluorescent probes, PET and MRI[3].

Fluorescent probes are widely used in biological systems like flies, mice and larval zebrafish. Some of the probes are also employed in studying neural systems. Protein based fluorescent probes and small molecule based fluorescent probes are the most popular tools for studying neural circuits.

Protein based fluorescent probes are usually the sensor of Ca^{2+} signals. Ca^{2+} signals can be widely detected in neural systems, ranging from complex neuronal networks to individual synapse. Therefore, imaging Ca^{2+} signals has become a popular method to analyze complex neural systems, especially olfactory receptor neurons. By measuring the kinetics of Ca^{2+} response, people can track the neuronal activity. As the powerful tools to detect Ca^{2+} signals, genetically encoded fluorescent calcium indicator proteins (FCIPs) have been employed in both vivo and vitro for Ca^{2+} imaging. FCIPs have many advantages including noninvasive loading procedure, application for long-term studies and the ability to target selected neurons[3]. Camgaroo (Camgaroo-1 and Camgaroo-2) is one of variant of yellow emitting fluorescent proteins (YFP). It has been used to image calcium signal in Drosophila mushroom bodies to study its roles in olfactory learning and memory[4]. G-CaMP, another Ca^{2+}-sensitive probe, been successfully used to image populations of glomerular activity in the Drosophila antennal lobe presynaptically or postsynaptically expressed in ORNs or in projection neurons[5]. However, the measurement requires careful interpretation and several control experiments. Better specificity, enhanced photostability is still needed.

Small molecule based fluorescent probes have been rapidly developed in the past years. Ca^{2+} sensitive dyes has been developed and employed in neural systems because of its stable and strong fluorescent signal, especially the voltage-sensitive dyes which have been reported to image the olfactory systems, such as Di8-ANEPPQ which label anterogradely at afferent axons of olfactory receptor neurons in zebrafis[6] and VoltageFluors[7] which detect synaptic and action potentials in cultured hippocampal neurons. However, the restriction of the Ca^{2+} sensitive dyes is that the background fluorescence is so strong, since some of the dyes can be uptake into all plasma membranes nonspecifically. It can obscure the boundary between the stained cells, make it difficult to tell the fluorescence changes against a high background of nonexcitable stained cells. The background signal can easily miss up the imaging.

PET imaging has been rapidly developed. It is also a popular method to investigate neural systems and it has been proved to be an advanced neuroimaging technique. PET usually employs the radioactive probe containing an isotope such as carbon-11, nitrogen-13 and fluorine-18. PET imaging can directly reflect the change of cerebral blood flow. Among the several radionuclides, $H_2{}^{15}O$ is widely used, because it can reflect the regional cerebral blood flow (rCBF), for example, [^{15}O]butanol-PET has been used to detect rCBF during monorhinic presentations. ^{18}F is another popular radionuclide, ^{18}F-FDG-PET has been used to study glucose metabolism in olfactory systems. Yet the resolution of the PET imaging is 1 mm which is relatively lower. This strategy can't be used to image a single synapse and reveal the connection between single neuron cells.

Compared with PET imaging, MRI probes has many advantages including high spatial resolution, long storage period, and low toxic labels. All of the advantages make MRI have a promising impact on imaging neural system. MRI has been employed to diagnose the injury of

brain soft tissues. However, many of the MRI probes have the problem to break the Blood-Brain Barrier. Even though some MRI probes have been successfully employed to investigate the neutral systems and get a high spatial resolution imaging, a new, general imaging technique with high resolution is still needed for studying neural circuits and cell-cell connection.

Another promising strategy to mapping neural circuit is using neurotropic viruses, like vesicular stomatitis virus[8] and rabies virus[9]. These kinds of viruses can travel through cell to cell via synapse so that they have been engineered to become tracers that can reveal the neural circuits and cell-cell connectivity in high resolution. However, these strategies are best suitable to the retrograde direction and viruses can be toxic. These strategies are not applicable in fixed systems, such as in embryonic development and the post-mortem human nervous system

Because of the all the weakness, my group try to find a new method to study neural circuits with high spatial and temporal precision. The research of our group is trying to develop a novel class of the trans-synaptic tracer which can be used to image neural circuits and visualize functional cell-cell interactions. Our strategy employs click chemistry and try to design and synthesis neurotransmitters that contain a cyclopropene tag and target it to the synapse where they will react with a biorthogonal partner to trigger fluorescence and image the synapse. Next we deliver neurotransmitter analogs to the interested part of brain or engineered cells through microinjection.

Because the neurotransmitter analogs have the similar structure of the essential neurotransmitter, we hypothesize that analogs can be packaged into synaptic vesicles by vesicular transporters and released at the synapse in neurons. Once the analogs packaged into synaptic vesicles or released at the synapse, they will react with pro-fluorescent tetrazine and trigger the fluorescence. By this

way, we can image the neural circuits. We also can visualize the location of different types of synaptic vesicles by this technique. We hope this technique will be a novel method to study neuroscience and conquer the disadvantages of the current methods mentioned above.

My work focuses on dopaminergic neural systems. Recent research has revealed that dopaminergic neural systems are related to many neural degenerative diseases[10,11,12]. Yet, the detailed mechanism is still unclear. I hope my research will be helpful. I have synthesized cyclopropene-modified dopamine analogs that can react with a tetrazine group. The molecules I have made will help reveal dopaminergic neural circuitry and provide details about normal and pathological brain function.

In past work, Dalibor Sames and co-workers has developed a notable dopamine analog, FFN511[13]. FFN511 is a fluorescent false neurotransmitters. Sames used FFN511 to observe the uptake and release of neurotransmitter from the individual presynaptic terminals. It has proved to be concentrated in dopaminergic vesicles and can be released at the synapse. During the experiments, Sames found that ethylene amine part was important for recognition by monoamine transporters. Dopamine, serotonin, and norepinephrine can be concentrated into synthetic vesicles by vesicular mono- amine transporter 2 (VMAT2) because of the ethylene amine part. Based on this point and the structure of dopamine, I have synthesized three cyclopropene analogs which are highly similar to dopamine. Current efforts focus on employing this neurotransmitter analogs in cultured dopaminergic neurons and larval zebrafish

Synthesis of cyclopropene-containing dopamine analogs

I have designed and synthesized three different dopamine analogs. All the analogs have two parts, the cyclopropene and the substituted dopamine structure (Figure 2). All the dopamine analogs are very similar to the original dopamine and they all contain the ethylene amine part, which is important for recognizing by monoamine transporter.

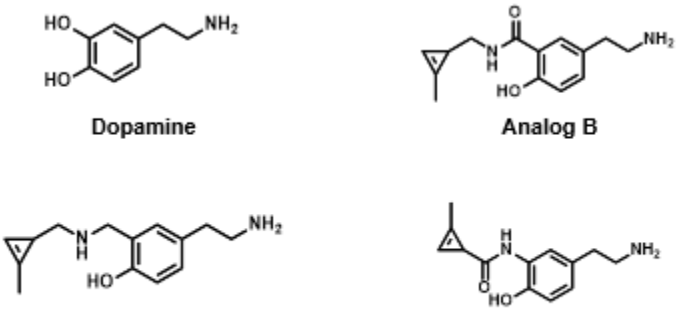

Figure 3: Structure of dopamine analog

For synthesis of the analogs, two kinds of intermediates are necessary, one is the intermediate

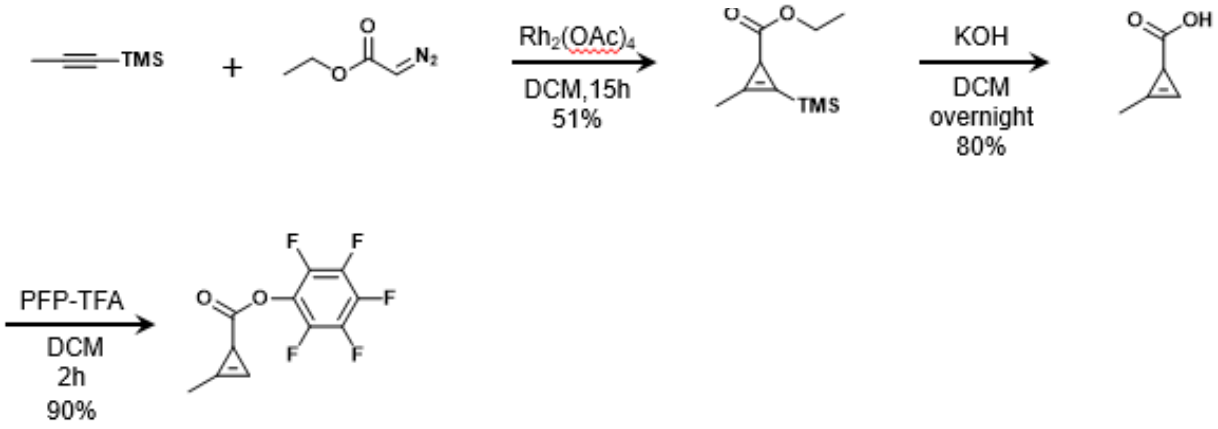

Figure 2: scheme for cyclopropene intermediate I

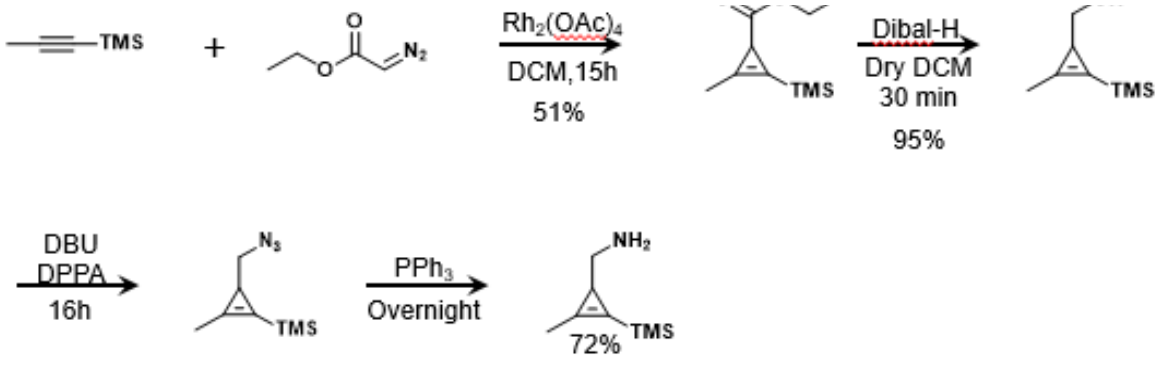

Figure 4: scheme for cyclopropene intermediate II

for cyclopropene, and the other one is the intermediate for substituted dopamine. I designed and

synthesised two different kinds of cyclopropene intermediate. The first one is an active ester (Figure 3), which is highly reactive with amines. However, several previous reports have noted that an electron withdrowing group on the C-3 carbon may lower the reaction rate of the cyclopropene-tetrazine ligation. Thus, I designed another cyclopropene intermediate, which is linked to the dopamine scaffold via an amine (Figure 4) and should be faster than the more electron withdrawing ester.

The other important part of the analogs is the substituted dopamine (Figure 5). The structure of the substituted dopamine is very similarly to the original dopamine. I have made three different kinds of substituted dopamine (Figure 6), amino substituted dopamine, aldehyde substituted dopamine, and active ester substituted dopamine. The synthesis for all the substituted dopamines begins with tyramine and use different coupling methods to assemble the dopamine analogs (Figure 6).

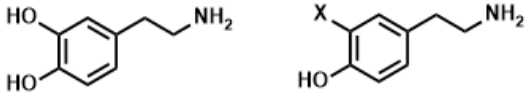

Figure 6: dopamine and substituted dopamine

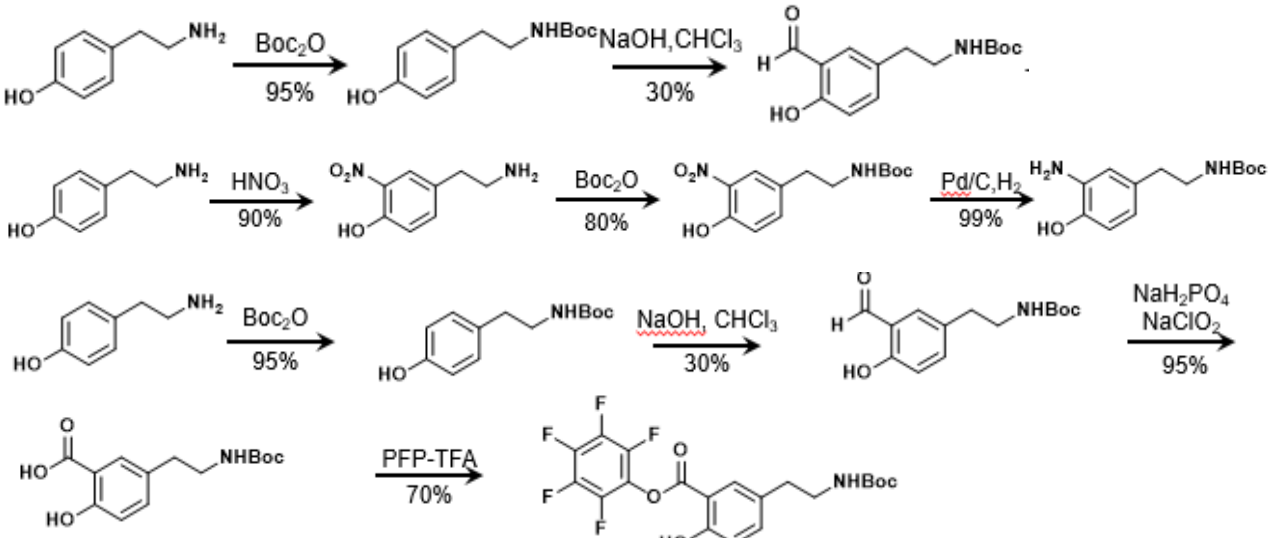

Figure 5: scheme for three different substituted dopamine

Now all the dopamine analogs are available, and we have already test the kinetic of dopamine analog C. The kinetic experiment gives us a very promising data that our molecules can rapidly react with tetrazine in vivo and image the neural circuit.

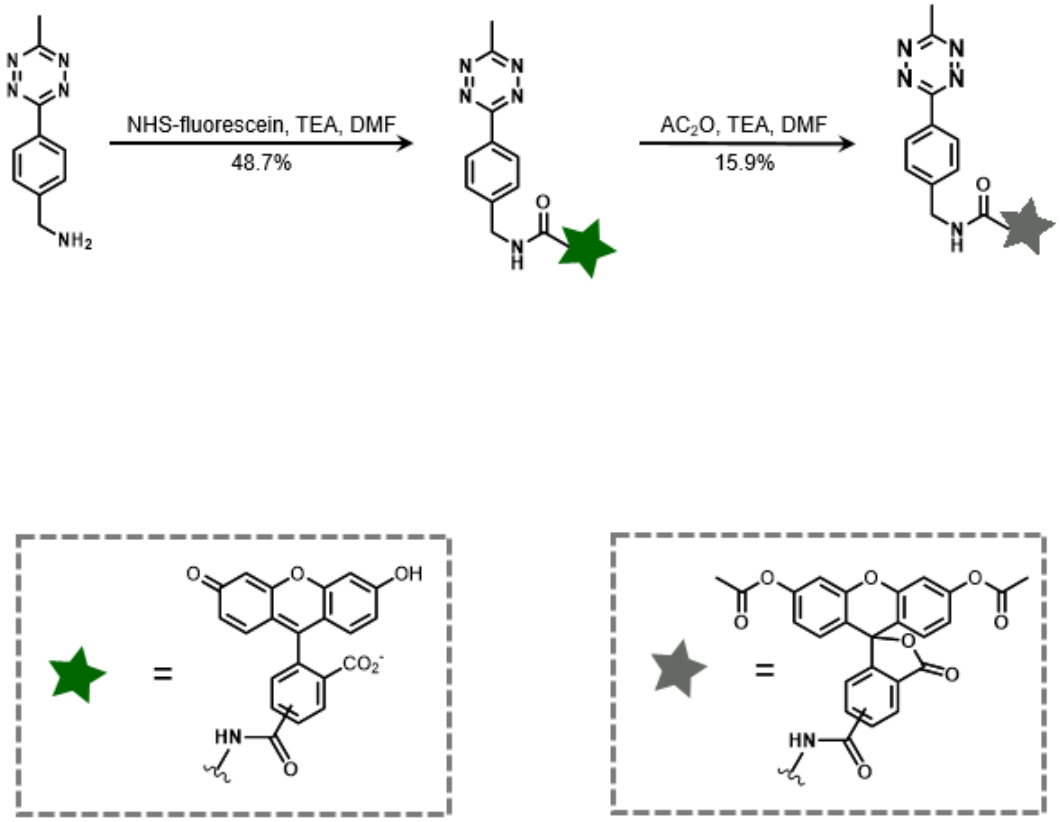

Figure 7: Synthetic scheme for tetrazines

Next, we will test dopamine analogs A-C in dopaminergic neurons with a pro-fluorescent tetrazine to make sure that the dopamine analogs can concentrate in dopaminergic vesicles (Figure 7). This tetrazine quenches fluorescence, which means when we connect the fluorophore with tetrazine, the molecule becomes non-fluorescent[14]. When the cyclopropene analogs react with tetrazine, the products of the reaction become fluorescence again. We will inject our analogs and tetrazine into dopaminergic neurons and use confocal microscopy to detect the signal of the

fluroescence and evaluate how efficent the analogs can concentrate into the vesicles to identify the best candidate for in vivo experiments.

Experiment section

General materials and methods. All chemical reagents were of analytical grade, obtained from commercial suppliers, and used without further purification unless otherwise specified. Rhodium (II) acetate (Rh_2OAc_4) was gently heated under vacuum until it became a free flowing powder (typically 15–20 s) before using it for reactions. Reactions were monitored by thin layer chromatography (TLC) on pre-coated glass TLC plates (Analtech UNIPLATE™ silica gel HLF w/ organic binder, 250 μm thickness, with UV254 indicator) or by LC/MS (Agilent LC-MSD, direct-injection mode, 1–10 μL, ESI). TLC plates were visualized by UV illumination or developed with either potassium permanganate stain ($KMnO_4$ stain: 1.5 g $KMnO_4$, 10 g K_2CO_3 and 1.25 mL of 10% NaOH dissolved in 200 mL H_2O), ceric ammonium molybdate stain (CAM stain: 12 g $(NH_4)_6Mo_7O_{24} \bullet 4H_2O$, 0.5 g $Ce(NH_4)_2(NO_3)_6$ and 15 mL of concentrated H_2SO_4 dissolved in 235 mL H_2O), or ninhydrin stain (1.5 g ninhydrin dissolved in 100 mL of n-BuOH and 3 mL of conc. AcOH). Flash chromatography was carried out using Sorbtech, 60 Å, 40–63 μm or Millipore 60 Å, 35-70 μm silica gel according to the procedure described by Still[15]. HPLC was performed using a Shimadzu HPLC (FCV-200AL) equipped with an Agilent reversed phase Zorbax Sb-Aq C18 column (4.6 × 250 mm or 21.2 × 250 mm) fitted with an Agilent stand-alone prep guard column. NMR spectra (^1H and ^{13}C) were obtained using a 400, 500, or 700 MHz Bruker spectrometer and analysed using Mestrenova 9.0. 1H and 13C chemical shifts (δ) were referenced to residual solvent peaks. High-resolution electrospray ionization (ESI) mass spectra were obtained at the Stony Brook University Institute for Chemical Biology and Drug Discovery Mass Spectrometry Facility with an Agilent LC-UV-TOF spectrometer.

General method 1 to remove TMS group. A solution of TMS protected compound (1 eq) in dry THF was added 1 M TBAF (1.2 eq) dropwise under N_2 at 0 ℃. After 12h, the reaction mixture was was diluted by water and DCM. The organic layer was combined, aqueous layer was further washed with DCM. The combined organic layers were dried over anhydrous Na_2SO_4, concentrated in vacuo, and purified by flash chromatography.

General method 2 to remove Boc group. A solution of boc protected compound was dissolved in 20% TFA/DCM (v/v) at 0 ℃. After 1h the reaction mixture was directly concentrated in vacuo. The crude was dissolved in water and purified by HPLC

Method for synthesis dopamine analog

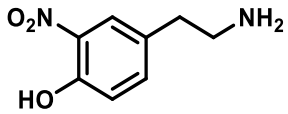

1

Compound 1 was synthesized essentially as previously described[16]. Tyramine (1.37 g, 10 mmol, 1 eq) was mixed with 30% HNO_3 (48 mmol, 4.8 eq). The resulting suspension was stirred at room temperature. The crude was diluted with water (20 mL) and applied onto a Dowex 50W-X2 (200–400 mesh) column (1.5 cm × 6 cm, H^+ form, equilibrated with water). The column was washed with water (100 mL) and then the product was eluted with 2 M HCl (20 mL/fraction). Fractions containing the target compound were combined and evaporated to dryness to give a yellow powder. (210mg, 91%).

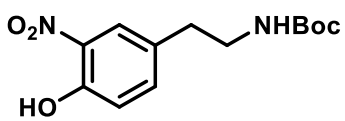

2

A solution of **1** (915 mg, 5 mmol, 1eq) in H_2O/THF (V/V=1:1), was added Boc_2O (2.16 g, 10 mmol, 2 eq) and $NaHCO_3$ (1.8 g. 20 mmol 4 eq) at room temperature. After 12h, the reaction

mixture was diluted by water and DCM. The organic layer was combined, aqueous layer was further washed with DCM. The combined organic layers were dried over anhydrous Na_2SO_4, concentrated in vacuo, and purified by flash chromatography (30 g silica, 20% ethyl acetate/hexanes (v/v)) to obtain **2** (1.4 g, 99%). ^{1}H NMR (500 MHz, Chloroform-d): δ= 10.50 (s, 1H), 7.94 (d, J = 2.2 Hz, 1H), 7.46 (dd, J = 8.6, 2.2 Hz, 1H), 7.13 (d, J = 8.6 Hz, 1H), 4.59 (s, 1H), 3.38 (q, J = 6.6 Hz, 2H), 2.82 (t, J = 7.1 Hz, 2H), 1.45 (s, 9H). ^{13}C NMR (126 MHz, Chloroform-d): δ= 156.18, 142.85, 134.69, 131.50, 119.43, 116.99, 79.47, 115.36, 41.98, 35.49, 28.45.

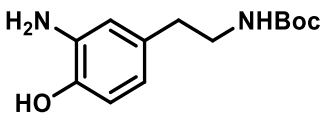

3

A solution of **2** (282 mg, 1 mmol, 1 eq) in DCM was added 20 mg Pd/C under H_2 in room temperature. After 12h, the reaction mixture pass through celite to get rid of Pd/C. Combine the organic layer, concentrated in vacuo to give 252 mg **3** as light yellow powder (232mg,100%). ^{1}H NMR (500 MHz, Chloroform-d): δ= 6.69 (d, J = 7.9 Hz, 1H), 6.58 (s, 1H), 6.47 (d, J = 8.0 Hz, 1H), 4.65 (s, 1H), 3.32 (t, J = 7.0 Hz, 2H), 2.65 (t, J = 7.2 Hz, 2H), 1.46 (s, 9H). ^{13}C NMR (126 MHz, Chloroform-d): δ= 156.57, 143.23, 135.08, 131.88, 119.81, 117.37, 115.73, 77.67, 42.36, 35.86, 28.83.

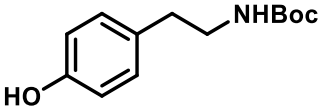

4

A solution of **tyramine** (640 mg, 5 mmol, 1eq) in H_2O/THF (V/V=1:1), was added Boc_2O (2.16 g, 10 mmol, 2 eq) and $NaHCO_3$ (1.8 g. 20 mmol 4 eq) at room temperature. After 12h, the reaction mixture was diluted by water and DCM. The organic layer was combined, aqueous layer was further washed with DCM. The combined organic layers were dried over anhydrous Na_2SO_4, concentrated in vacuo, and purified by flash chromatography (30 g silica, 20% ethyl acetate/hexanes (v/v)) to obtain **4.** (1.1 g, 99%).^{1}H NMR (500 MHz, Chloroform-d): δ= 7.07 (d, J

= 8.4 Hz, 2H), 6.84 – 6.74 (m, 2H), 4.56 (s, 1H), 3.36 (d, J = 7.2 Hz, 2H), 2.74 (t, J = 7.1 Hz, 2H), 1.46 (s, 9H).

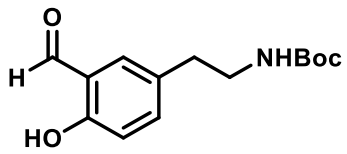

5

A solution of **4** (460 mg, 2 mmol, 1 eq) in 2.4 ml 10 N NaOH was heated to 65 ℃. Then 2 ml of CH_3Cl was adding in 3 portions over 15 min. The mixture was heated at reflux in chloroform for 4h. After cooling, the mixture was acidified to pH 1 with 12 N HCl. The organic layer was combined, aqueous layer was further washed with DCM. The combined organic layers were dried over anhydrous Na_2SO_4, concentrated in vacuo, and purified by flash chromatography (25 g silica, 20% ethyl acetate/hexanes (v/v)) to obtain **5** (330 mg, 65%). ^{1}H NMR (500 MHz, Chloroform-d): δ= 10.91 (s, 1H), 9.89 (d, J = 0.7 Hz, 1H), 7.39 (d, J = 8.0 Hz, 2H), 7.00 – 6.92 (m, 1H), 4.58 (s, 1H), 3.38 (q, J = 6.8 Hz, 2H), 2.81 (t, J = 7.1 Hz, 2H), 1.45 (s, 9H). ^{13}C NMR (126 MHz, Chloroform-d): δ= 196.49, 160.27, 155.83, 137.63, 133.44, 130.46, 120.51, 117.84, 80.10, 41.70, 36.13, 28.40.

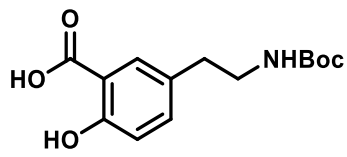

6

A solution of 5 (265 mg, 1 mmol, 1 eq) in 2 ml MeOH, was mixed with a solution of $KMnO_4$ (157 mg, 1 mmol, 1 eq) and Na2HPO4 (143 mg, 1 mmol, 1 eq) in H_2O (2 ml). The product stream was eluted into a stirred biphasic mixture prepared from 1 M HCl (3 ml) saturated with sodium chloride and sodium thiosulfate (20 mg) and EtOAc. The organic layer was combined, aqueous layer was further washed with EtOAc. The combined organic layers were dried over anhydrous Na_2SO_4, concentrated in vacuo to provide 6 (252 mg, 91%).

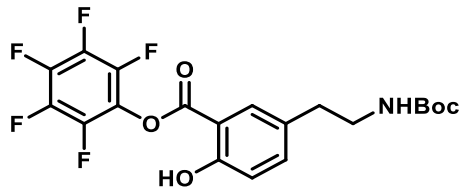

7

A solution of **6** (100 mg, 0.35 mmol, 1 eq) in 2 ml dry DCM, was added PFP-TFA (120 mg, 0.42 mmol, 1.2 eq) and TEA (43 mg, 0.42 mmol, 1.2 eq). After 1h, the reaction mixture mixture was diluted by water and DCM. The organic layer was combined, aqueous layer was further washed with DCM. The combined organic layers were dried over anhydrous Na_2SO_4, concentrated in vacuo, and purified by flash chromatography (6 g silica, 100 % DCM) to obtain **7** (125 mg, 80%). ^{1}H NMR (500 MHz, Chloroform-d): 9.76 (s, 1H), 7.89 (d, J = 2.3 Hz, 1H), 7.47 (dd, J = 8.7, 2.2 Hz, 1H), 7.05 (d, J = 8.6 Hz, 1H), 4.66 (s, 1H), 3.40 (q, J = 6.6 Hz, 2H), 2.83 (t, J = 7.2 Hz, 2H), 1.45 (s, 9H).^{13}C NMR (126 MHz, Chloroform-d): δ= 166.01, 161.16, 156.09, 143.65, 142.36, 140.22, 138.83, 138.38, 137.00, 130.54, 130.26, 118.38, 109.64, 79.77, 41.74, 35.19, 29.71, 28.33.

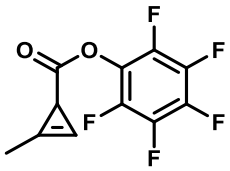

8

Cyclopropene PFP ester was synthesized as previously described[1].

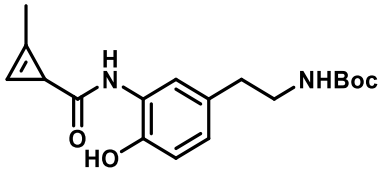

9

A solution of 2 (252 mg, 1 mmol, 1 eq) in 5 ml dry DMF was added cyclopropene PFP ester (290 mg, 1.1 mmol, 1.1 eq) under N_2 and heated to 50°C. After 24h, the reaction mixture was diluted by DCM and water. The organic layer was combined, aqueous layer was further washed with DCM. The combined organic layers were dried over anhydrous Na_2SO_4, concentrated in vacuo, and purified by flash chromatography (15 g silica, 45% ethyl acetate/hexanes (v/v)) to obtain **9** (282 mg, 85%). ^{1}H NMR (500 MHz, CD3Cl): δ= 9.39

(s, 1H), 7.79 (s, 1H), 6.93 (m, 2H), 6.79 (s, 1H), 6.53 (s, 1H), 4.61 (s, 1H), 3.31 (q, 2H), 2.68 (t, 2H), 2.29 (d, 2H), 2.25 (d, 1H), 1.46 (s, 9H). ^{13}C NMR (126 MHz, $CDCl_3$): δ= 176.66, 156.02, 147.38, 130.62, 127.09, 125.88, 122.00, 119.96, 113.49, 95.69, 79.41, 41.88, 35.20, 28.43, 22.85, 10.66.

Cyclopropene alcohol was synthesized as previously described[17].

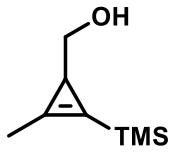

10

Cyclopropene amine was synthesized as previously described [17].

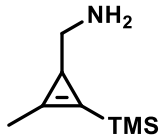

11

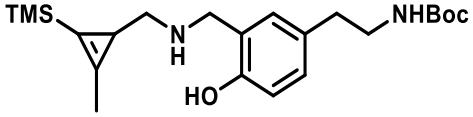

12

A solution of **5** (70 mg, 0.26 mmol, 1 eq) in MeOH was added cyclopropene amine (70 mg, 0.45 mmol, 1.7 eq) at 0 ℃. After 1h, $NaBH_4$ (20 mg, 0.5 mmol, 1.8 eq) was add to the reaction mixture. After another 1h, the reaction was diluted with water and DCM, The combined organic layers were dried over anhydrous Na_2SO_4, concentrated in vacuo, and purified by flash chromatography (6 g silica, 40% ethyl acetate/hexanes (v/v), 1% TEA) to obtain **12** (73 mg, 70%). ^{1}H NMR (500 MHz, $CDCl_3$): δ 6.98 (dd, J = 8.2, 2.2 Hz, 1H), 6.82 (s, 1H), 6.78 (d, J = 8.2 Hz, 1H), 4.55 (s, 1H), 3.97 (s, 2H), 3.39 – 3.30 (m, 2H), 2.71 (dt, J = 14.1, 5.7 Hz, 3H), 2.50 (dd, J = 11.9, 5.0 Hz, 1H), 2.23 (s, 3H), 1.50 (t, J = 4.7 Hz, 1H), 1.45 (s, 9H), 0.18 (s, 9H). ^{13}C NMR (126 MHz, Chloroform-d):

δ=157.03, 155.92, 136.18, 128.97, 128.72, 128.51, 122.79, 116.35, 115.39,112.05, 79.14, 58.6755.93, 52.54, 42.04, 35.27, 28.43, 27.98, 19.52, 13.39, -1.03.

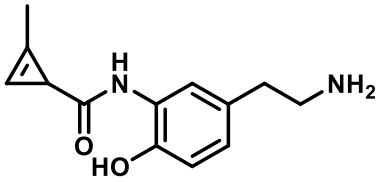

13

Compound **13** was obtained by general method 2 from compound 9. ^{1}H NMR (500 MHz, $CDCl_3$): δ= 9.39 (s, 1H), 7.79 (s, 1H), 6.93 (m, 2H), 6.79 (s, 1H), 6.53 (s, 1H), 4.61 (s, 1H), 3.31 (q, 2H), 2.68 (t, 2H), 2.29 (d, 2H), 2.25 (d, 1H). ^{13}C NMR (126 MHz, $CDCl_3$): δ= 178.04, 148.40, 128.73, 127.67, 126.45, 123.49, 117.13, 114.11, 96.39, 42.09, 33.96, 23.54, 10.66.

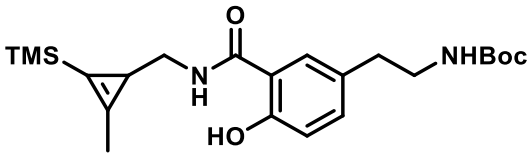

14

A solution of **7** (145 mg, 0.32 mmol, 1eq) in dry DMF was added cyclopropene amine (60 mg, 0.38 mmol, 1.2eq) and TEA (49 mg, 0.48mml, 1.5 eq) under N_2. After 18h, the reaction mixture was diluted by DCM and water. The organic layer was combined, aqueous layer was further washed with DCM. The combined organic layers were dried over anhydrous Na_2SO_4, concentrated in vacuo, and purified by flash chromatography (8 g silica,10 % ethyl acetate/hexanes (v/v)) to obtain **14** (80 mg, 60%).^{1}H NMR (500 MHz, Chloroform-d): δ= 7.27 – 7.17 (m, 2H), 6.92 (d, J = 8.4 Hz, 1H), 6.49 (d, J = 7.2 Hz, 1H), 4.65 (s, 1H), 3.47 – 3.33 (m, 3H), 3.25 (dt, J = 13.6, 5.3 Hz, 1H), 2.75 (t, J = 7.1 Hz, 2H), 2.24 (s, 3H), 1.58 (dd, J = 5.2, 4.4 Hz, 1H), 1.43 (s, 9H), 0.19 (s, 9H).^{13}C NMR (126 MHz, Chloroform-d): δ= 169.54, 160.05,

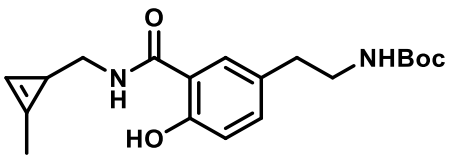

15

156.04, 135.92, 134.39, 128.67, 125.20, 118.58, 114.48, 111.54, 79.38, 46.59, 41.45, 35.38, 28.40, 19.25, 13.17. -1.03.

Compound **15** was obtained by general method 1

^{1}H NMR (500 MHz, Chloroform-d) δ 12.35 (s, 1H), 7.27 – 7.17 (m, 2H), 6.93 (d, J = 8.4 Hz, 1H), 6.73 – 6.63 (m, 1H), 6.48 (s, 1H), 4.61 (s, 1H), 3.48 (ddd, J = 13.7, 5.7, 4.1 Hz, 1H), 3.40 (q, J = 6.9 Hz, 2H), 3.32 (dt, J = 13.7, 5.1 Hz, 1H), 2.77 (t, J = 7.2 Hz, 2H), 2.18 (d, J = 1.1 Hz, 3H), 1.69 (td, J = 4.4, 1.6 Hz, 1H), 1.45 (s, 9H). ^{13}C NMR (126 MHz, Chloroform-d): δ= 169.79, 160.07, 156.09, 134.45, 128.57, 125.17, 121.51,118.57, 114.42, 102.80, 79.45, 45.67, 41.34, 35.35, 28.41, 17.86, 11.61.

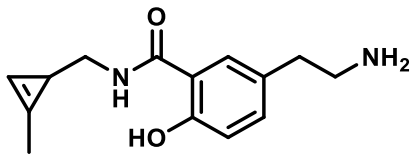

16

Compound **16** was obtained by general method 2.

^{1}H NMR (500 MHz, Chloroform-d) δ 12.35 (s, 1H), 7.27 – 7.17 (m, 2H), 6.93 (d, J = 8.4 Hz, 1H), 6.73 – 6.63 (m, 1H), 6.48 (s, 1H), 4.61 (s, 1H), 3.48 (ddd, J = 13.7, 5.7, 4.1 Hz, 1H), 3.40 (q, J = 6.9 Hz, 2H), 3.32 (dt, J = 13.7, 5.1 Hz, 1H), 2.77 (t, J = 7.2 Hz, 2H), 2.18 (d, J = 1.1 Hz, 3H), 1.69 (td, J = 4.4, 1.6 Hz, 1H).^{13}C NMR (126 MHz, Chloroform-d): δ= 169.79, 160.07, 156.09, 134.45, 128.57, 125.17, 121.51,118.57, 114.42, 102.80, 79.45, 45.67, 41.34, 35.35, 17.86, 11.61.

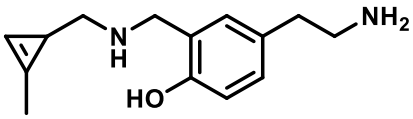

17

Compound **17** was obtained by general method 1 and 2 from compound **14**.

^{1}H NMR (500 MHz, Methanol-d4): δ= 7.23 – 7.15 (m, 2H), 6.89 (d, J = 8.2 Hz, 1H), 6.80 (d, J = 1.6 Hz, 1H), 4.18 (s, 2H), 3.11 (t, J = 7.9 Hz, 2H), 3.05 (dd, J = 12.7, 4.8 Hz, 1H), 2.87 (dd, J = 9.1, 6.6 Hz, 2H), 2.75 (dd, J = 12.8, 6.2 Hz, 1H), 2.16 (d, J = 1.0 Hz, 3H), 1.65 (ddd, J = 6.2, 4.7, 1.5 Hz, 1H). ^{13}C NMR (126 MHz, Methanol-d4): δ= 156.64, 132.82, 132.47, 129.18, 121.41, 119.51, 116.75, 102.93, 55.94, 47.52, 41.99, 33.58, 15.10, 11.17.

NMRs for the molecules synthesized in chapter I

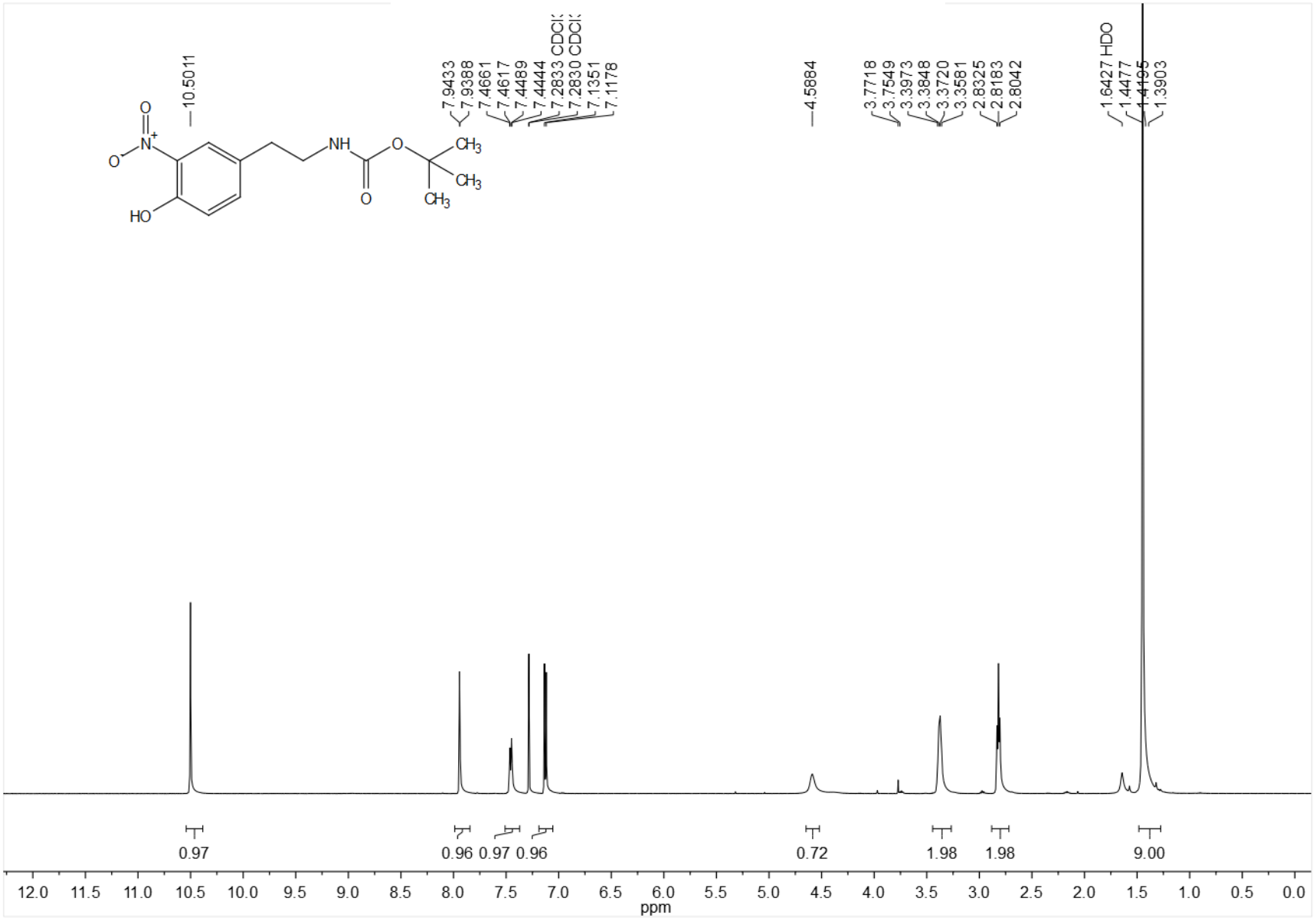

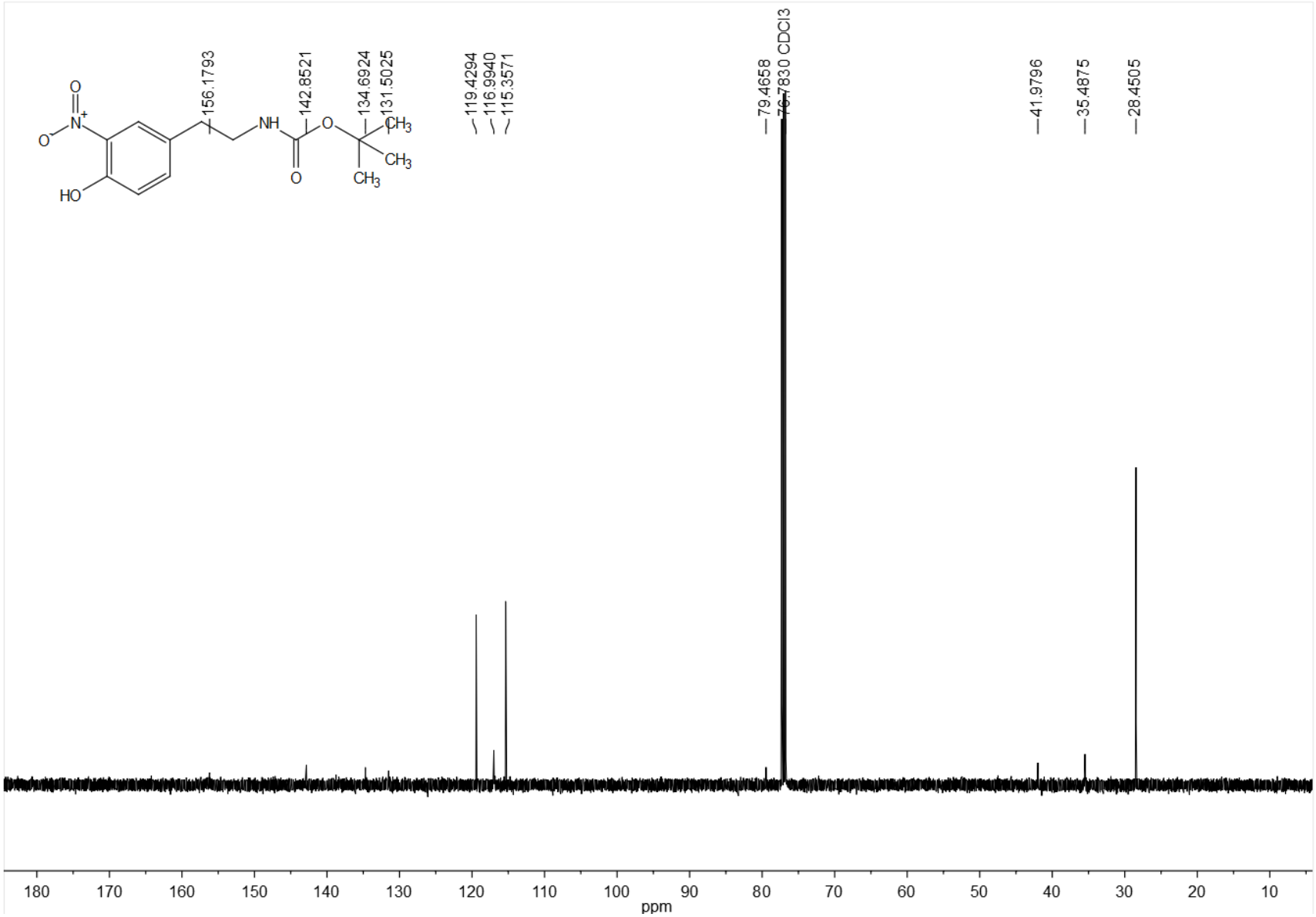
156.1793
142.8521
134.6924
131.5025
119.4294
116.9940
115.3571
79.4658
76.7830 CDCl3
41.9796
35.4875
28.4505
NH
O
HO
CH3
CH3
CH3
180
170
160
150
140
130
120
110
100
90
80
70
60
50
40
30
20
10
ppm

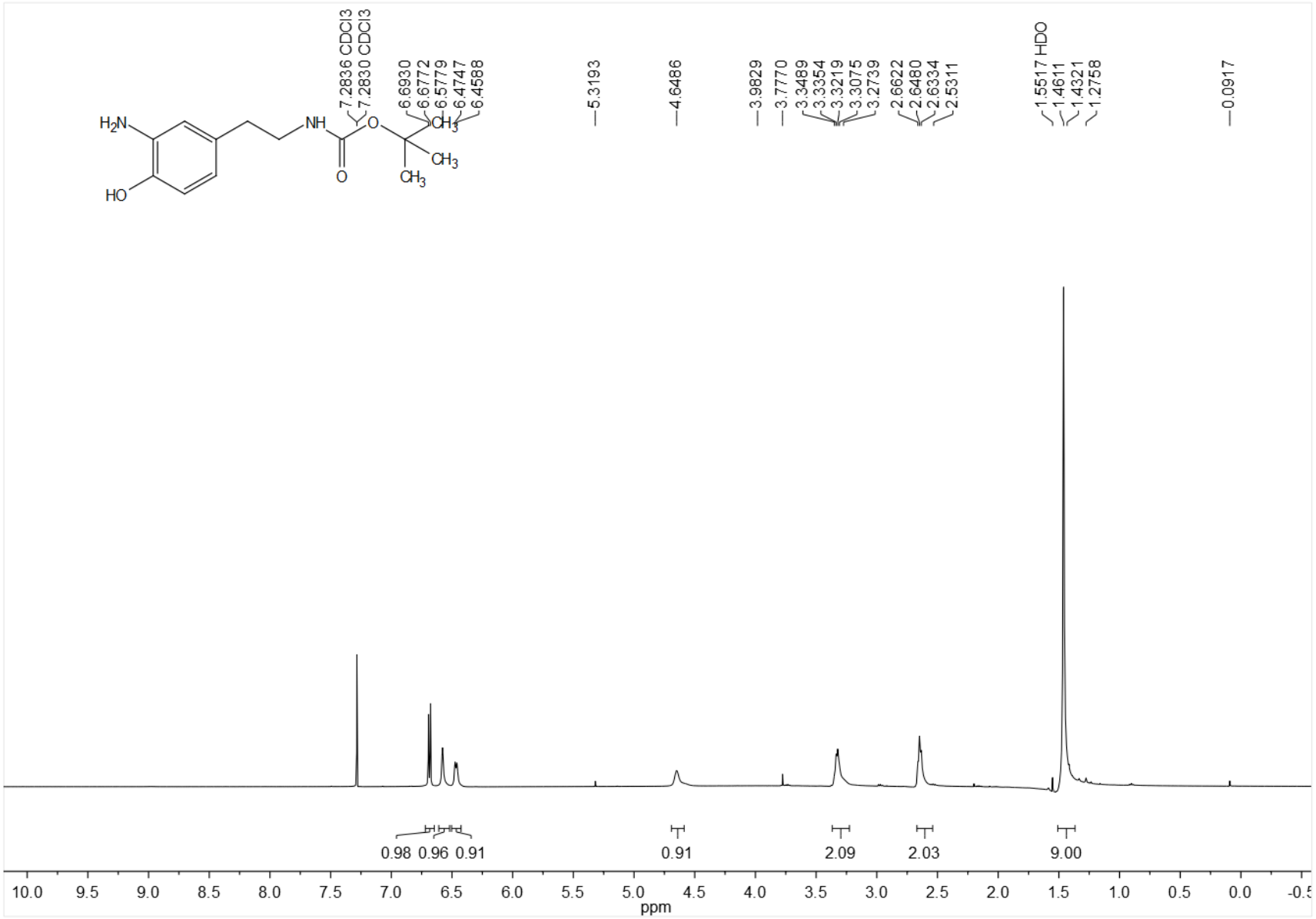
7.2836 CDCl3
7.2830 CDCl3
6.6930
6.6772
6.5779
6.4747
6.4588
5.3193
4.6486
3.9829
3.7770
3.3489
3.3354
3.3219
3.3075
3.2739
2.6622
2.6480
2.6334
2.5311
1.5517 HDO
1.4611
1.4321
1.2758
0.0917
H2N
NH
O
CH3
CH3
CH3
HO
0.98 0.96 0.91
0.91
2.09
2.03
9.00
10.0 9.5 9.0 8.5 8.0 7.5 7.0 6.5 6.0 5.5 5.0 4.5 4.0 3.5 3.0 2.5 2.0 1.5 1.0 0.5 0.0
ppm

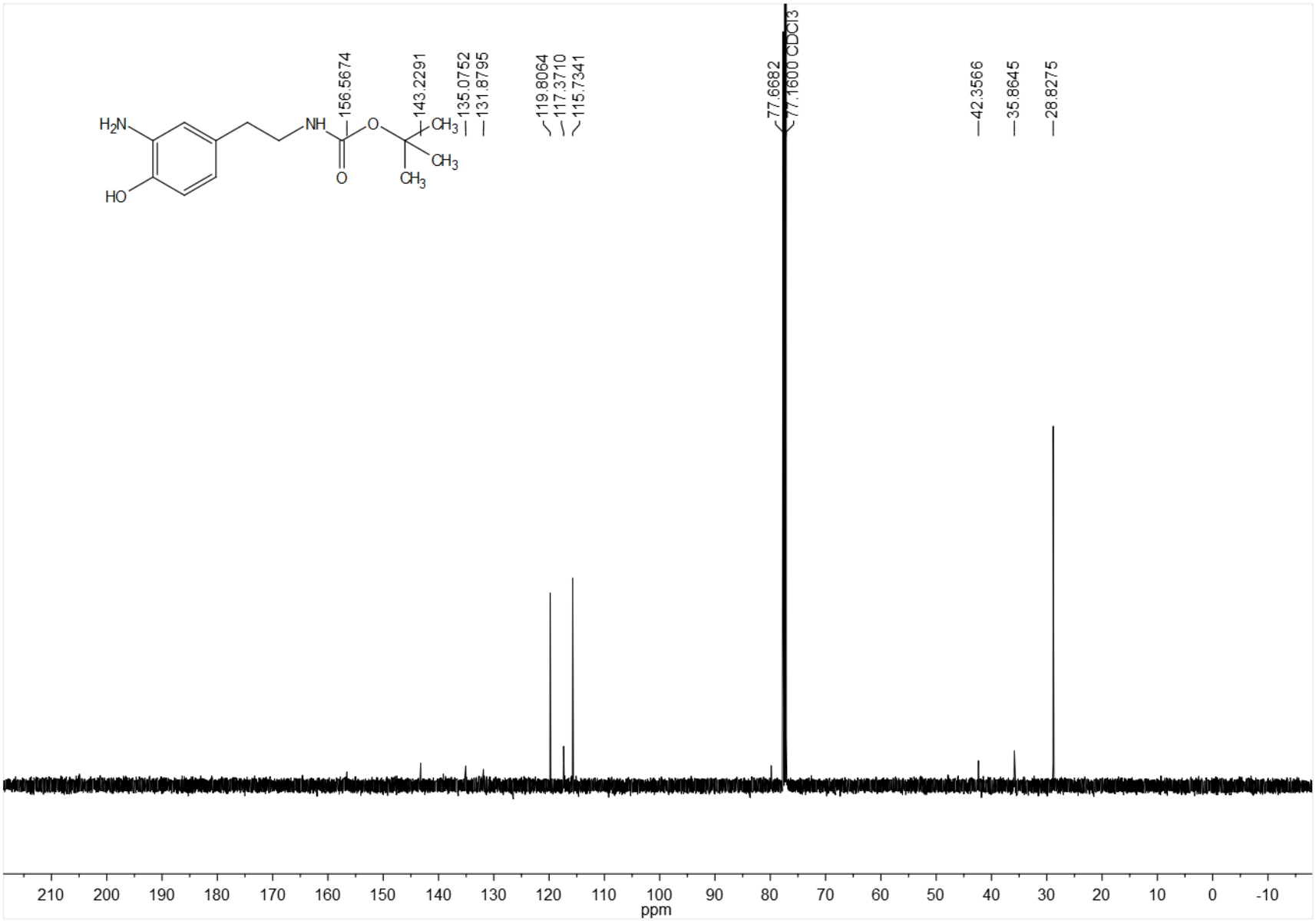
H2N
HO
NH
O
O
CH3
CH3
CH3
156.5674
143.2291
135.0752
131.8795
119.8064
117.3710
115.7341
77.6682
77.1600 CDCl3
42.3566
35.8645
28.8275
210 200 190 180 170 160 150 140 130 120 110 100 90 80 70 60 50 40 30 20 10 0 -10
ppm

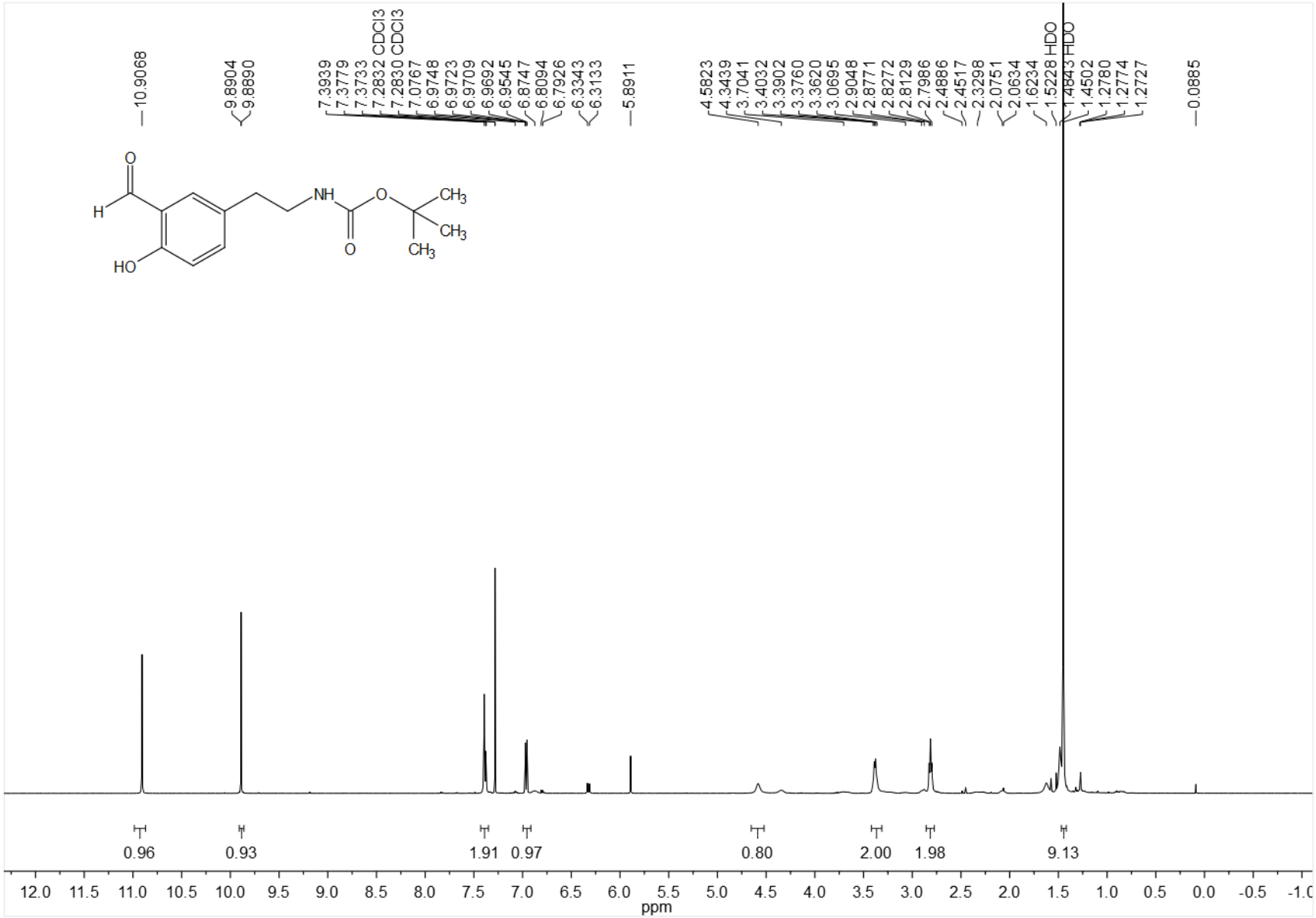
10.9068
9.8904
9.8890
7.3939
7.3779
7.3733
7.2832 CDCl3
7.2830 CDCl3
7.0767
6.9748
6.9723
6.9709
6.9692
6.9545
6.8747
6.8094
6.7926
6.3343
6.3133
5.8911
4.5823
4.3439
3.7041
3.4032
3.3902
3.3760
3.3620
3.0695
2.9048
2.8771
2.8272
2.8129
2.7986
2.4886
2.4517
2.3298
2.0751
2.0634
1.6234
1.5228 HDO
1.4843 HDO
1.4502
1.2780
1.2774
1.2727
0.0885
O
H
HO
NH
O
O
CH3
CH3
CH3
0.96
0.93
1.91
0.97
0.80
2.00
1.98
9.13
12.0 11.5 11.0 10.5 10.0 9.5 9.0 8.5 8.0 7.5 7.0 6.5 6.0 5.5 5.0 4.5 4.0 3.5 3.0 2.5 2.0 1.5 1.0 0.5 0.0 -0.5 -1.0
ppm

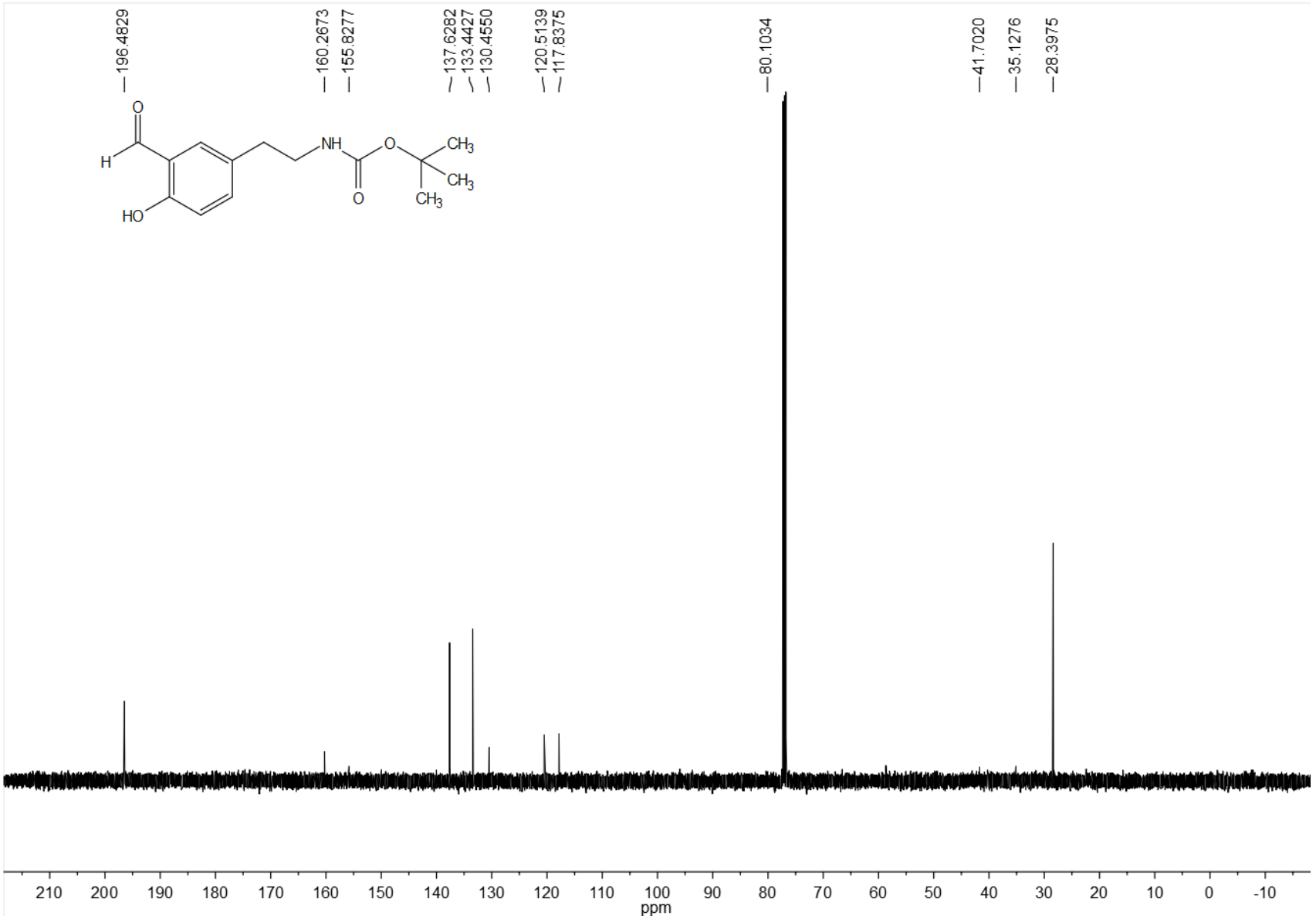
196.4829
160.2673
155.8277
137.6282
133.4427
130.4550
120.5139
117.8375
80.1034
41.7020
35.1276
28.3975
O
H
HO
NH
O
O
CH3
CH3
CH3
210
200
190
180
170
160
150
140
130
120
110
100
90
80
70
60
50
40
30
20
10
0
-10
ppm

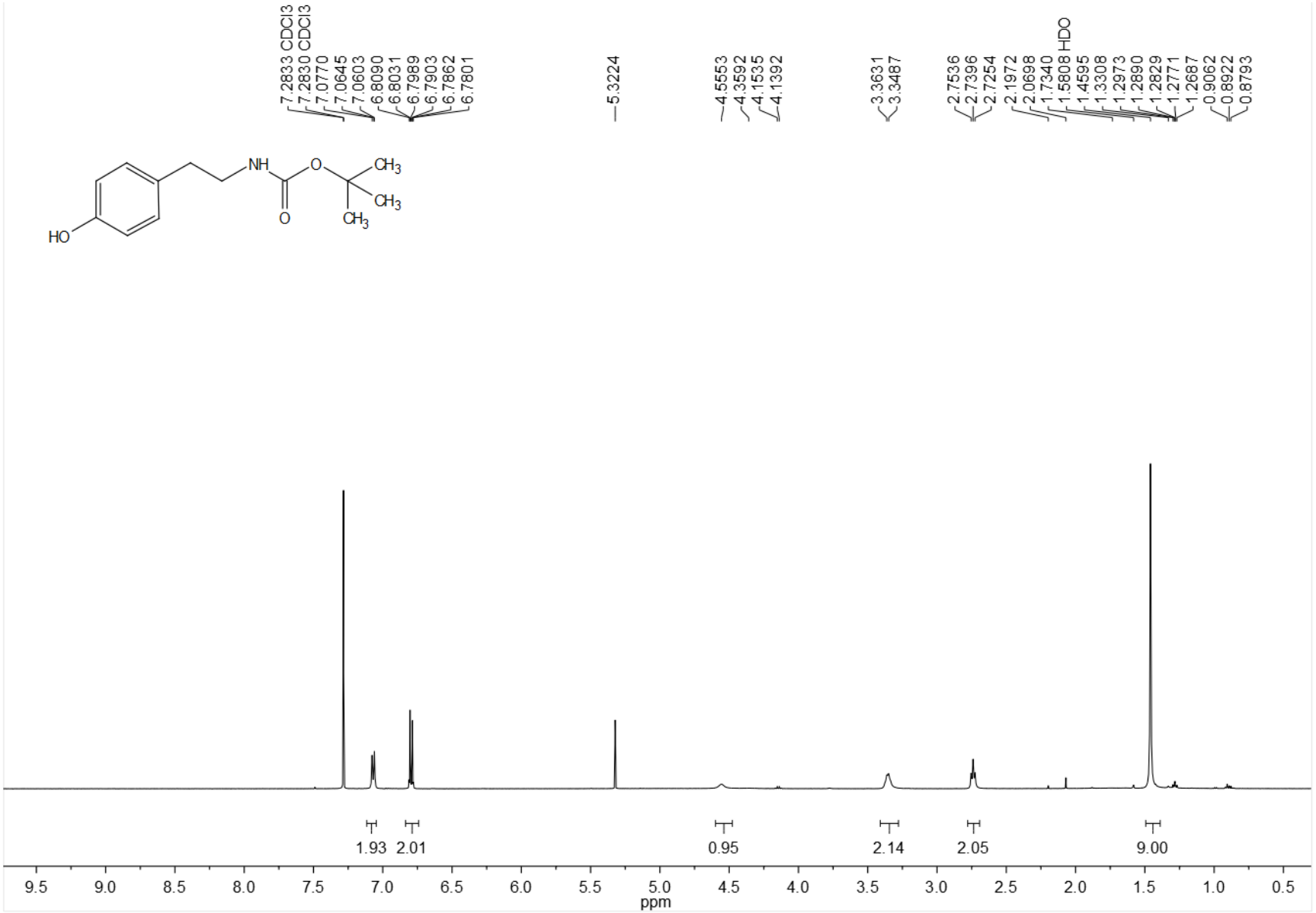
7.2833 CDCl3
7.2830 CDCl3
7.0770
7.0645
7.0603
6.8090
6.8031
6.7989
6.7903
6.7862
6.7801
5.3224
4.5553
4.3592
4.1535
4.1392
3.3631
3.3487
2.7536
2.7396
2.7254
2.1972
2.0698
1.7340
1.5808 HDO
1.4595
1.3308
1.2973
1.2890
1.2829
1.2771
1.2687
0.9062
0.8922
0.8793
NH
O
O
CH3
CH3
CH3
HO
1.93
2.01
0.95
2.14
2.05
9.00
9.5
9.0
8.5
8.0
7.5
7.0
6.5
6.0
5.5
5.0
4.5
4.0
3.5
3.0
2.5
2.0
1.5
1.0
0.5
ppm

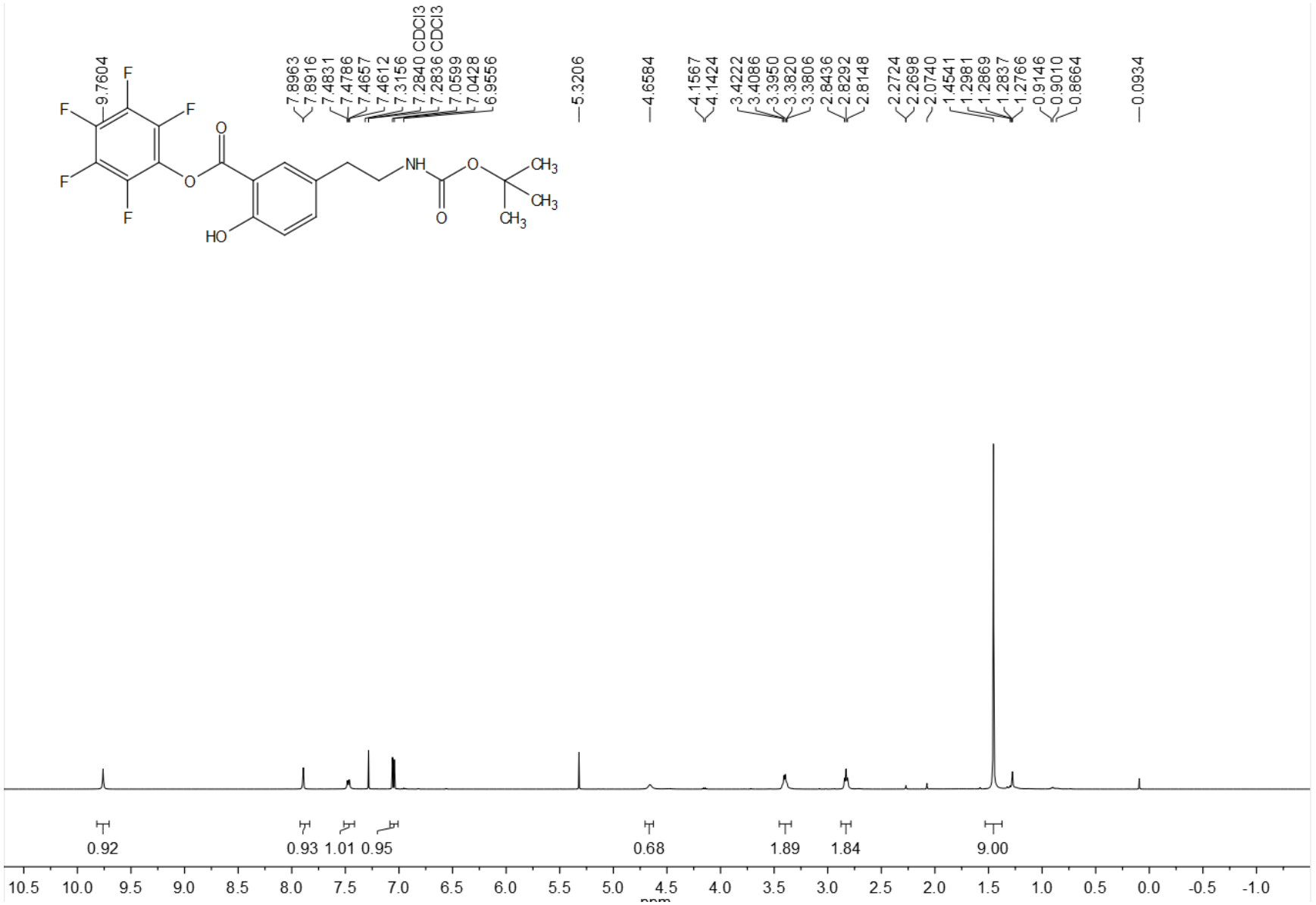
9.7604
7.8963
7.8916
7.4831
7.4786
7.4657
7.4612
7.3156
7.2840 CDCl3
7.2836 CDCl3
7.0599
7.0428
6.9556
5.3206
4.6584
4.1567
4.1424
3.4222
3.4086
3.3950
3.3820
3.3806
2.8436
2.8292
2.8148
2.2724
2.2698
2.0740
1.4541
1.2981
1.2869
1.2837
1.2766
0.9146
0.9010
0.8664
0.0934
F
F
F
F
O
O
HO
NH
O
O
CH3
CH3
CH3
0.92
0.93
1.01
0.95
0.68
1.89
1.84
9.00
10.5
10.0
9.5
9.0
8.5
8.0
7.5
7.0
6.5
6.0
5.5
5.0
4.5
4.0
3.5
3.0
2.5
2.0
1.5
1.0
0.5
0.0
-0.5
-1.0
ppm

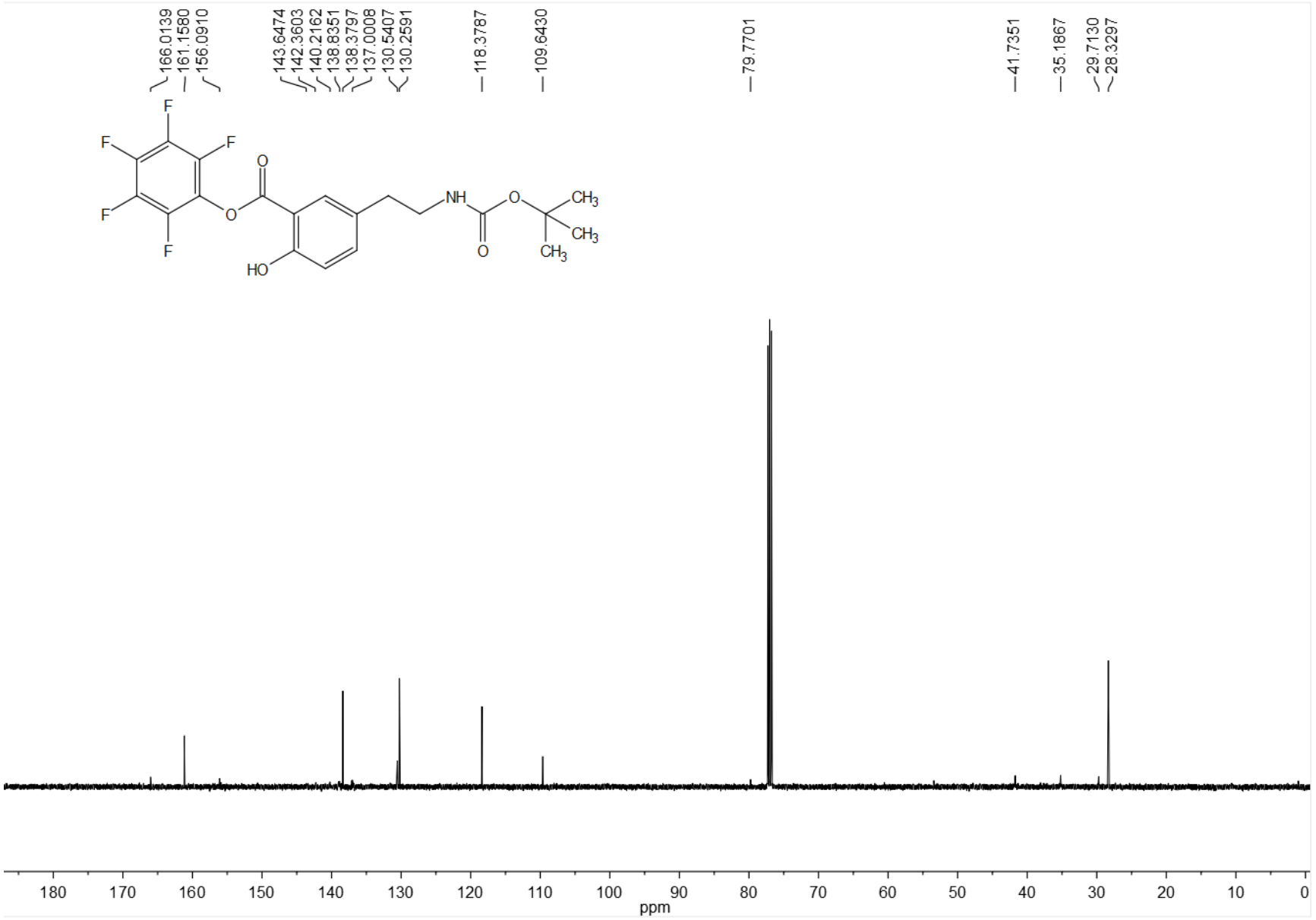
166.0139
161.1580
156.0910
143.6474
142.3603
140.2162
138.8351
138.3797
137.0008
130.5407
130.2591
118.3787
109.6430
79.7701
41.7351
35.1867
29.7130
28.3297
F
F
F
F
O
O
NH
O
CH3
CH3
CH3
O
HO
180
170
160
150
140
130
120
110
100
90
80
70
60
50
40
30
20
10
0
ppm

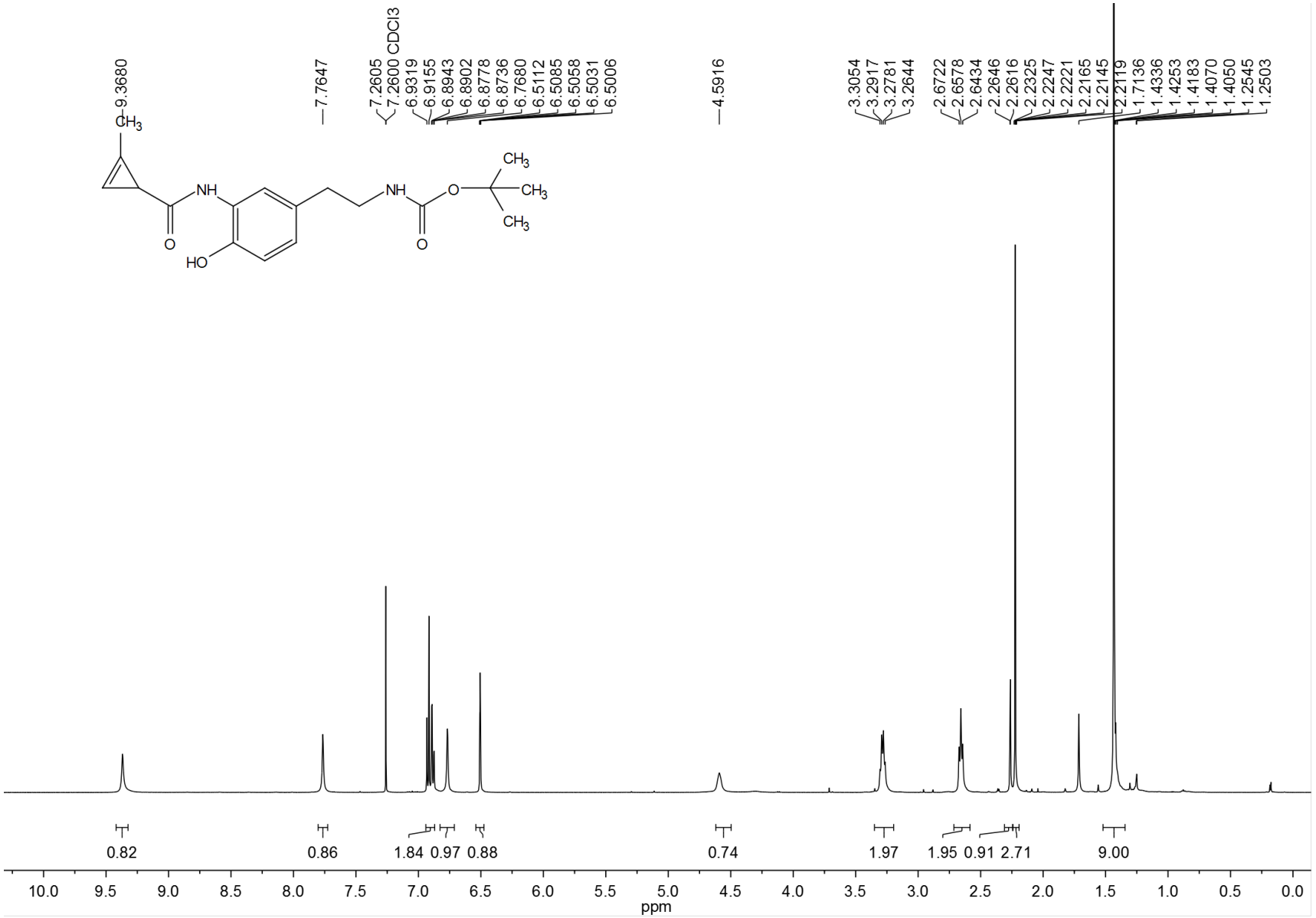
9.3680
7.7647
7.2605
7.2600 CDCl3
6.9319
6.9155
6.8943
6.8902
6.8778
6.8736
6.7680
6.5112
6.5085
6.5058
6.5031
6.5006
4.5916
3.3054
3.2917
3.2781
3.2644
2.6722
2.6578
2.6434
2.2646
2.2616
2.2325
2.2247
2.2221
2.2165
2.2145
2.2119
1.7136
1.4336
1.4253
1.4183
1.4070
1.4050
1.2545
1.2503
CH3
NH
NH
O
O
HO
CH3
CH3
CH3
0.82
0.86
1.84
0.97
0.88
0.74
1.97
1.95
0.91
2.71
9.00
10.0
9.5
9.0
8.5
8.0
7.5
7.0
6.5
6.0
5.5
5.0
4.5
4.0
3.5
3.0
2.5
2.0
1.5
1.0
0.5
0.0
ppm

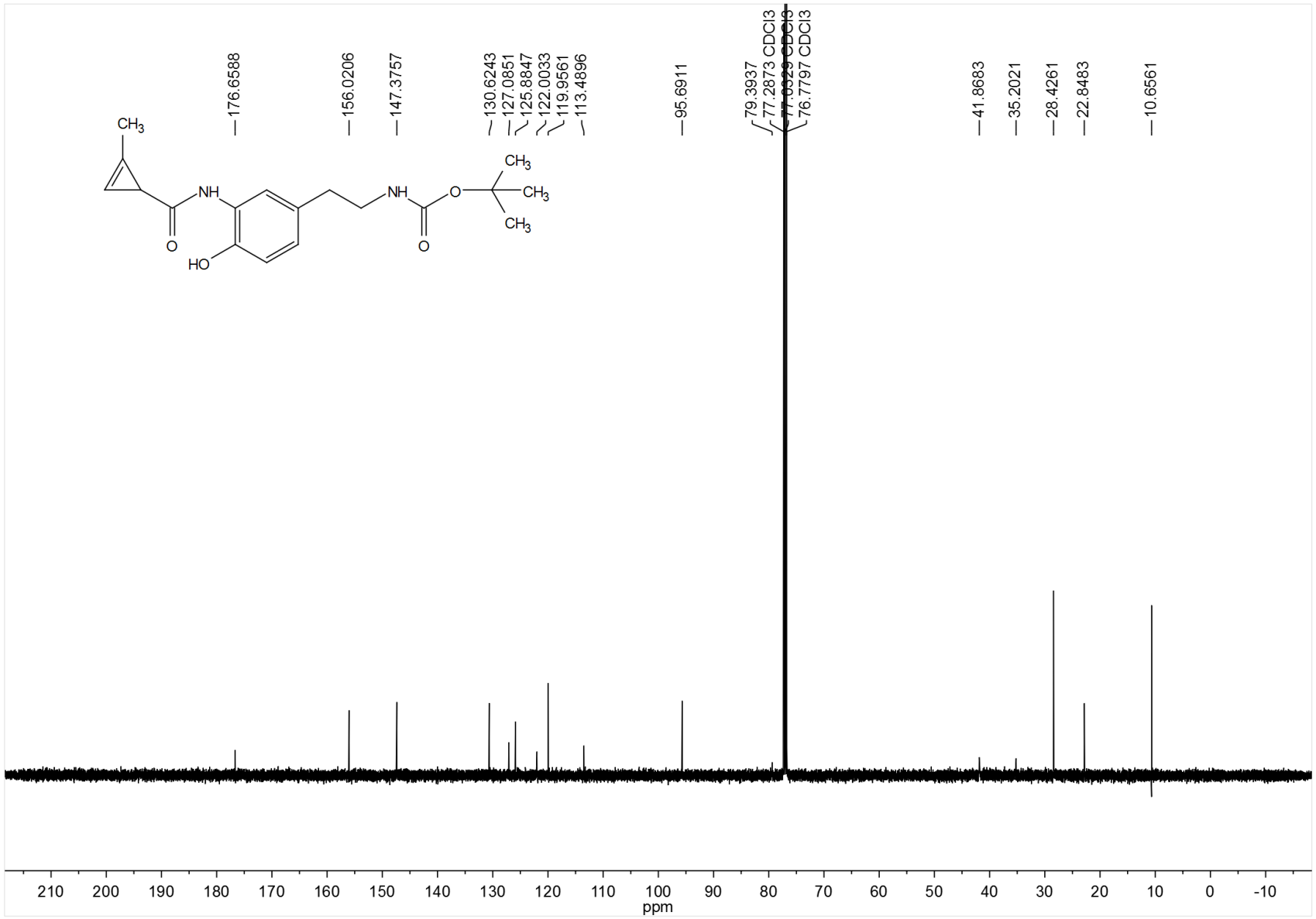
176.6588
156.0206
147.3757
130.6243
127.0851
125.8847
122.0033
119.9561
113.4896
95.6911
79.3937
77.2873 CDCl3
76.7797 CDCl3
41.8683
35.2021
28.4261
22.8483
10.6561
CH3
NH
O
HO
NH
O
O
CH3
CH3
CH3
210 200 190 180 170 160 150 140 130 120 110 100 90 80 70 60 50 40 30 20 10 0 -10
ppm

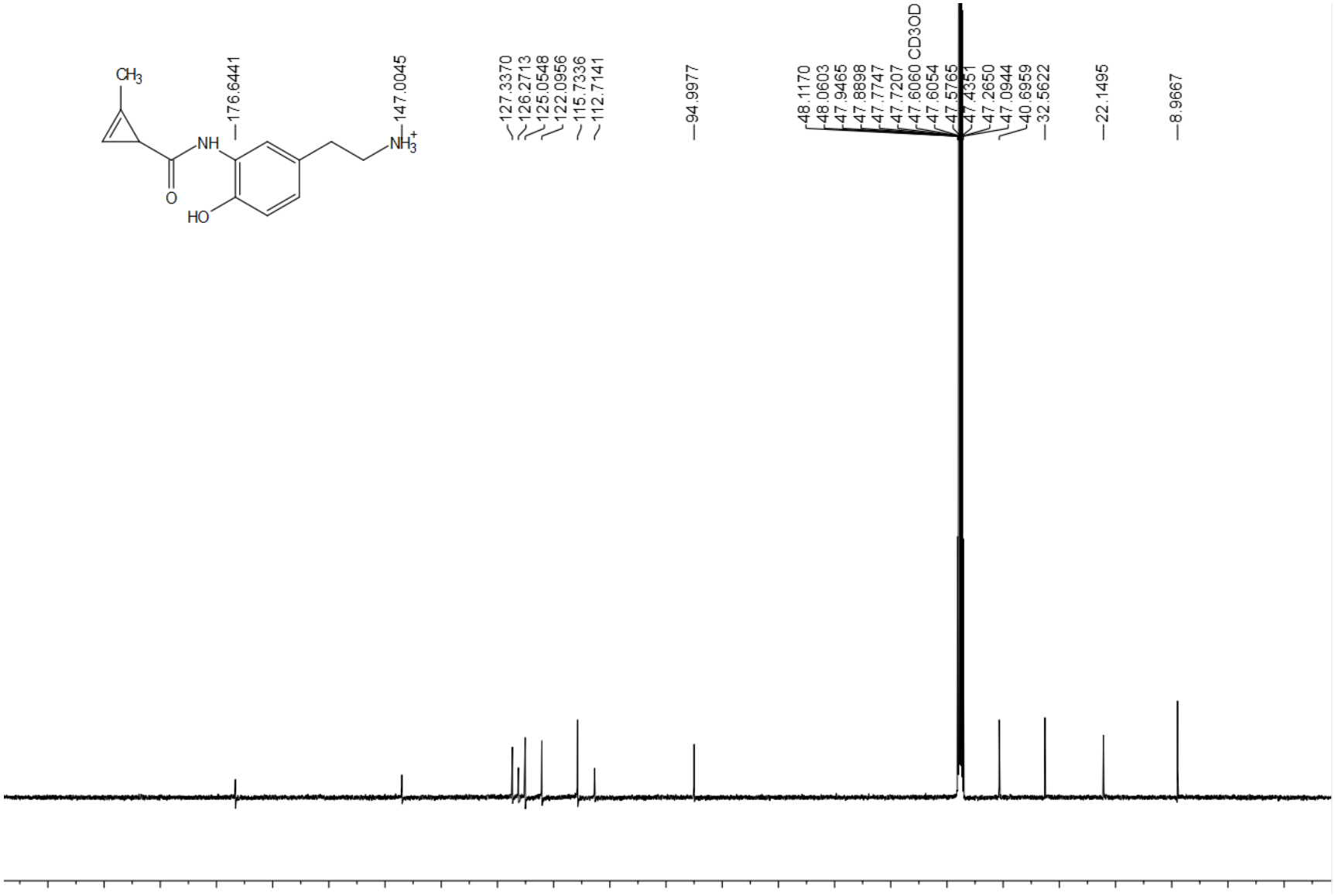
CH3
NH
O
HO
NH3+
176.6441
147.0045
127.3370
126.2713
125.0548
122.0956
115.7336
112.7141
94.9977
48.1170
48.0603
47.9465
47.8898
47.7747
47.7207
47.6060 CD3OD
47.6054
47.5765
47.4351
47.2650
47.0944
40.6959
32.5622
22.1495
8.9667

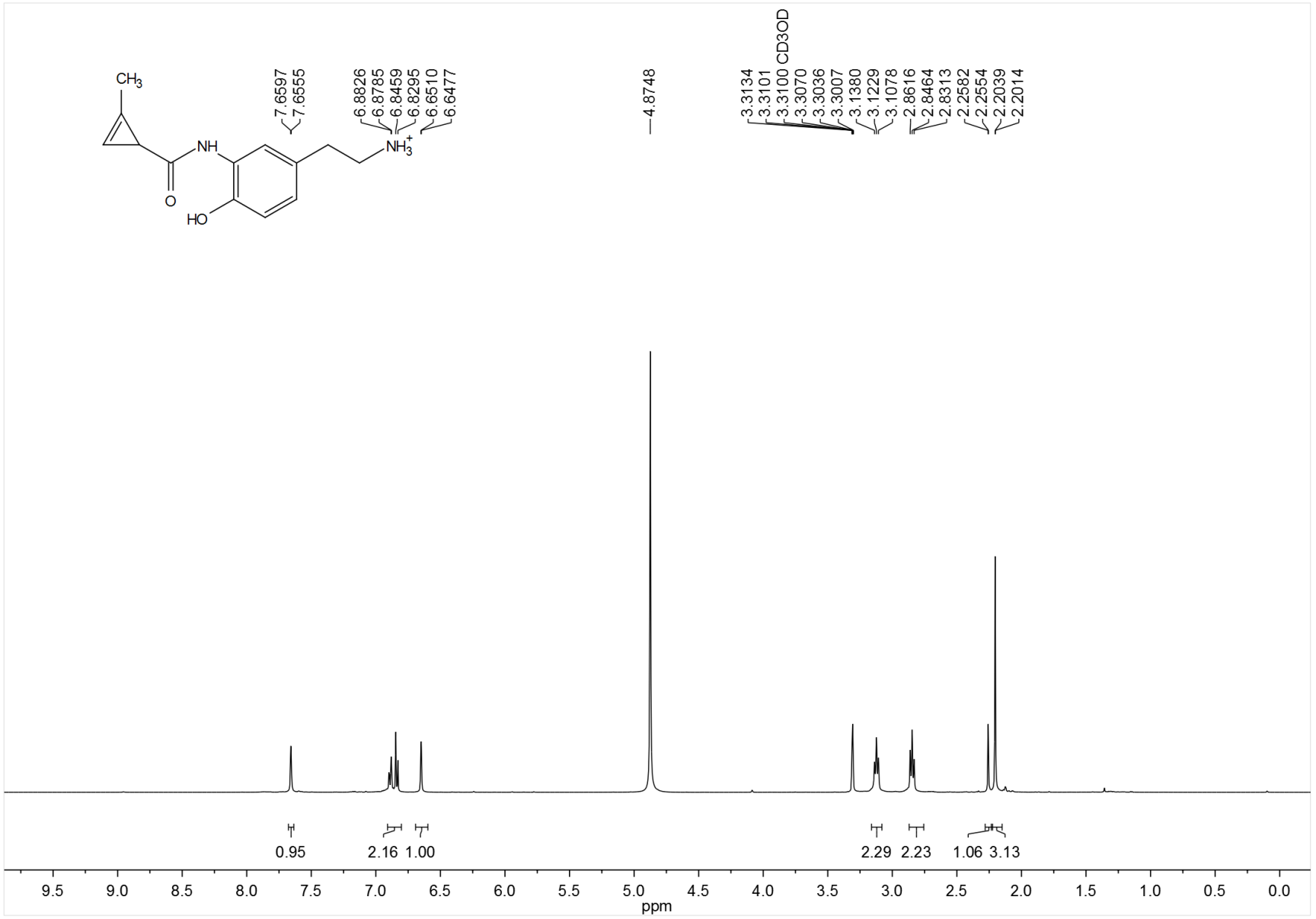
CH3
NH
O
HO
NH3+
7.6597
7.6555
6.8826
6.8785
6.8459
6.8295
6.6510
6.6477
4.8748
3.3134
3.3101
3.3100
CD3OD
3.3070
3.3036
3.3007
3.1380
3.1229
3.1078
2.8616
2.8464
2.8313
2.2582
2.2554
2.2039
2.2014
0.95
2.16
1.00
2.29
2.23
1.06
3.13
9.5
9.0
8.5
8.0
7.5
7.0
6.5
6.0
5.5
5.0
4.5
4.0
3.5
3.0
2.5
2.0
1.5
1.0
0.5
0.0
ppm

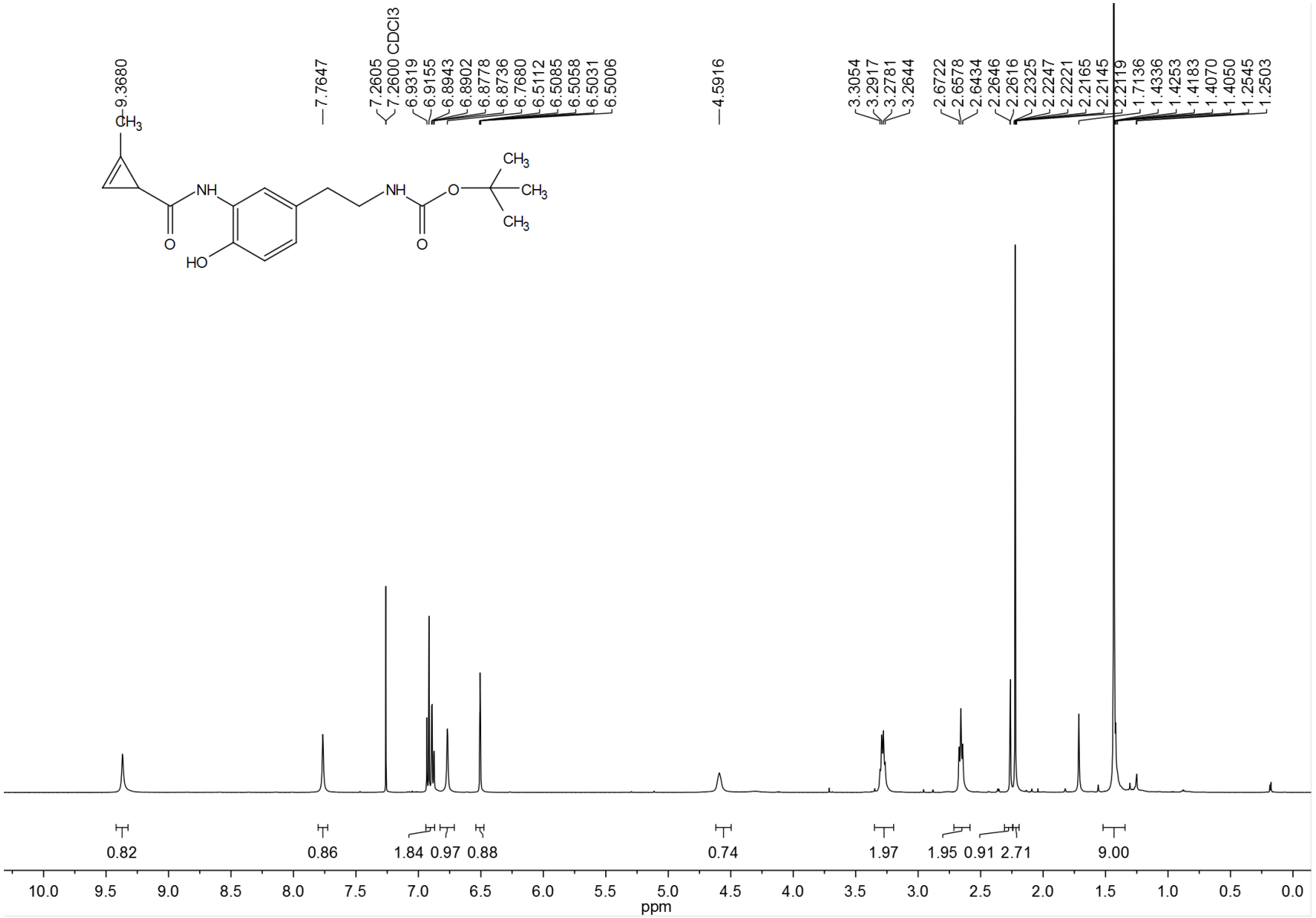
9.3680
7.7647
7.2605
7.2600 CDCl3
6.9319
6.9155
6.8943
6.8902
6.8778
6.8736
6.7680
6.5112
6.5085
6.5058
6.5031
6.5006
4.5916
3.3054
3.2917
3.2781
3.2644
2.6722
2.6578
2.6434
2.2646
2.2616
2.2325
2.2247
2.2221
2.2165
2.2145
2.2119
1.7136
1.4336
1.4253
1.4183
1.4070
1.4050
1.2545
1.2503
CH3
NH
NH
O
O
HO
CH3
CH3
CH3
0.82
0.86
1.84
0.97
0.88
0.74
1.97
1.95
0.91
2.71
9.00
10.0
9.5
9.0
8.5
8.0
7.5
7.0
6.5
6.0
5.5
5.0
4.5
4.0
3.5
3.0
2.5
2.0
1.5
1.0
0.5
0.0
ppm

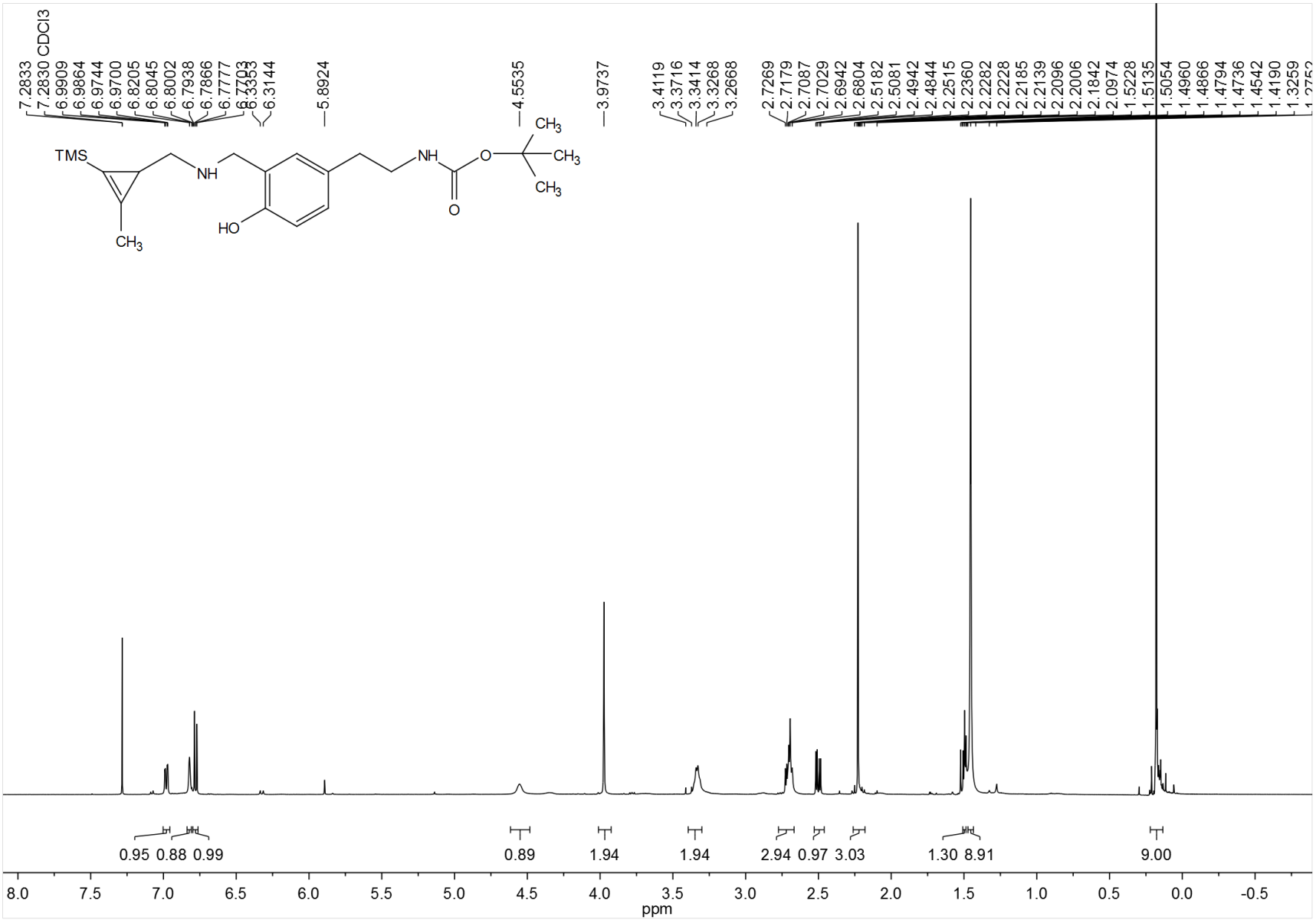
7.2833
7.2830 CDCl3
6.9909
6.9864
6.9744
6.9700
6.8205
6.8045
6.8002
6.7938
6.7866
6.7777
6.3353
6.3144
5.8924
4.5535
3.9737
3.4119
3.3716
3.3414
3.3268
3.2668
2.7269
2.7179
2.7087
2.7029
2.6942
2.6804
2.5182
2.5081
2.4942
2.4844
2.2515
2.2360
2.2282
2.2228
2.2185
2.2139
2.2096
2.2006
2.1842
2.0974
1.5228
1.5135
1.5054
1.4960
1.4866
1.4794
1.4736
1.4542
1.4190
1.3259
TMS
NH
NH
O
O
CH3
CH3
CH3
HO
CH3
0.95 0.88 0.99
0.89
1.94
1.94
2.94 0.97 3.03
1.30 8.91
9.00
8.0
7.5
7.0
6.5
6.0
5.5
5.0
4.5
4.0
3.5
3.0
2.5
2.0
1.5
1.0
0.5
0.0
-0.5
ppm

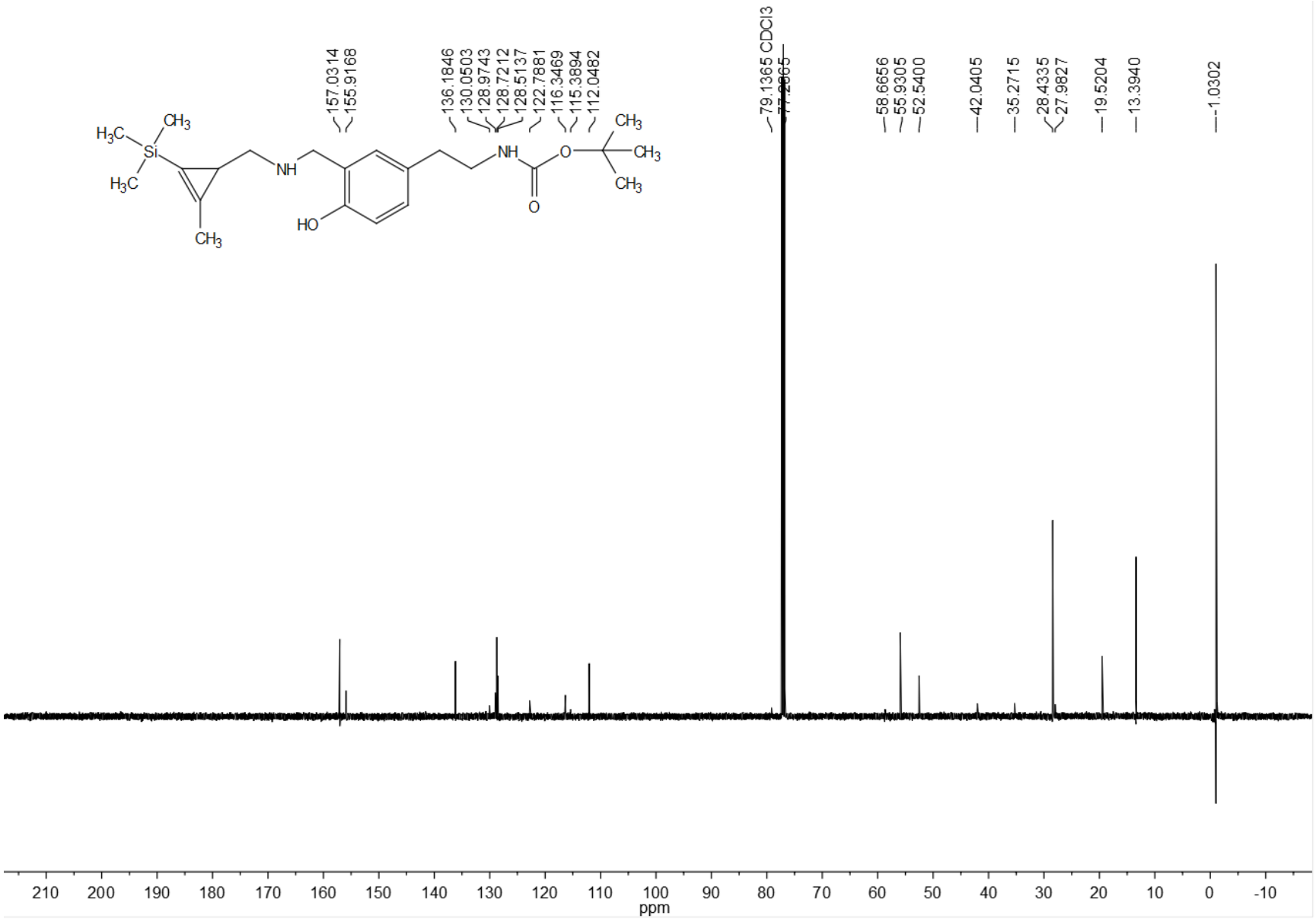
157.0314
155.9168
136.1846
130.0503
128.9743
128.7212
128.5137
122.7881
116.3469
115.3894
112.0482
79.1365 CDCl3
77.2865
58.6656
55.9305
52.5400
42.0405
35.2715
28.4335
27.9827
19.5204
13.3940
-1.0302
ppm

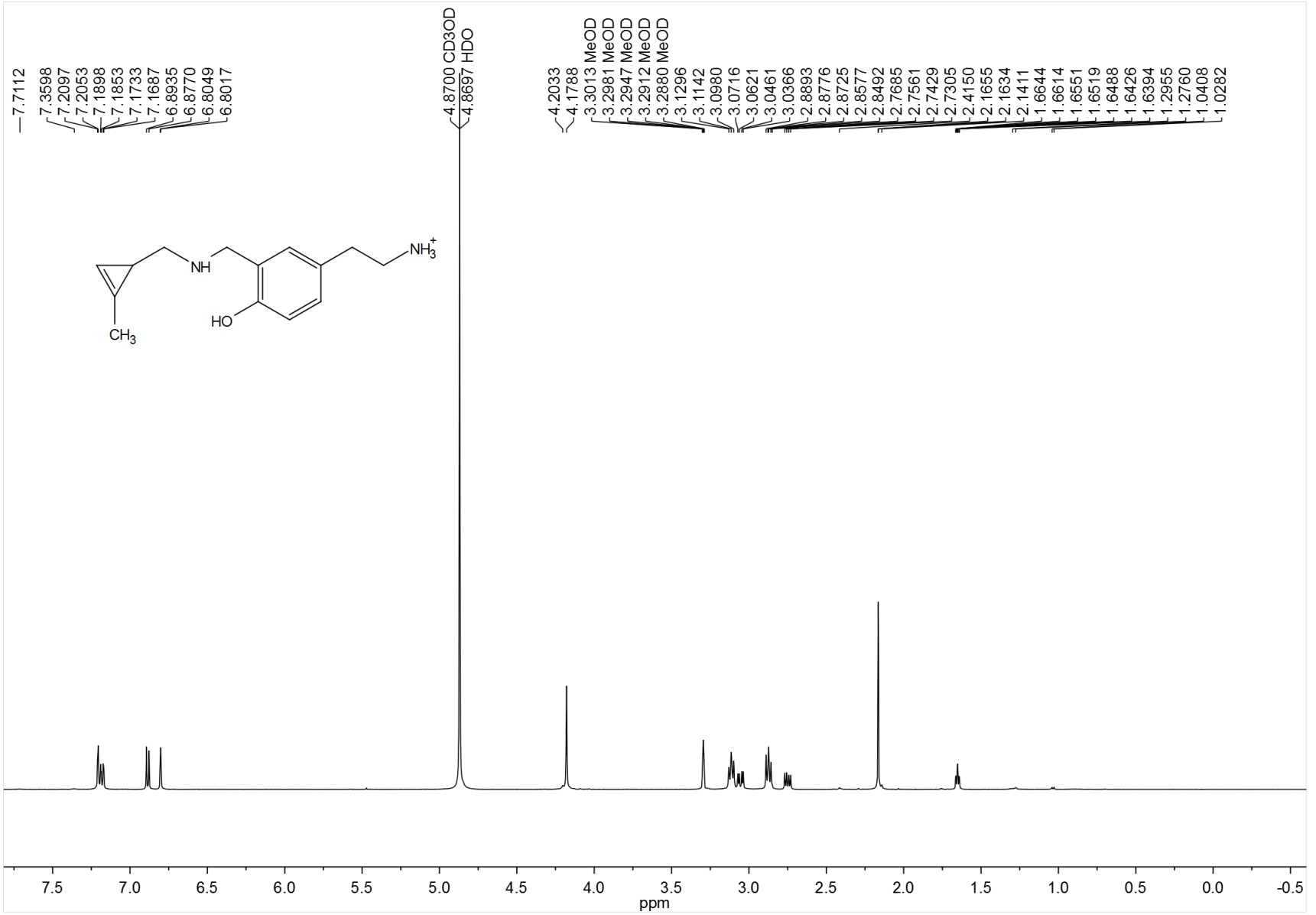
7.7112
7.3598
7.2097
7.2053
7.1898
7.1853
7.1733
7.1687
6.8935
6.8770
6.8049
6.8017
4.8700 CD3OD
4.8697 HDO
4.2033
4.1788
3.3013 MeOD
3.2981 MeOD
3.2947 MeOD
3.2912 MeOD
3.2880 MeOD
3.1296
3.1142
3.0980
3.0716
3.0621
3.0461
3.0366
2.8893
2.8776
2.8725
2.8577
2.8492
2.7685
2.7561
2.7429
2.7305
2.4150
2.1655
2.1634
2.1411
1.6644
1.6614
1.6551
1.6519
1.6488
1.6426
1.6394
1.2955
1.2760
1.0408
1.0282
NH
NH3+
HO
CH3
7.5
7.0
6.5
6.0
5.5
5.0
4.5
4.0
3.5
3.0
2.5
2.0
1.5
1.0
0.5
0.0
-0.5
ppm

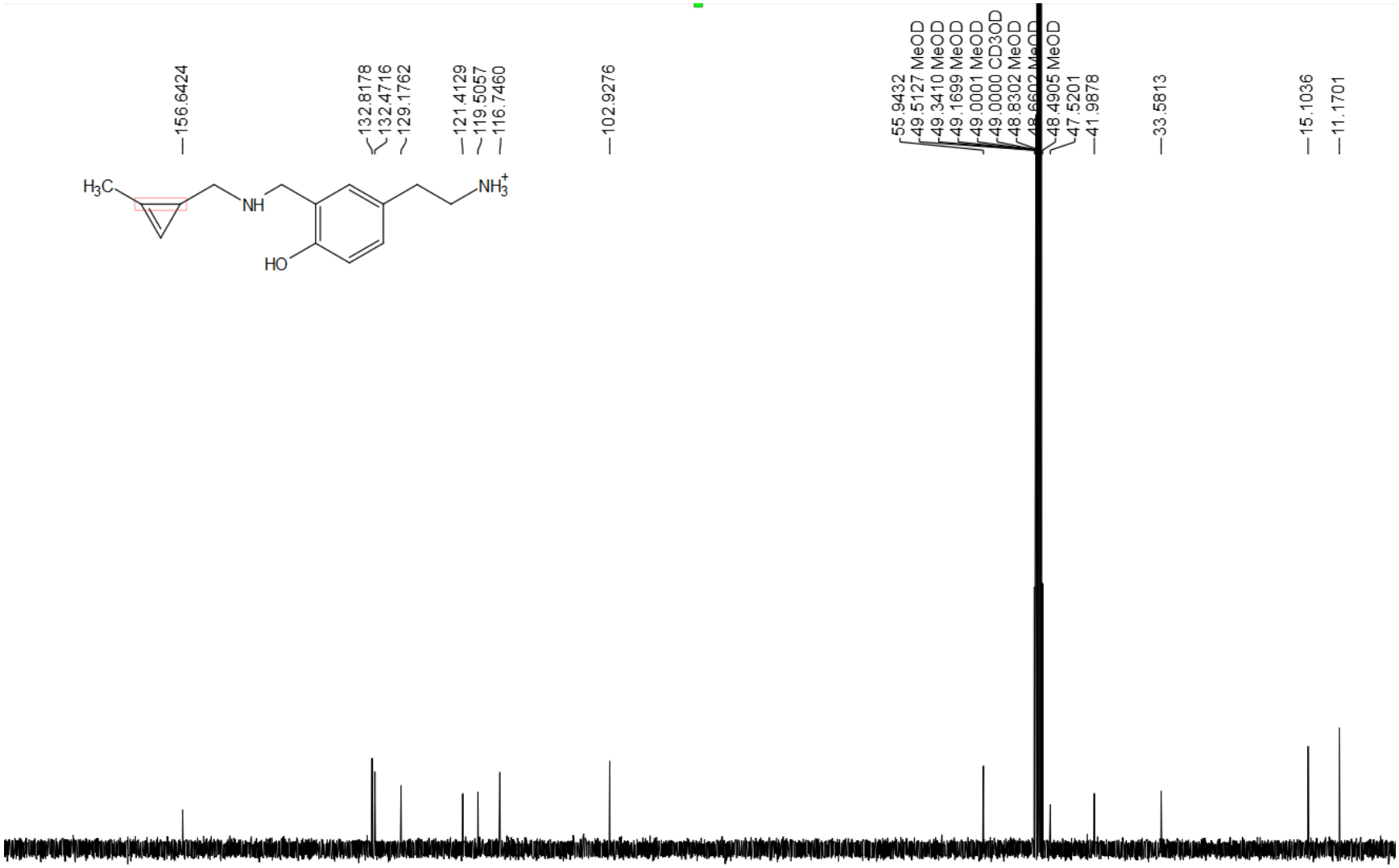
156.6424
132.8178
132.4716
129.1762
121.4129
119.5057
116.7460
102.9276
55.9432
49.5127 MeOD
49.3410 MeOD
49.1699 MeOD
49.0001 MeOD
49.0000 CD3OD
48.8302 MeOD
48.4905 MeOD
47.5201
41.9878
33.5813
15.1036
11.1701
H3C
NH
NH3+
HO

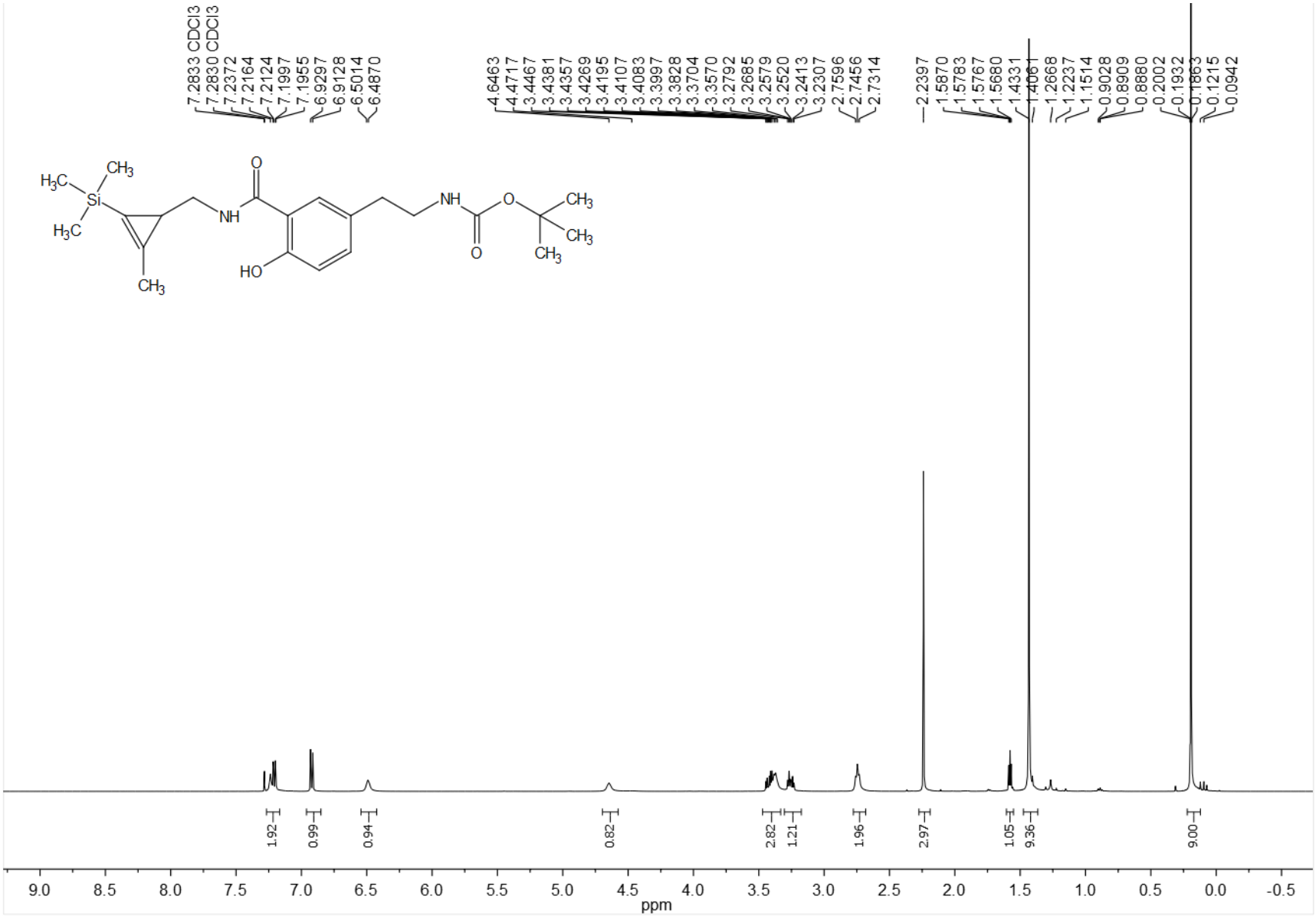
7.2833 CDCl3
7.2830 CDCl3
7.2372
7.2164
7.2124
7.1997
7.1955
6.9297
6.9128
6.5014
6.4870
4.6463
4.4717
3.4467
3.4381
3.4357
3.4269
3.4195
3.4107
3.4083
3.3997
3.3828
3.3704
3.3570
3.2792
3.2685
3.2579
3.2520
3.2413
3.2307
2.7596
2.7456
2.7314
2.2397
1.5870
1.5783
1.5767
1.5680
1.4331
1.4061
1.2668
1.2237
1.1514
0.9028
0.8909
0.8880
0.2002
0.1932
0.1863
0.1215
0.0942
1.92
0.99
0.94
0.82
2.82
1.21
1.96
2.97
1.05
9.36
9.00
ppm

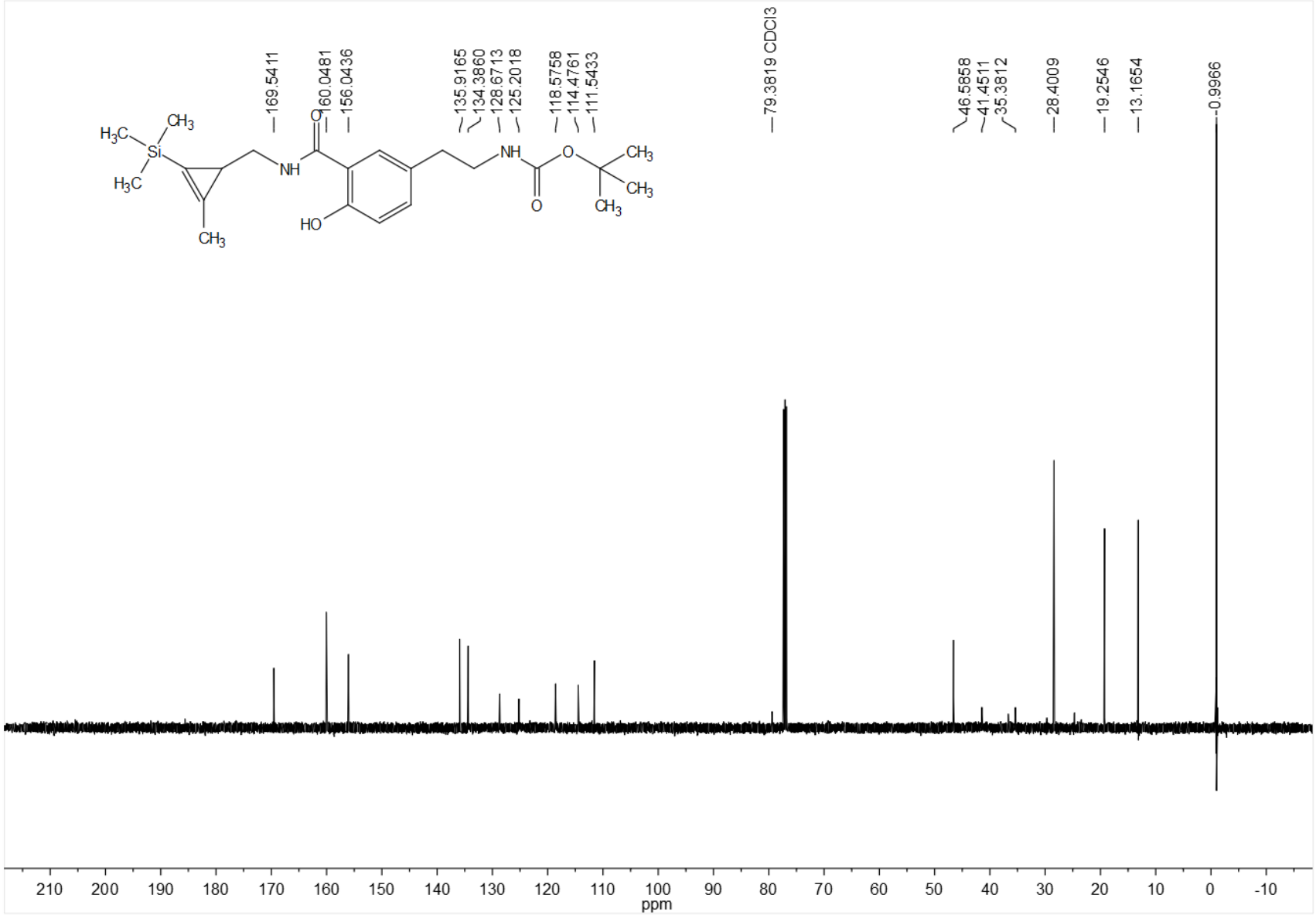
169.5411
160.0481
156.0436
135.9165
134.3860
128.6713
125.2018
118.5758
114.4761
111.5433
79.3819 CDCl3
46.5858
41.4511
35.3812
28.4009
19.2546
13.1654
0.9966
ppm

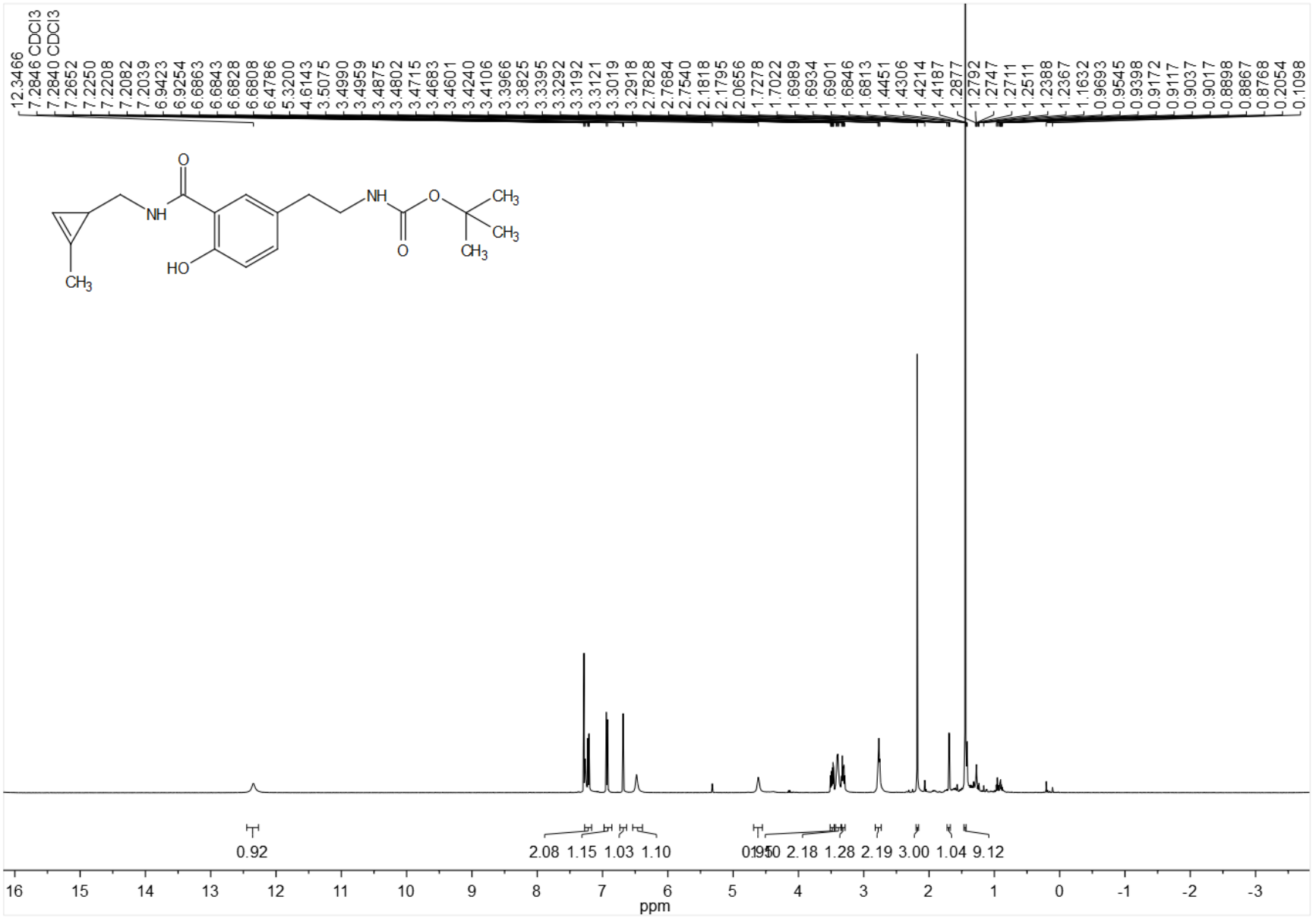
12.3466
7.2846 CDCl3
7.2840 CDCl3
7.2652
7.2250
7.2208
7.2082
7.2039
6.9423
6.9254
6.6863
6.6843
6.6828
6.6808
6.4786
5.3200
4.6143
3.5075
3.4990
3.4959
3.4875
3.4802
3.4715
3.4683
3.4601
3.4240
3.4106
3.3966
3.3825
3.3395
3.3292
3.3192
3.3121
3.3019
3.2918
2.7828
2.7684
2.7540
2.1818
2.1795
2.0656
1.7278
1.7022
1.6989
1.6934
1.6901
1.6846
1.6813
1.4451
1.4306
1.4214
1.4187
1.2877
1.2792
1.2747
1.2711
1.2511
1.2388
1.2367
1.1632
0.9693
0.9545
0.9398
0.9172
0.9117
0.9037
0.9017
0.8898
0.8867
0.8768
0.2054
0.1098
O
NH
HO
CH3
NH
O
O
CH3
CH3
CH3
0.92
2.08
1.15
1.03
1.10
2.18
1.28
2.19
3.00
1.04
9.12
16
15
14
13
12
11
10
9
8
7
6
5
4
3
2
1
0
-1
-2
-3
ppm

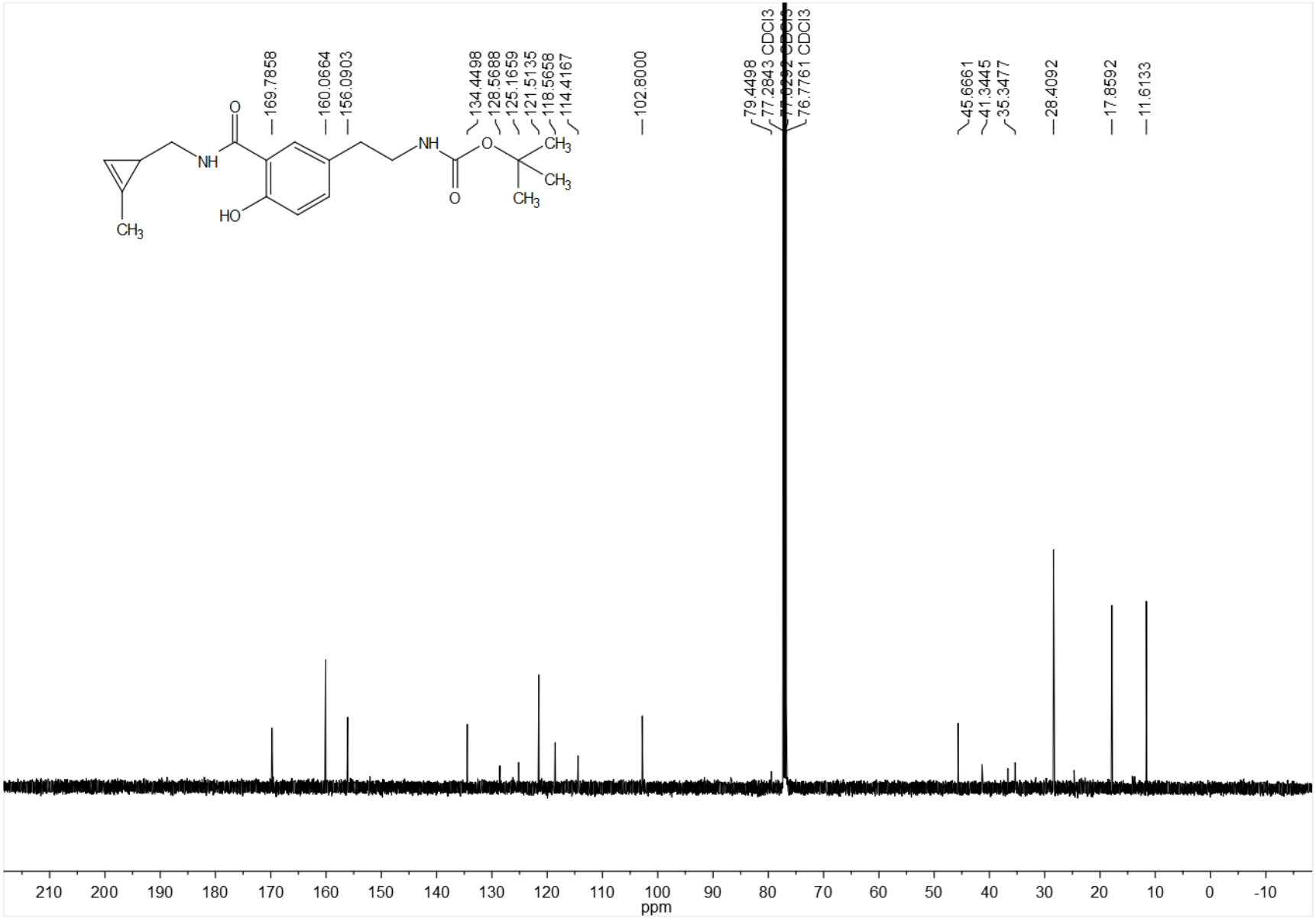
169.7858
160.0664
156.0903
134.4498
128.5688
125.1659
121.5135
118.5658
114.4167
102.8000
79.4498
77.2843 CDCl3
76.7761 CDCl3
45.6661
41.3445
35.3477
28.4092
17.8592
11.6133
NH
NH
O
O
O
HO
CH3
CH3
CH3
CH3
210 200 190 180 170 160 150 140 130 120 110 100 90 80 70 60 50 40 30 20 10 0 -10
ppm

Chapter II: Development of spirocyclopropene, a new chemical biology tool to control cyclopropene reactivity

Introduction

In chapter I, we developed a general method to study neural circuits which respresent a certain kind of cell-cell connection that the cells talk with each other by neurotransmitters. However, there are a lot of other kinds of functional cells in brain. They talk with each other by different ways, not just neurotransmitters. Some kinds of cell-cell connections are related to centain neuron degenerative diseases. So a novel method to study functional cell-cell interactions is needed. In order to do that, we try to develop a new kind of bioorthogonal reactions which we can control the reactivity by light or enzyme. My work is trying to design and synthesize that kind of bioorthogonal tools as the start of the whole strategy.

Here I describe the development of a strategy to control cyclopropene reactivity with tetrazines. The ultimate goal of this research will be its application to visualizing neural circuits using lipophilic bioorthogonal tracers that contain a lipid anchor linked to a cyclopropene.

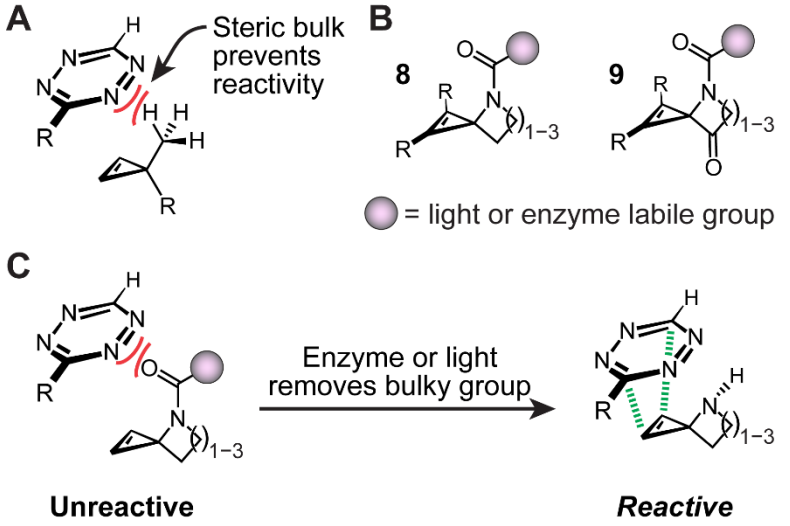

Figure 8: Developing a turn-on cyclopropene. (A) Bulky groups prevent reaction between cyclopropene and tetrazine. (B) Proposed turn-on cyclopropene scaffolds. (C) Schematic for the use of turn-on cyclopropenes.

Cyclopropene-tetrazine reaction is one of the most popular biorthogonal reaction. This kind of click chemistry can react rapidly via inverse-electron-demand Diels−Alder (IED-DA) reactions. The remarkable speed of cyclopropene-tetrazine raction is very useful for sensitive bio-imaging.

We are trying to control the reactivity of this tracer. However, there is still no technique for controlling the reactivity for this reaction. So now we are focusing on make a ‘ turn-on’ biorthogonal tools which we can easily control the reactivity of the reaction.

Lin and co-workers described a spirocyclopropene for reaction with tetrazole in 2016[18]. Lin showed that the projection of hydrogens on the exocyclic 4- or 5-membered ring affect the reactivity because of the steric hindrance which inspired us to design a new kind of spirocyclopropene that contain a nitrogen for caging the reactivity. We can attach a bulk group on the nitrogen which can be cleaved by light or enzyme (Figure 8). We think that the bulky group can efficiently cage the reactivity of spirocyclopropene-tetrazine reaction. When we remove that bulky group by enzyme or UV light (Figure 8), the spirocyclopropene can rapidly react with tetrazine. Then we can control the reactivity of the cyclopropene-tetrazine reaction precisely. Since it has a lipid anchor on the molecule, we can directly apply this new tracer to a fixed brain. Because it is a lipophilic molecule, it can diffuse along the cell’s membrane and get to the certain part we want it to go. Now we are still interested in synapse, which connects two neuron cells.

We hoped that the when the tracer reached the synapse, the fluorescence activator is released by a specific protease that is targeted to the synapse by conjugation to an antibody. The cyclopropene then activates the pro-fluorescent lipid’s fluorescence which was quenched by a tetrazine on the connected neuron, which has been uniformly applied throughout the system.

Synthesis of 3-N-substituted spirocyclopropenes

We have designed three kinds of spirocyclopropene. At very beginning, we tried to make the spirocyclopropene which has no electron withdrawing group on the exocyclic ring. However,

when we tried to eliminate the bromine from the cyclopropane intermediate, it formed either alkane when the R group was proton or allene when the R group was something else (Figure 10).

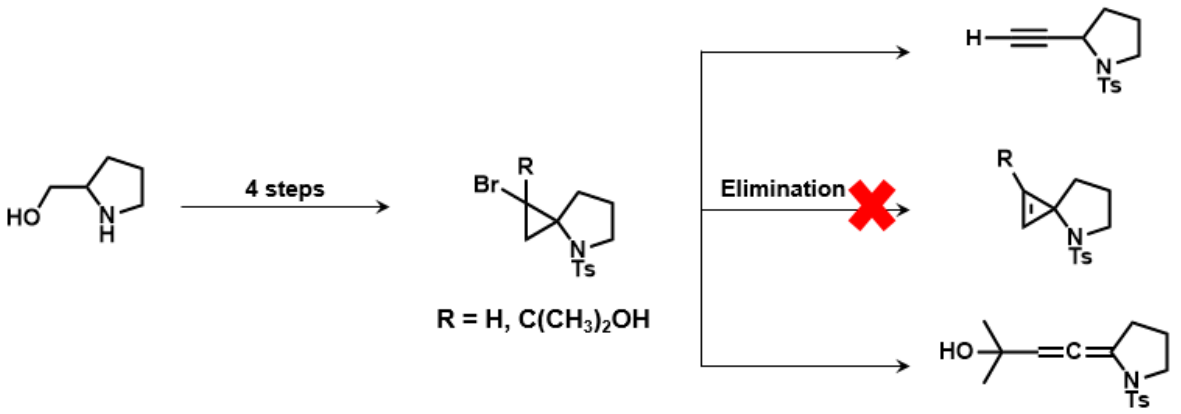

Figure 10: Elimination product of spirocyclopropane with mono bromine

So, we designed three series of spirocyclopropene. They all have an electron withdrawing group on the exocyclic ring (Figure 11). We hoped that the electron withdrawing could stabilize the structure of spirocyclopropene. My work focuses on the synthesis of the difluoro-substituted spirocyclopropene.

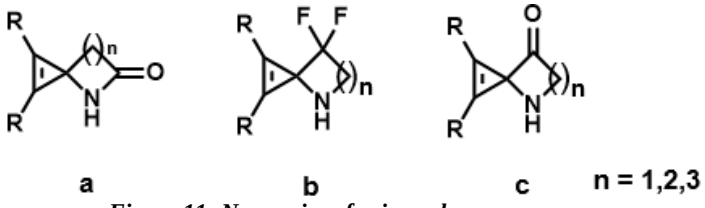

Figure 11: New series of spirocyclopropene

I started with a five member ring intermediate which can be made in three steps from commercially available starting materials. I used Diethylaminosulfur trifluoride to replace the ketone with two fluorines and then used LAH to reduce the ester to an alcohol. Then I added a 4-Toluenesulfonyl group on the alcohol and used 1, 8-Diazabicyclo [5.4.0] undec-7-ene to do the

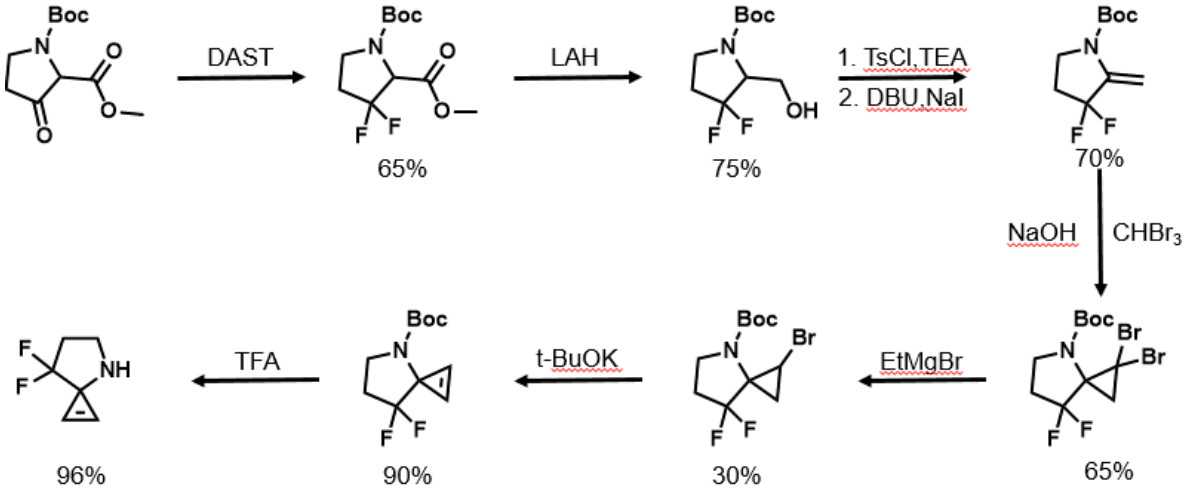

Figure 9: synthesis of di-fluoro spirocyclopropene

elimination and obtained alkane. Then I found a method to synthesis the bromo spiro-cyclopropane. The final step was using t-BuOK to do the elimination of bromo spiro-cyclopropanes and obtained di-fluoro spirocyclopropene (Figure 12).

When we tested the kinetics of the original di-fluoro spirocyclopropene, we found that it was unstable in pH 7.4 or even higher. Multiple reports have noted that putting a functional group on the C1 carbon of cyclopropene, even a methyl group could stabilize the cyclopropene.

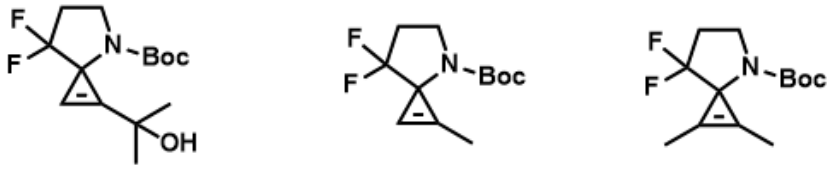

Figure 10: new type of di-fluoro spirocyclopropene with function group

Accordingly, we employed a strategy to functionalize the C1 position to improve stability and add a synthetic handle for attached biomolecules of interest (Figure 12). Analyzing the stability of the monomethyl spirocyclopropene revealed that it was stable at pH 7.4 and had good reactivity with tetrazine.

Synthesis of photoactivatable di-fluoro spirocyclopropene

In the meantime, I attached a light-protected group on the difluorospirocyclopropene. I chose an o-nitrobenzyl protecting group, which can be cleaved by UV light and is widely used in chemical biology[19] (Figure 14). This bulky group is in ideal position to block the cyclopropene face that tetrazine approaches and should thus inhibit the reaction.

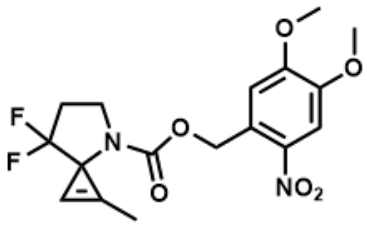

Figure 11: photoactivatable di-fluoro spirocyclopropene

To ensure low reactivity with tetrazine, I dissolved 1 mmol di-fluoro spirocyclopropene, and 0.25 mmol tetrazine in 200 μL PBS solution and tracked the reaction by HPLC. I injected the reaction in HPLC after 3h, 24h, 48h and 7 days. Fortunately, we observed no reaction products or consumption of starting material by HPLC, which indicated a very sluggish reaction between tetrazine and photocaged spirocyclopropene.

In the future work, we will try to get the precise kinetics date about the caged and uncaged spirocyclopropene. Next, we will try to put the enzyme cleavable group on the nitrogen. Then we can control the reactivity by enzyme.

Experiment section

General materials and methods. All chemical reagents were of analytical grade, obtained from commercial suppliers, and used without further purification unless otherwise specified. Rhodium

(II) acetate (Rh_2OAc_4) was gently heated under vacuum until it became a free flowing powder (typically 15–20 s) before using it for reactions. Reactions were monitored by thin layer chromatography (TLC) on pre-coated glass TLC plates (Analtech UNIPLATE™ silica gel HLF w/ organic binder, 250 μm thickness, with UV254 indicator) or by LC/MS (Agilent LC-MSD, direct-injection mode, 1–10 μL, ESI). TLC plates were visualized by UV illumination or developed with either potassium permanganate stain ($KMnO_4$ stain: 1.5 g $KMnO_4$, 10 g K_2CO_3 and 1.25 mL of 10% NaOH dissolved in 200 mL H_2O), ceric ammonium molybdate stain (CAM stain: 12 g $(NH_4)_6Mo_7O_{24} \bullet 4H_2O$, 0.5 g $Ce(NH_4)_2(NO_3)_6$ and 15 mL of concentrated H_2SO_4 dissolved in 235 mL H_2O), or ninhydrin stain (1.5 g ninhydrin dissolved in 100 mL of n-BuOH and 3 mL of conc. AcOH). Flash chromatography was carried out using Sorbtech, 60 Å, 40–63 μm or Millipore 60 Å, 35-70 μm silica gel according to the procedure described by Still[15]. HPLC was performed using a Shimadzu HPLC (FCV-200AL) equipped with an Agilent reversed phase Zorbax Sb-Aq C18 column (4.6 × 250 mm or 21.2 × 250 mm) fitted with an Agilent stand-alone prep guard column. NMR spectra (1H and 13C) were obtained using a 400, 500, or 700 MHz Bruker spectrometer and analysed using Mestrenova 9.0. 1H and 13C chemical shifts (δ) were referenced to residual solvent peaks. High-resolution electrospray ionization (ESI) mass spectra were obtained at the Stony Brook University Institute for Chemical Biology and Drug Discovery Mass Spectrometry Facility with an Agilent LC-UV-TOF spectrometer.

Scheme 1

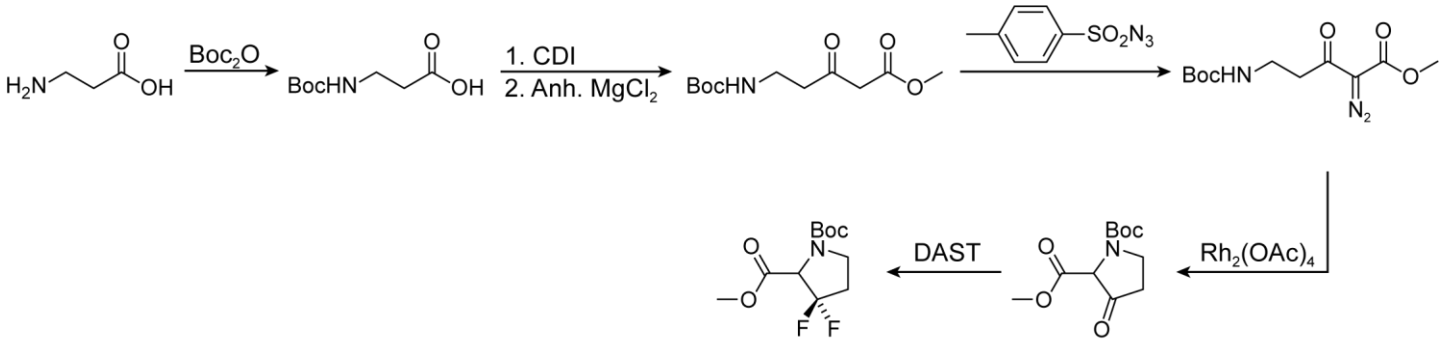

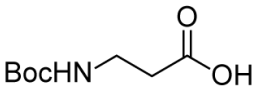

1

To a solution of β-alanine (20.0 g, 224.49 mmol, 1 eq) in 2M NaOH (200 mL) and THF (200 mL) was added Boc_2O (49.98 g, 228.98 mmol,1.02 eq). The reaction mixture was stirred at rt for 16 h, concentrated in vacuo to remove THF, and diluted with DCM (50 mL). The organic layer was discarded and the aqueous layer was acidified to pH 1-2 using 2M HCl. Th aqueous layer was washed with EtOAc (3×75 mL) and the combined organic layers were dried over anhydrous Na_2SO_4, and concentrated in vacuo to obtain an oil which solidified upon cooling to give 1 as a white powder (42.2 g, quantitative). Rf = 0.1-0.5 (50% EtOAc/hexanes, visualized w/ Ninhydrin stain). ^{1}H NMR (25:75 % mixture of rotamers, 500 MHz, $CDCl_3$): δ= 11.68 (s, 1H), 6.32 (s, 0.27H), 5.16 (s, 0.62H), 3.39–3.32 (m, 2H), 2.56–2.51 (m, 2H), 1.50–1.30 (m, 9H). ^{13}C NMR (rotamers,126 MHz, $CDCl_3$): δ= 177.53, 176.47, 157.69, 156.11, 81.25, 79.79, 37.25, 35.99, 34.54, 28.45. MS (ESI): Calcd for $C_8H_{15}NO_4$ $[M]^+$: 189.1, found: 134.1 $[M\text{-}C(CH_3)_3+2H]^+$, 190.1 $[MH]^+$.

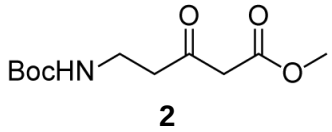

2

2 was synthesized based on a modification to a previously described strategy. To a suspension of **1** (19.78 g, 104.50 mmol, 1 eq) in THF (200 mL) was added CDI (20.49 g, 125 mmol, 1.2 eq) and the mixture was stirred at rt for 4 h during which it turned homogenous. To this activated ester (Rf = 0.25, 50% EtOAc/hexanes, visualized w/ UV) was added a mixture of $MgCl_2$ (9.95 g, 104.50 mmol, 1 eq) and name (32.64 g, 209 mmol, 2 eq) in one portion. The suspension was stirred at rt for 16 h, quenched with water, and concentrated in vacuo to remove THF. The reaction mixture was then diluted with DCM (150 mL) and 1M HCl (150 mL), and stirred at rt for 15 min to dissolved the white solid. The aqueous layer was acidified to pH 1-2 using 1M HCl and extracted with DCM. The combined organic layers were washed with brine, dried over anhydrous Na_2SO_4 and concentrated in vacuo to obtain a crude pale yellow oil which was used without further purification (26.2 g). Rf = 0.31 (30% EtOAc/hexanes, visualized w/ UV). ^{1}H NMR (16:84 % mixture of rotamers, 500 MHz, $CDCl_3$): δ= 5.88 (s, 0.16 H), 5.21 (s, 0.82 H), 3.54 (s, 2H), 3.51 (s, 3H), 3.15 (q, J = 6.1 Hz, 2H), 2.59 (t, J = 6.1 Hz, 2H), 1.25–1.20 (m, 9H). ^{13}C NMR (rotamers,126 MHz, $CDCl_3$): δ= 202.22, 168.89, 155.96, 79.27, 52.14, 48.74, 42.71, 40.76, 28.11. MS (ESI): Calcd for $C_{11}H_{19}NO_5$ $[M]^+$: 245.1, found: 146.1 $[M\text{-}Boc^+2H]^+$, 190.1 $[M\text{-}C(CH_3)3+2H]+$, 246.1 $[MH]^+$.

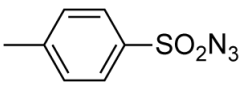

3

To an ice-cold solution of TsCl (10.0 g, 52.46 mmol, 1.0 eq) in acetone (100 mL) and water (50 mL) was added NaN3 (3.58 g, 55.09 mmol, 1.05 eq) and the reaction was allowed to warm to rt over 4 h. Reaction was concentrated in vacuo at 27 °C to remove acetone. The aqueous layer was washed with DCM (3×50 mL). The combined organic layers were dried over anhydrous Na2SO4 and concentrated in vacuo to obtain 3 as a transparent oil which solidified upon freezing (10.3 g,

quantitative). Rf = 0.80 (20% EtOAc/hexanes, visualized w/ UV). ^{1}H NMR (700 MHz, CDCl3) : δ= 7.77 (d, J = 8.6 Hz, 2H), 7.36 (d, J = 8.4 Hz, 2H), 2.41 (s, 3H). ^{13}C NMR (175 MHz, $CDCl_3$): δ= 146.24, 135.20, 130.17, 127.27, 21.47. MS (ESI): Calcd for $C_7H_7SO_2N_3$ $[M]^+$: 197.0, found: 220.0 $[MNa]^+$, 417.0 $[2M+Na]^+$.

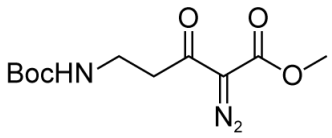

4

To a solution of crude β-ketoester **3** (26.2 g, 106.8 mmol, 1 eq) in MeCN (400 mL) was added tosyl azide (21.42 g, 108.9 mmol, 1.02 eq). Et_3N (44.4 mL, 320.4 mmol, 3 eq) was added dropwise and the mixture was stirred at rt for 2 h. The reaction mixture was concentrated in vacuo, and diluted with DCM and water. The organic layer was collected and the aqueous layer was further washed with DCM. The combined organic layers were washed with brine, dried over anhydrous Na_2SO_4, concentrated in vacuo, and purified by flash chromatography (180 g silica, 30% ethyl acetate/hexanes (v/v)) to obtain 4 as a yellow oil (27.0 g, 95.2 % over two steps). Rf = 0.43 (30% EtOAc/hexanes, visualized w/ UV). ^{1}H NMR (500 MHz, $CDCl_3$): δ= 5.17 (t, J = 6.2 Hz, 1H), 3.51 (s, 3H), 3.08 (q, J = 6.2 Hz, 2H), 2.71 (t, J = 6.2 Hz, 2H), 1.07 (s, 9H). ^{13}C NMR (126 MHz, $CDCl_3$): δ= 190.74, 160.95, 155.24, 78.09, 75.30, 51.60, 40.15, 35.03, 27.71. MS (ESI): Calcd for $C_{11}H_{17}N_3O_5$ $[M]^+$: 271.1, found: 272.1 $[MH]^+$, 294.1 $[MNa]^+$.

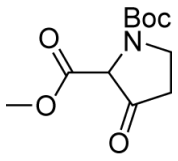

5

To a solution of **4** (25.5 g, 94.06 mmol, 1 eq) in dry toluene (350 mL) was added Rh_2OAc_4 (208 mg, 0.47 mmol, 0.005 eq) and the mixture was stirred at 90 °C for 1 h. The reaction mixture was concentrated in vacuo and passed through silica gel (60 g) using ether to obtain 5 as an oil which solidified upon cooling (20.85 g, 91.2%). Rf = 0.27 (30% EtOAc/hexanes, visualized w/ UV). ^{1}H NMR (33:67 % mixture of rotamers, 700 MHz, CDCl3): δ= 4.14 (m, 1H), 3.55–3.48 (m, 1H), 3.45–3.39 (m, 4H), 2.43–2.36 (m, 1H), 2.35–2.31 (m, 1H),

1.14–1.06 (2×s, 9H). ^{13}C NMR (rotamers, 175 MHz, $CDCl_3$): δ= 204.04, 203.51, 166.31, 166.03, 153.42, 153.07, 80.04, 65.05, 64.65, 52.16, 52.12, 41.74, 41.07, 36.40, 35.70, 27.57, 27.44. MS (ESI): Calcd for $C_{11}H_{17}NO_5$ $[M]^+$: 243.1, found: 144.1 $[M\text{-}Boc+2H]^+$, 188.1 $[M\text{-}C(CH_3)_3+2H]^+$, 244.1 $[MH]^+$, 487.2 $[2M+H]^+$.

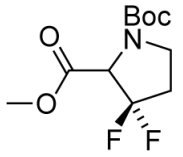

6

6 was synthesized based on a modification of a recently described strategy. 5 (6.5 g, 26.74 mmol, 1 equiv) was added to a flame dried flask under argon and cooled down to 0 °C. DAST (10.6 mL, 80.21 mmol, 3 equiv) was added dropwise using syringe and the resulting solution was allowed to warm to rt overnight. The yellow-orange solution was cooled down to 0°C, diluted with DCM, and quenched using dropwise addition of a saturated $NaHCO_3$ (~200 mL) until pH 8-9. The mixture was stirred for 30 min at 0°C and the resulting biphasic mixture was separated. The aqueous layer was further extracted with DCM. The combined organic layers were washed with brine, dried over anhydrous Na_2SO_4, concentrated in vacuo, and purified by flash chromatography (100 g silica, 10% ethyl acetate/hexanes (v/v)) to obtain 6 as a pale-yellow oil (4.3 g, 61%). Rf = 0.27 (10% EtOAc/hexanes, visualized w/ $KMnO_4$). (4.51 g, 16.16 mmol, 64% yield). ^{1}H NMR (50:60 % mixture of rotamers, 500 MHz, $CDCl_3$): δ= 4.50–4.38 (m, 1H), 3.77 (s, 3H), 3.77–3.68 (m, 1H), 3.55–3.47 (m, 2H), 2.51–2.27 (m, 2H), 1.40 (2×s, 9H). ^{13}C NMR (126 MHz, $CDCl_3$) δ= 167.99, 167.96, 167.92, 167.89, 153.77, 153.16, 128.68, 128.01, 126.65, 125.99, 124.63, 124.00, 81.22, 81.15, 65.41, 65.17, 64.93, 64.83, 64.59, 64.35, 52.90, 52.75, 43.48, 43.44, 42.94, 42.91, 33.62, 33.43, 33.25, 33.02, 32.84, 32.65, 28.33, 28.21. ^{19}F NMR (376 MHz, $CDCl_3$): δ= (-94.24)–(-95.29) (m, 1F), (-105.89)–(-108.12) (m, 1F). MS (ESI): Calcd for $C_{11}H_{17}F_2NO_4$, 265.1; found, 166.1 $[M\text{-}Boc+2H]^+$, 210.1 $[M\text{-}C(CH_3)_3+2H]^+$, 266.1 $[MH]^+$.

Scheme 2

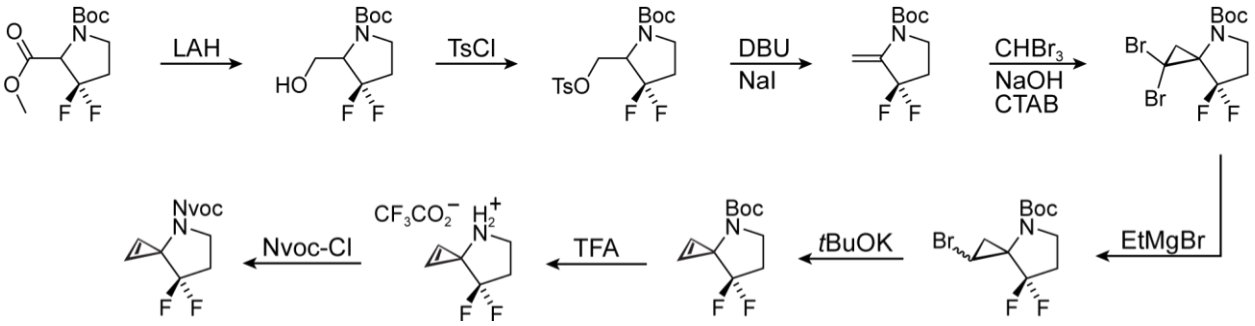

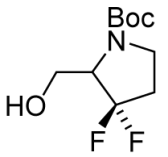

7

To a solution of 6 (540 mg, 2.03 mmol, 1 eq) in anhydrous THF (5 mL) at 0 °C was added LAH (85 mg, 2.24 mmol, 1.1 eq) in portions. The resulting suspension was stirred for 30 min at 0 °C. The reaction was quenched with ice cold water, diluted with DCM (10 mL) and separated. The organic layer was collected and the aqueous layer was further washed with DCM. The combined organic layers were washed with brine, dried over anhydrous Na_2SO_4, concentrated in vacuo, and purified by flash chromatography (11 g silica, 20% EtOAc/hexanes (v/v)) to obtain 7 as a colourless oil (474 mg, 99%). A similar reaction starting with 5.0 g of S6 produced 3.35 g of S7 (75% yield). Rf = 0.17 (20% EtOAc/hexanes, visualized w/ $KMnO_4$ stain). ^{1}H NMR (16:84 % mixture of rotamers, 400 MHz, $CDCl_3$): δ= 3.98–3.85 (m, 1.5H), 3.85 (s,1H), 3.69–3.67 (m, 1H), 3.51–3.44 (m, 1.5H), 2.57–2.22 (m, 2H), 1.44–1.43 (m, 9H). ^{13}C NMR (rotamers, 100 MHz, $CDCl_3$): δ= 155.88, 155.57, 154.23, 153.39, 128.73, 126.75, 124.72, 99.60, 99.02, 81.15, 80.92, 64.34, 64.12, 63.90, 62.73, 62.50, 61.29, 60.49, 60.05, 49.13, 48.99, 43.48, 42.87, 33.29, 33.11, 32.93, 28.47, 28.40. MS (ESI): Calcd for $C_{10}H_{17}F_2NO_3$ $[M]^+$: 237.1, found: 138.1 $[M\text{-}Boc+2H]^+$, 182.1 $[M\text{-}C(CH_3)_3+2H]^+$, 238.1 $[MH]^+$, 260.1 $[MNa]^+$.

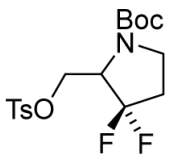

8

To a solution of 7 (5.20 g, 21.93 mmol, 1 eq) in DCM (50 mL) was added TsCl (5.01g, 26.32 mmol, 1.2 eq), Et3N (2.88 g, 28.52 mmol, 1.3 eq), and DMAP (53mg, 0.43 mmol, 0.02 equiv). The reaction mixture was then heated to 45 °C and stirred at this temperature for 16 h. The reaction mixture was diluted with water and the crude product extracted with DCM (4×30 mL). The combined organic layers were washed with brine, dried over anhydrous Na_2SO_4, concentrated in vacuo, and purified by flash chromatography (130 g silica, 10% EtOAc/hexanes (v/v)) to obtain 8 as a colourless oil (7.3 g, 85%). Rf = 0.37 (20% EtOAc/hexanes, visualized w/ UV). ^{1}H NMR (47:53 % mixture of rotamers, 500 MHz, $CDCl_3$): δ= 7.70–7.67 (m, 1H), 7.28 (d, J = 8.5 Hz, 2H), 5.14 (m, 0.34H), 4.56–4.36 (m, 1H), 4.27–4.25 (m, 0.32H), 4.11–4.04 (m, 1H), 4.00–3.93 (m, 1H), 3.87–3.75 (m, 0.39H), 3.47–3.33 (m, 1.25H), 2.36 (s, 3H), 2.36–2.21 (m, 1.30H), 1.35 (m, 9H). ^{13}C NMR (rotamers, 126 MHz, $CDCl_3$): δ= 153.93, 153.65, 153.55, 153.27, 153.10, 152.90, 151.74, 151.46, 144.98, 144.86, 144.79, 144.60, 132.58, 132.54, 132.27, 129.76, 129.70, 129.63, 127.55, 127.52, 127.50, 80.77, 80.49, 80.41, 80.09, 66.37, 66.35, 65.69, 65.67, 65.58, 65.24, 60.83, 60.59, 60.37, 58.37, 58.14, 48.78, 48.73, 48.28, 48.23, 42.77, 42.30, 3.98, 32.77, 32.34, 32.15, 31.98, 28.00, 27.91, 21.26. ^{13}C DEPT-135 NMR (rotamers, 126 MHz, $CDCl_3$): δ= (up) 129.76, 129.70, 60.97, 60.74, 60.50, 58.51, 58.28, 42.91, 42.43, 28.14, 28.05, 21.40. (down) 66.51, 66.50, 65.83, 65.79, 65.75, 48.92, 48.87, 48.42, 48.37, 33.30, 33.13, 32.95, 32.48, 32.28,32.10. HRMS (ESI): Calcd for $C_{17}H_{23}F_2NO_5S$ $[M+NH_4]^+$: 409.1603, found: 409.1602.

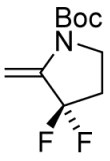

9

To a solution of 8 (1.10 g, 2.81 mmol, 1 eq) in glyme (30 mL) was added NaI (1.35 g, 9 mmol, 3 eq), and DBU (915 mg, 6 mmol, 2 eq). The reaction mixture was refluxed for 4 h, diluted with water (20 mL), and extracted with Et_2O (3×30 mL). The combined organic layers were washed with brine, dried

over anhydrous Na_2SO_4, concentrated in vacuo, and purified by flash chromatography (130 g silica, 10% EtOAc/hexanes (v/v)) to obtain x as a pale-yellow oil (0.51 g, 82.3%). We found the alkene to be unstable on silica and, therefore, used it without the flash chromatography for future production of 9. Rf = 0.88 (20% EtOAc/hexanes, visualized w/ UV). ^{1}H NMR (500 MHz, $CDCl_3$): δ= 5.56 (br s, 1H), 4.90 (s, 1H), 3.67 (t, J = 7.1 Hz, 2H), 2.31 (m, ,2H), 1.52 (s, 9H). ^{13}C NMR (126 MHz, $CDCl_3$): δ= 152.10, 140.35, 125.06, 123.14, 121.18, 92.84, 83.94, 43.79, 31.97, 31.76, 31.57, 28.40. HRMS (ESI): Calcd for $C_{10}H_{15}F_2NO_5$ $[M+H]^+$: 220.1144, found: 220.1148.

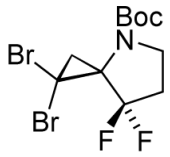

10

To a solution of 9 (2.19 g, 10.00 mmol, 1 eq) in $CHBr_3$ (1.8 mL, 5.1 g, 20.00 mmol, 2 eq) and DCM (3 mL) was added CTAB (0.364 g, 1.00 mmol, 0.1 eq) and the mixture was stirred vigorously. To this was added NaOH (18 mL, 50% w/v) dropwise. The brown-black reaction mixture was stirred for 24 h at rt. To this reaction was added additional $CHBr_3$ and CTAB based on TLC and the process was repeated until complete consumption of reactant. Complete consumption of reactant was a necessity as the product have same Rf as the reactant. Upon completion, the reaction mixture was diluted with DCM and water. The organic layer was collected, washed with brine and concentrated under reduced pressure. The crude obtained was purified by flash chromatography (120 g silica, 2.5% EtOAc/hexanes (v/v)) to obtain 10 as a light-yellow oil (2.07 g, 65%) Rf = 0.28 (2.5% EtOAc/hexanes, visualized w/ UV). ^{1}H NMR (700 MHz, $CDCl_3$): δ= 3.86 (br s, 1H), 3.59 (m, 1H), 2.51–2.45 (m, 1H), 2.40–2.32 (m, 1H), 2.27 (d, J = 9.9 Hz, 1H), 1.57–1.52 (m, 1H), 1.45 (s, 9H). ^{13}C NMR (176 MHz, $CDCl_3$): δ= 153.62, 124.93, 123.44, 122.04, 81.50, 52.66, 52.51, 52.48, 52.32, 31.74, 28.44, 22.81, 14.28. HRMS (ESI): Calcd for $C_{11}H_{15}Br_2F_2NO_2$ $[M+Na]^+$: 411.9330, found: 411.9306.

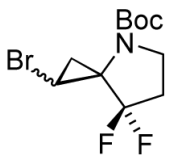

11

To an ice-cold solution of 10 (800 mg, 2 mmol, 1 eq) in anhydrous THF (6.0 mL) under N2 was added 3M EtMgBr (0.8 mL, 2.4 mmol, 1.2 eq) and $Ti(OiPr)_4$ (60 mg, 0.064 mL, 0.2 mmol, 0.1 eq) and the mixture was stirred at the same temperature for 1 hour. The reaction was quenched by ice-water and diluted with DCM. The organic layer was collected and the aqueous layer was further washed with DCM. The combined organic layers were dried over anhydrous Na_2SO_4, concentrated in vacuo, and purified by flash chromatography (120 g silica, 2.5% EtOAc/hexanes (v/v)) to give crude 11 as a mixture of diastereomers which was used for the next step without further purification. Rf = 0.50 (5% EtOAc/hexanes, visualized w/ UV). ^{1}H NMR (500 MHz, $CDCl_3$): δ= 3.89 (br s, 1H), 3.62 (t, J = 7.4 Hz, 0.56H), 3.55 (td, J = 10.5, 4.5 Hz, 0.78H), 3.21 (m, 0.65H), 2.50–2.39 (m, 0.82H), 2.37–2.21 (m, 1.53H), 1.75 (t, J = 8.8 Hz, 0.79H), 1.54 (2×s, 1.16 H), 1.46 (2×s, 9H). MS (ESI): Calcd for $C_{11}H_{16}BrF_2NO_2$ [M]+: 311.0, found: 256.0 $[M\text{-}C(CH_3)_3+2H]^+$, 258.1 $[M+2\text{-}C(CH_3)_3+2H]^+$, 312.0 $[MH]^+$, 314.0 $[M+2+H]^+$.

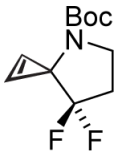

12

The crude 11 (amount) was dissolved in anhydrous THF (5.0 mL) and cooled down to 0 °C. To this solution was added KOtBu (0.72 mmol, 88mg, 1.2eq) at 0 °C and the reaction was stirred at the same temperature for 1 h. The reaction was quenched with water and diluted with DCM. The organic layer was collected and the aqueous layer was further washed with DCM. The combined organic layers were dried over anhydrous Na_2SO_4, concentrated in vacuo, and purified by flash chromatography (100 g silica, 20% EtOAc/hexanes(v/v)) to obtain pure12 as a pale-yellow oil (140 mg, 30% combine 2 step). Rf = 0.23 (5% EtOAc/hexanes, visualized w/ $KMnO_4$). ^{1}H NMR (500 MHz, $CDCl_3$): δ= 7.28 (br s, 2H), 3.56 (t, J = 6.0 Hz), 2.35 (m, 2H), 1.40 (s, 9H). ^{13}C NMR (126 MHz, $CDCl_3$): δ= 154.20, 126.57, 124.63, 122.68, 111.59, 80.12, 47.82, 47.55, 47.27,

41.02, 32.14, 31.95, 31.75, 28.59. HRMS (ESI): Calcd for $C_{11}H_{15}F_2NO_2$ $[M+Na]^+$: 411.9330, found: 411.9306.

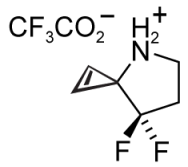

13

To a solution of 12 (40 mg, 0.17 mmol) in DCM (2.0 mL) at 0 °C was added TFA (0.4 mL). After stirring the reaction at the same temperature for 1 h, it was concentrated in vacuo (<25 °C) to obtain pure 13 as a TFA salt (41 mg, %). ^{1}H NMR (700 MHz, CD_3OD): δ= 7.79 (s, 2H), 3.53 (t, J = 4.3 Hz, 2H), 2.69 (m, 2H). ^{13}C NMR (176 MHz, CD_3OD): δ= 161.45, 161.24, 161.02, 160.81, 125.70, 124.31, 122.92, 119.69, 118.04, 116.41, 114.77, 108.98, 54.81, 40.84, 40.82, 40.79, 34.17, 34.02, 33.88, 28.67. HRMS (ESI): Calcd for $C_6H_7F_2N$ $[M+Na]^+$: 411.9330, found: 411.9306.

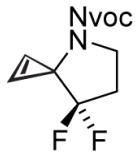

14

T o a solution of 13 (17 mg, 0.07 mmol, 1eq) in CHCl3/ Et2O (2 mL, 9:1 v/v) at 0 °C was added $NaHCO_3$ (13.4 mg, 0.16mmol, 2.3 eq) and 4,5-Dimethoxy-2-nitrobenzyl chloroformate (23.15 mg, 0.08 mmol, 1.2 eq) respectively. The reaction was allowed to warm to rt and stirred for 15 h. It was then diluted with DCM and water. The organic layer was collected and the aqueous layer was further washed with DCM. The combined organic layers were dried over anhydrous Na_2SO_4, concentrated in vacuo, and purified by flash chromatography to give crude S14 (100 g silica, 20% EtOAc/hexanes(v/v)). It was further purified by HPLC .^{1}H NMR (700 MHz, $CDCl_3$): δ= 7.68 (s, 1H), 7.32 (s, 2H), 6.93 (s, 1H), 5.45 (s, 2H), 3.97 (s, 3H), 3.95 (s, 3H), 3.67 (t, J = 6.0 Hz, 2H), 2.41 (m, 2H). ^{13}C NMR (176 MHz, $CDCl_3$): δ= 153.44, 148.39, 140.29, 127.51, 111.45, 110.90, 108.40, 63.74, 56.56, 53.57, 41.21, 32.11, 31.92, 31.74, 29.58, 29.50, 29.39, 29.22. HRMS (ESI): Calcd for $C_{16}H_{16}F_2N_2O_6$ $[M]^+$: 377.0976, found: 411.9306.

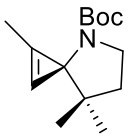

15

To a solution of LiHDMS (200 µL, 1M in THF,9.2 mmol, 1.5 eq) in 1 ml dry THF was add 12 (30 mg, 0.12 mmol, 1 eq) under N_2 at – 30°C. After 5 min, 13 µL Me_2SO_4 (1.05 eq) was added to the solution. After 30 min, the reaction was quenched with water and diluted with DCM. The organic layer was collected and the aqueous layer was further washed with DCM. The combined organic layers were dried over anhydrous Na_2SO_4, concentrated in vacuo, and purified by flash chromatography. (8 g silica, 3% EtOAc/hexanes(v/v)) to obtain 16 20 mg (60 %).

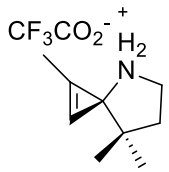

16

To a solution of 15 (40 mg, 0.17 mmol) in DCM (2.0 mL) at 0 °C was added TFA (0.4 mL). After stirring the reaction at the same temperature for 1 h, it was concentrated in vacuo (<25 °C) to obtain pure 16 as a TFA salt. ^{1}H NMR (500 MHz, Methanol-d4): δ= 7.19 (dp, J = 3.2, 1.1 Hz, 1H), 3.52 (t, J = 7.5 Hz, 2H), 2.67 (ttd, J = 12.7, 7.4, 1.5 Hz, 2H), 2.29 (d, J = 1.1 Hz, 3H) . ^{13}C NMR (126 MHz, CD_3OD): δ= 118.35, 118.31, 118.28, 100.47, 100.44, 100.43, 100.40, 40.80, 40.77, 40.74, 34.42, 34.22, 34.01, 8.65. Peaks for two quaternary carbons (CO and CF_2) and TFA were not observed. HRMS (ESI): Calcd for $C_7H_9F_2N$ $[M+H]^+$:146.0776, found: 1

NMRs for the molecules synthesized in chapter II

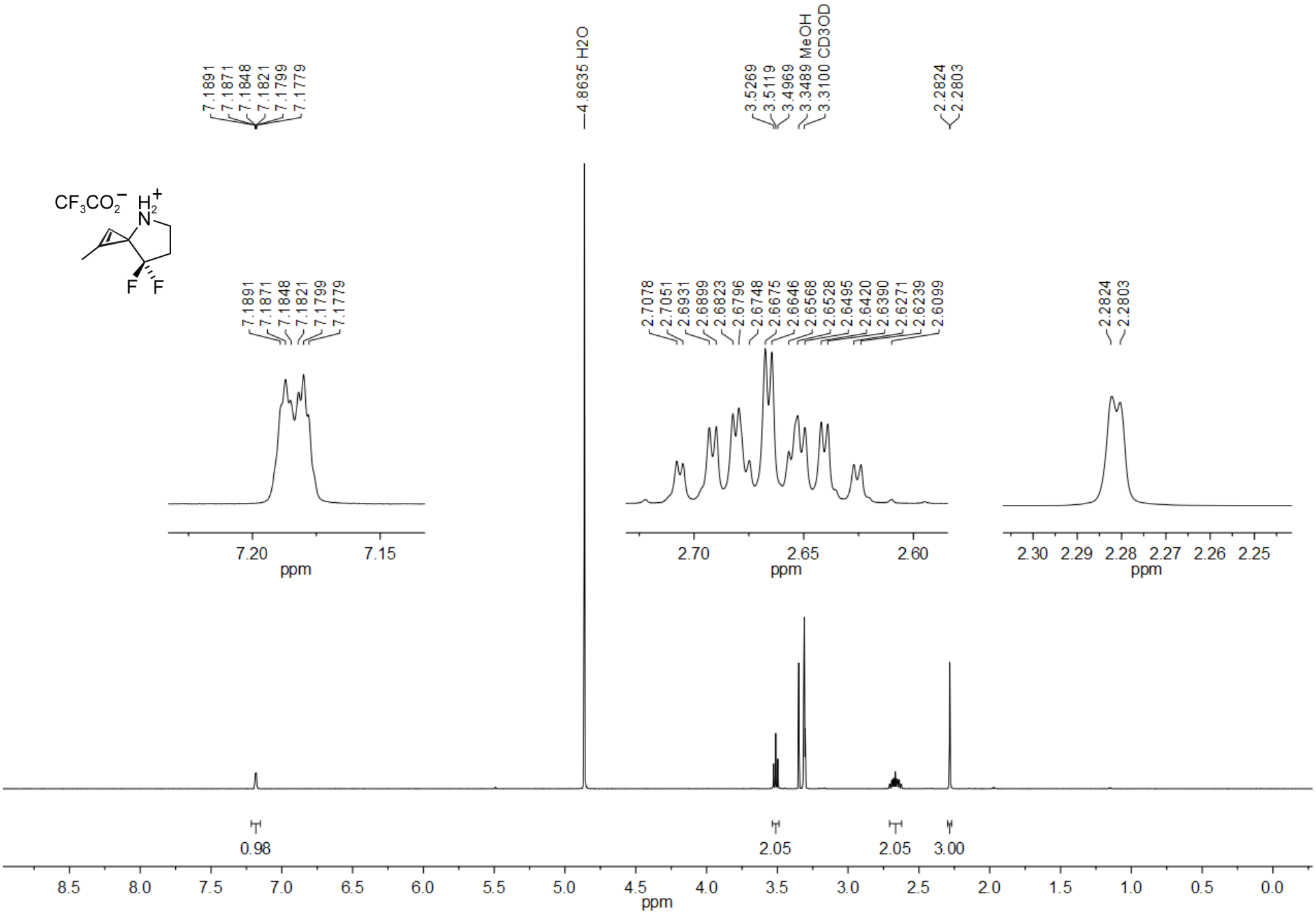

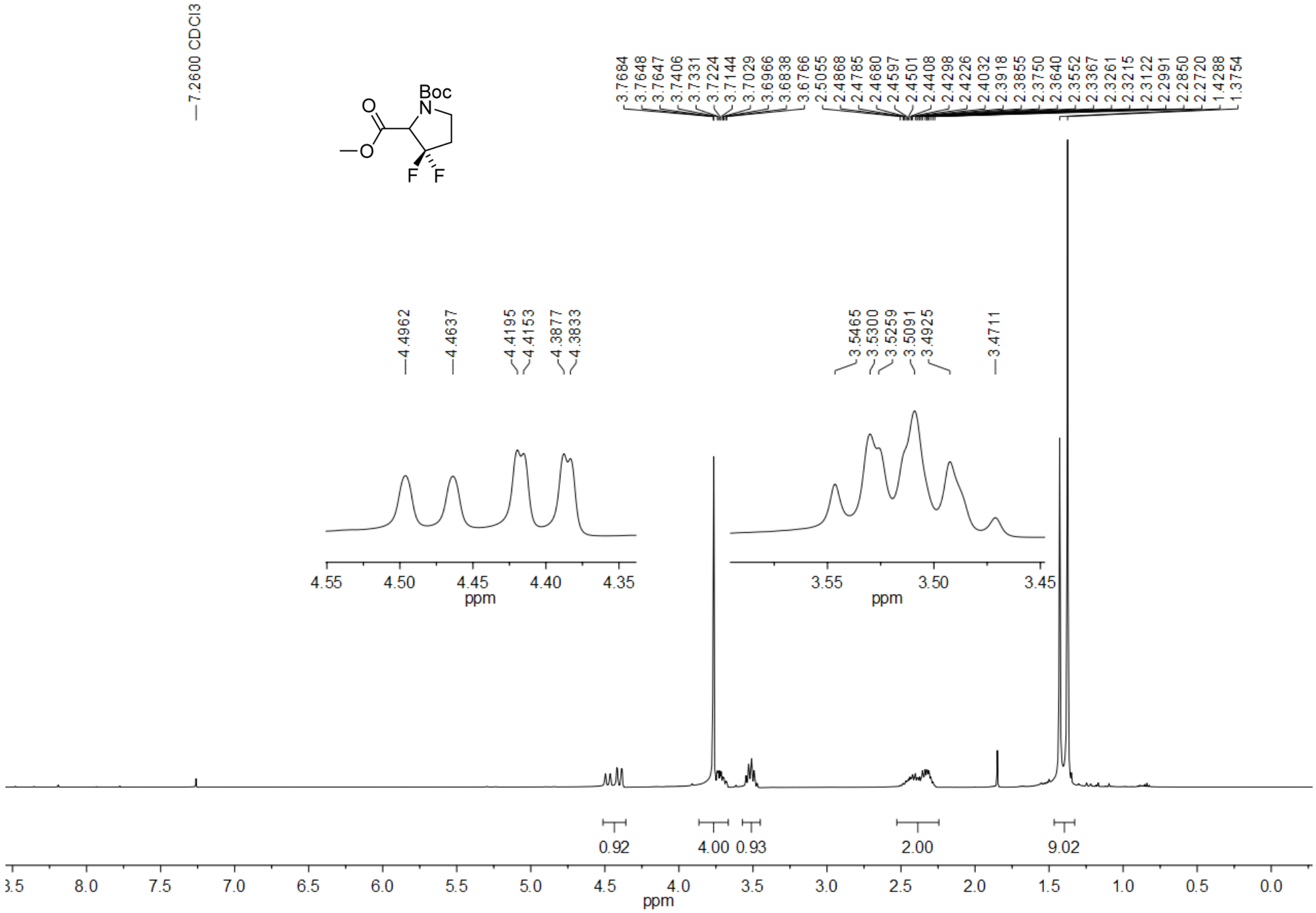
7.2600 CDCl3
Boc
N
O
O
F
F
3.7684
3.7648
3.7647
3.7406
3.7331
3.7224
3.7144
3.7029
3.6966
3.6838
3.6766
2.5055
2.4868
2.4785
2.4680
2.4597
2.4501
2.4408
2.4298
2.4226
2.4032
2.3918
2.3855
2.3750
2.3640
2.3552
2.3367
2.3261
2.3215
2.3122
2.2991
2.2850
2.2720
1.4288
1.3754
4.4962
4.4637
4.4195
4.4153
4.3877
4.3833
3.5465
3.5300
3.5259
3.5091
3.4925
3.4711
4.55
4.50
4.45
4.40
4.35
ppm
3.55
3.50
3.45
ppm
0.92
4.00
0.93
2.00
9.02
8.0
7.5
7.0
6.5
6.0
5.5
5.0
4.5
4.0
3.5
3.0
2.5
2.0
1.5
1.0
0.5
0.0
ppm

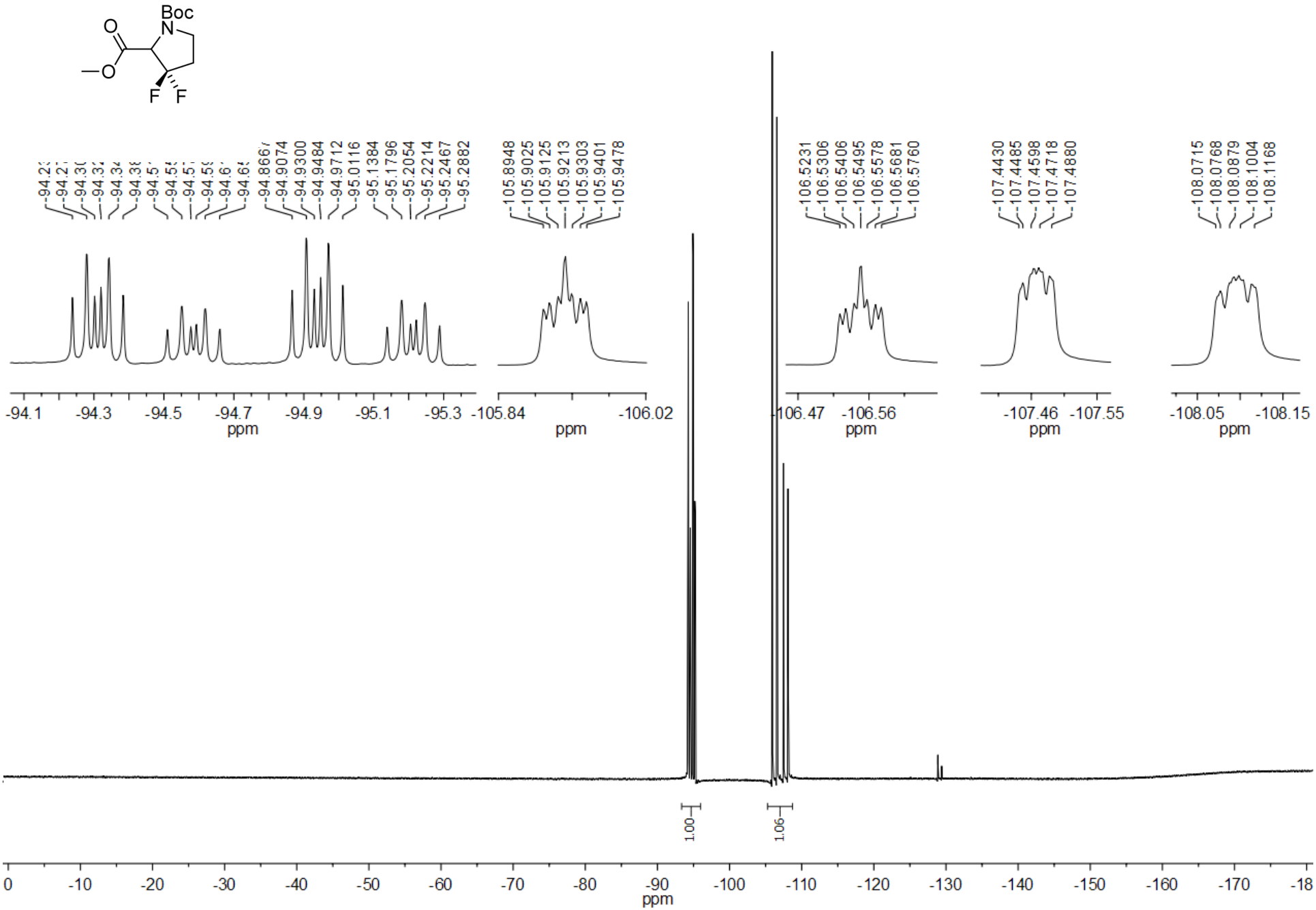
Boc
O
N
O
F
F
-94.866
-94.907
-94.930
-94.948
-94.971
-95.012
-95.138
-95.180
-95.205
-95.221
-95.247
-95.288
-105.895
-105.903
-105.921
-105.930
-105.940
-105.948
-106.523
-106.531
-106.540
-106.549
-106.558
-106.568
-106.576
-107.443
-107.448
-107.460
-107.472
-107.488
-108.072
-108.077
-108.088
-108.100
-108.117
-94.1
-94.3
-94.5
-94.7
-94.9
-95.1
-95.3
ppm
-105.84
-106.02
ppm
-106.47
-106.56
ppm
-107.46
-107.55
ppm
-108.05
-108.15
ppm
1.00
1.06
0
-10
-20
-30
-40
-50
-60
-70
-80
-90
-100
-110
-120
-130
-140
-150
-160
-170
-18
ppm

^{19}F CPD NMR (376 MHz)

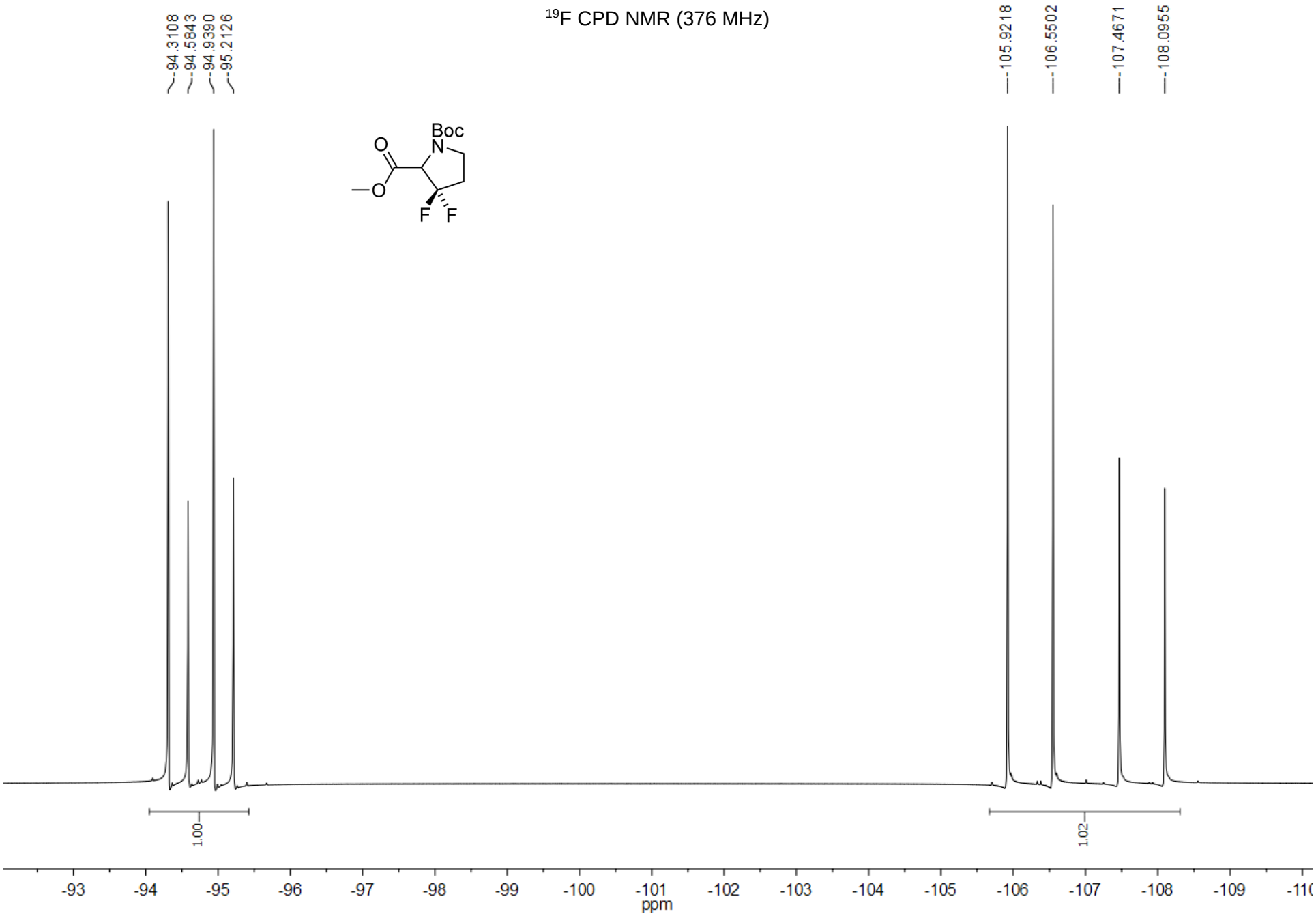

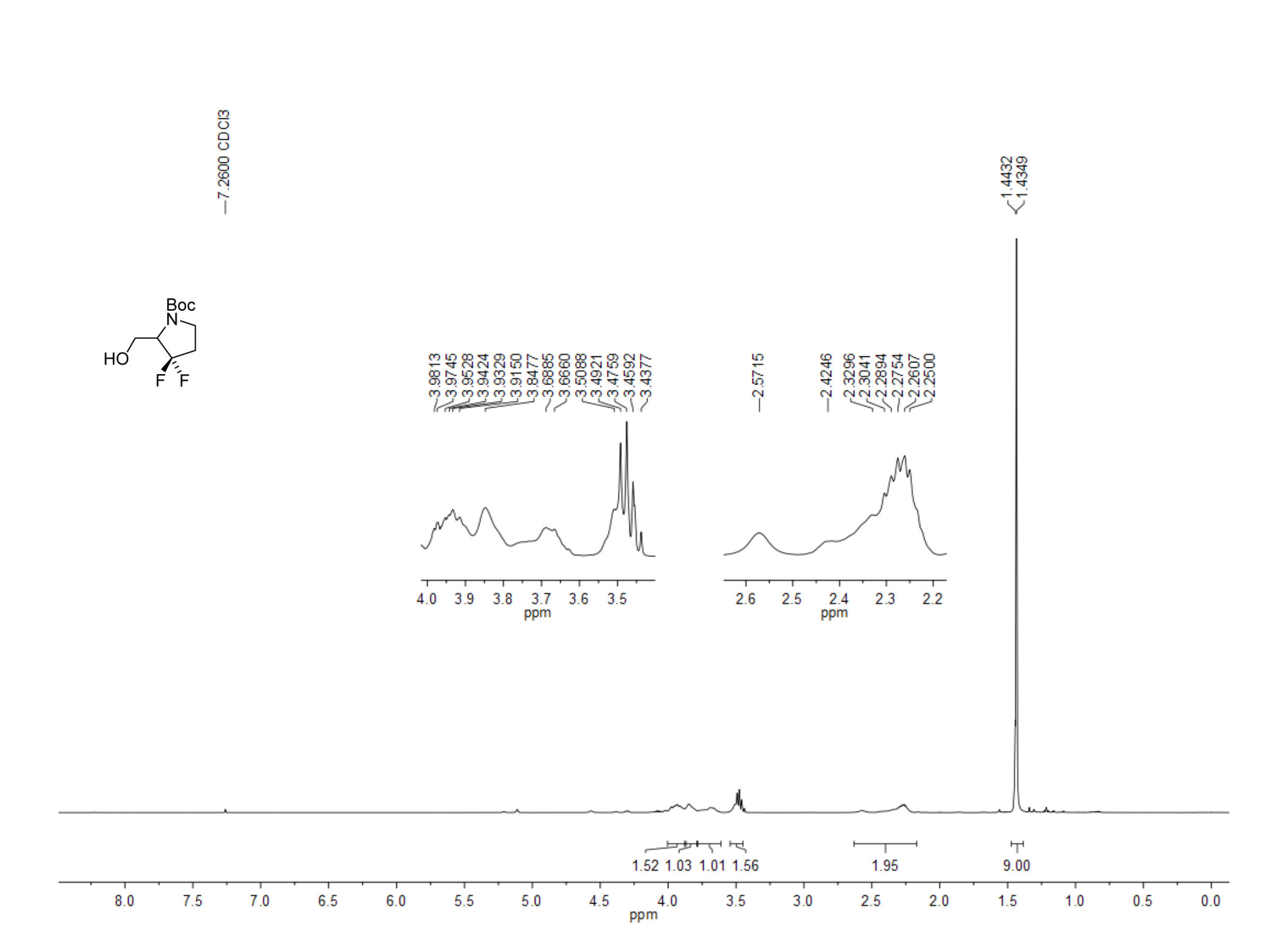
7.2600 CDCl3
1.4432
1.4349
Boc
N
HO
F
F
3.9813
3.9745
3.9528
3.9424
3.9329
3.9150
3.8477
3.6885
3.6660
3.5088
3.4921
3.4759
3.4592
3.4377
2.5715
2.4246
2.3296
2.3041
2.2894
2.2754
2.2607
2.2500
4.0 3.9 3.8 3.7 3.6 3.5
ppm
2.6 2.5 2.4 2.3 2.2
ppm
1.52 1.03 1.01 1.56
1.95
9.00
8.0 7.5 7.0 6.5 6.0 5.5 5.0 4.5 4.0 3.5 3.0 2.5 2.0 1.5 1.0 0.5 0.0
ppm

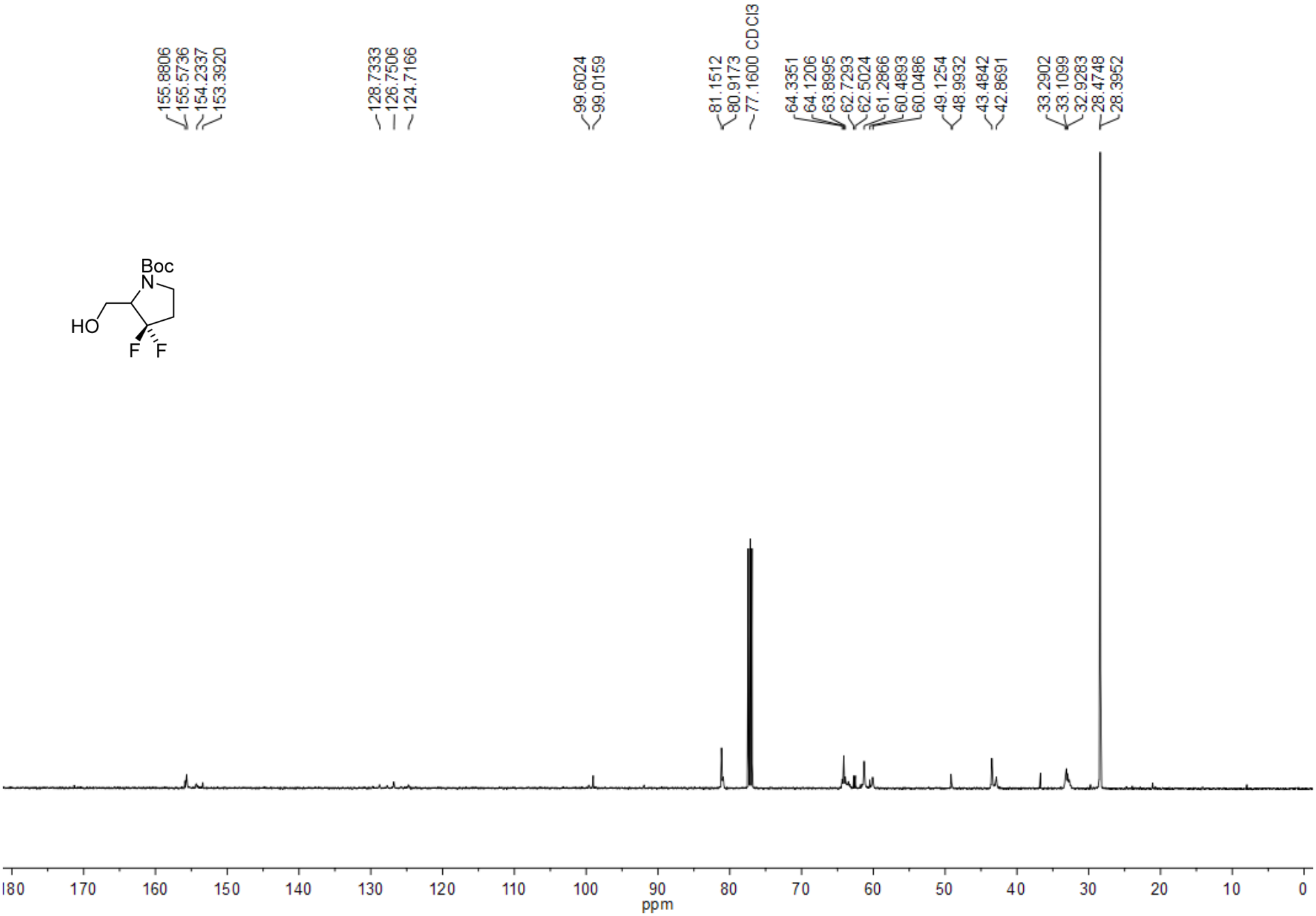
155.8806
155.5736
154.2337
153.3920
128.7333
126.7506
124.7166
99.6024
99.0159
81.1512
80.9173
77.1600 CDCl3
64.3351
64.1206
63.8995
62.7293
62.5024
61.2866
60.4893
60.0486
49.1254
48.9932
43.4842
42.8691
33.2902
33.1099
32.9283
28.4748
28.3952
Boc
N
HO
F
F
180
170
160
150
140
130
120
110
100
90
80
70
60
50
40
30
20
10
0
ppm

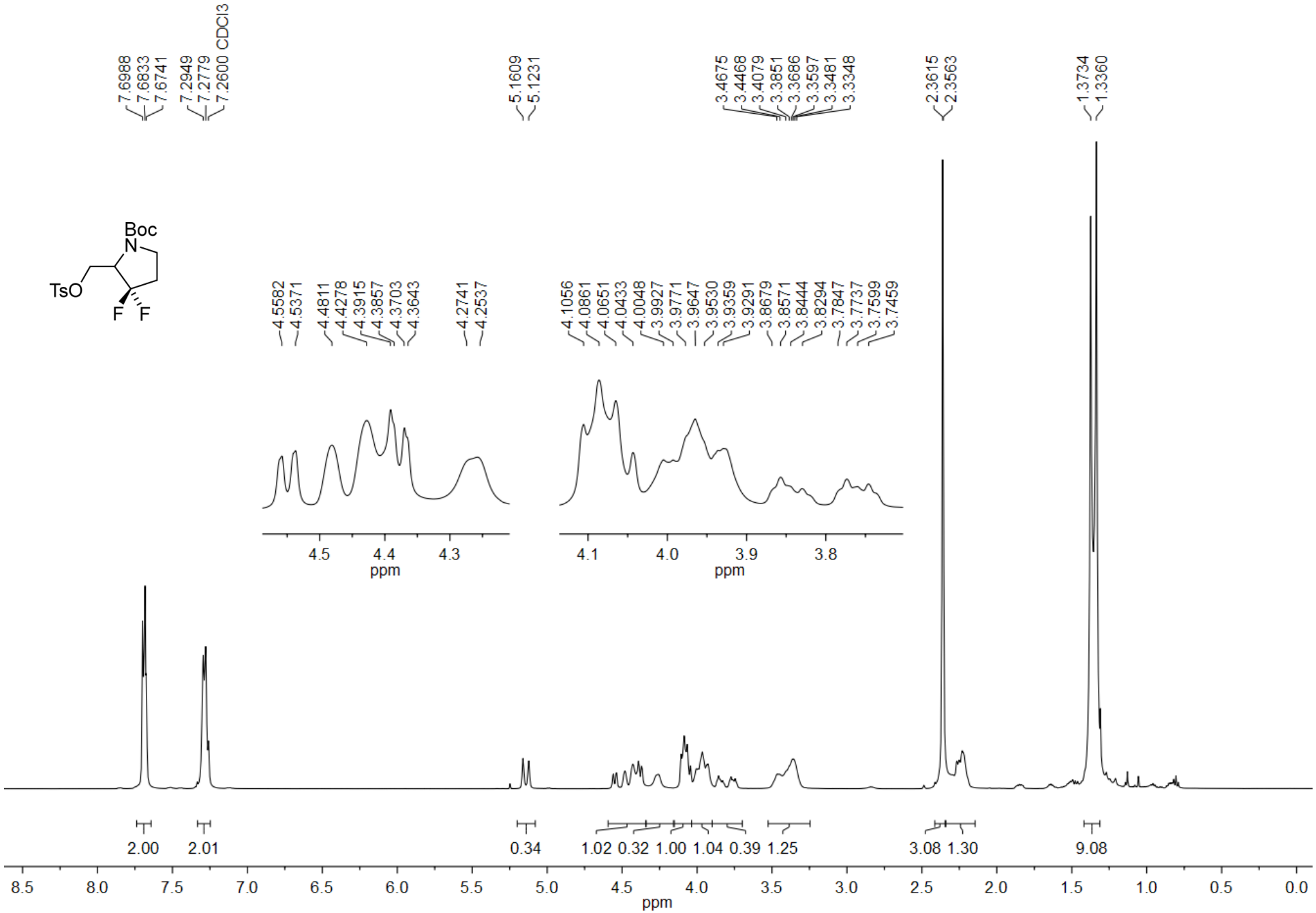
7.6988
7.6833
7.6741
7.2949
7.2779
7.2600 CDCl3
5.1609
5.1231
3.4675
3.4468
3.4079
3.3851
3.3686
3.3597
3.3481
3.3348
2.3615
2.3563
1.3734
1.3360
Boc
N
TsO
F
F
4.5582
4.5371
4.4811
4.4278
4.3915
4.3857
4.3703
4.3643
4.2741
4.2537
4.1056
4.0861
4.0651
4.0433
4.0048
3.9927
3.9771
3.9647
3.9530
3.9359
3.9291
3.8679
3.8571
3.8444
3.8294
3.7847
3.7737
3.7599
3.7459
4.5
4.4
4.3
ppm
4.1
4.0
3.9
3.8
ppm
2.00
2.01
0.34
1.02
0.32
1.00
1.04
0.39
1.25
3.08
1.30
9.08
8.5
8.0
7.5
7.0
6.5
6.0
5.5
5.0
4.5
4.0
3.5
3.0
2.5
2.0
1.5
1.0
0.5
0.0
ppm

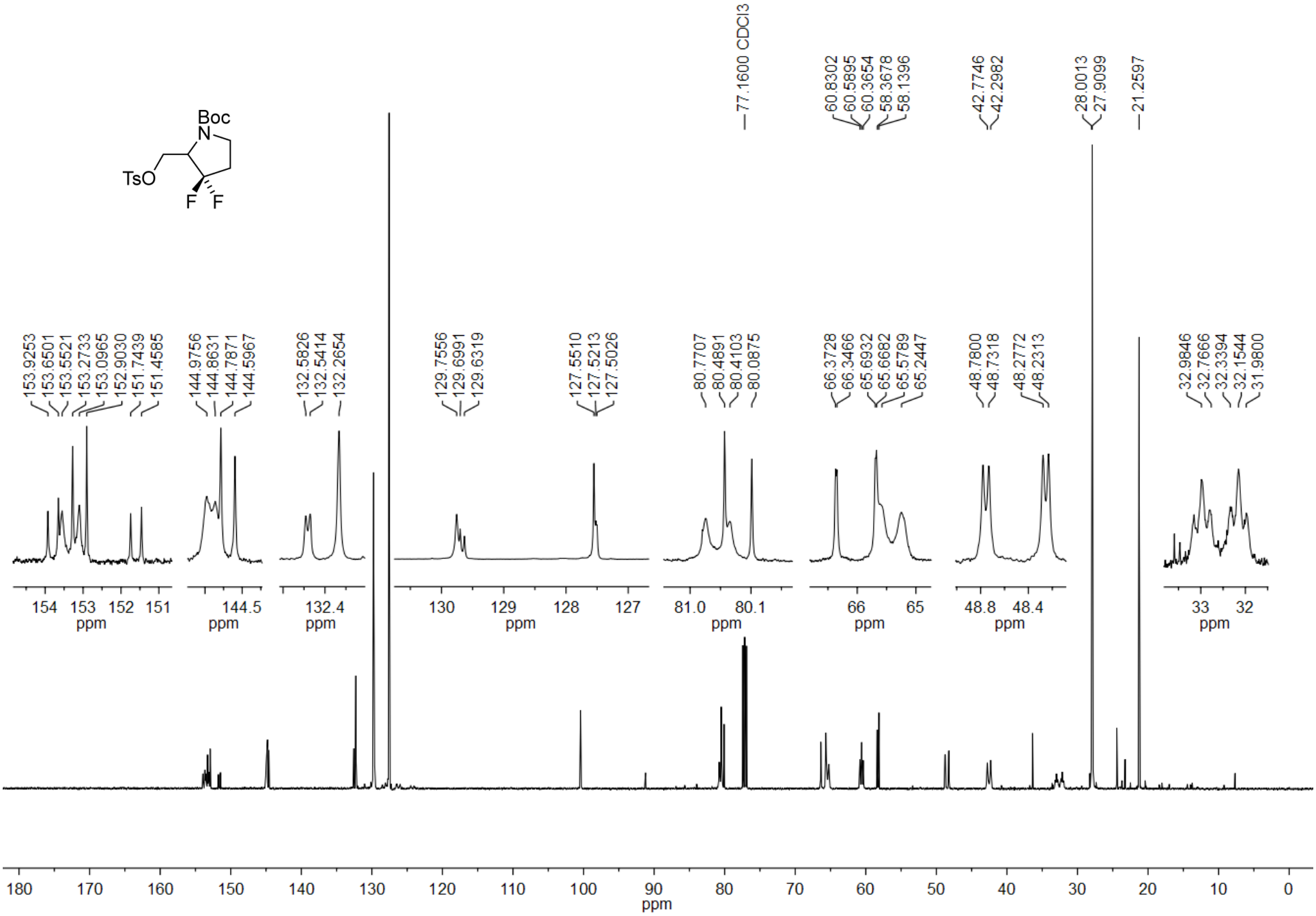
Boc
N
TsO
F
F
77.1600 CDCl3
60.8302
60.5895
60.3654
58.3678
58.1396
42.7746
42.2982
28.0013
27.9099
21.2597
153.9253
153.6501
153.5521
153.2733
153.0965
152.9030
151.7439
151.4585
144.9756
144.8631
144.7871
144.5967
132.5826
132.5414
132.2654
129.7556
129.6991
129.6319
127.5510
127.5213
127.5026
80.7707
80.4891
80.4103
80.0875
66.3728
66.3466
65.6932
65.6682
65.5789
65.2447
48.7800
48.7318
48.2772
48.2313
32.9846
32.7666
32.3394
32.1544
31.9800
154 153 152 151
ppm
144.5
ppm
132.4
ppm
130 129 128 127
ppm
81.0 80.1
ppm
66 65
ppm
48.8 48.4
ppm
33 32
ppm
180 170 160 150 140 130 120 110 100 90 80 70 60 50 40 30 20 10 0
ppm

DEPT-135 ^{13}C NMR (500 MHz)

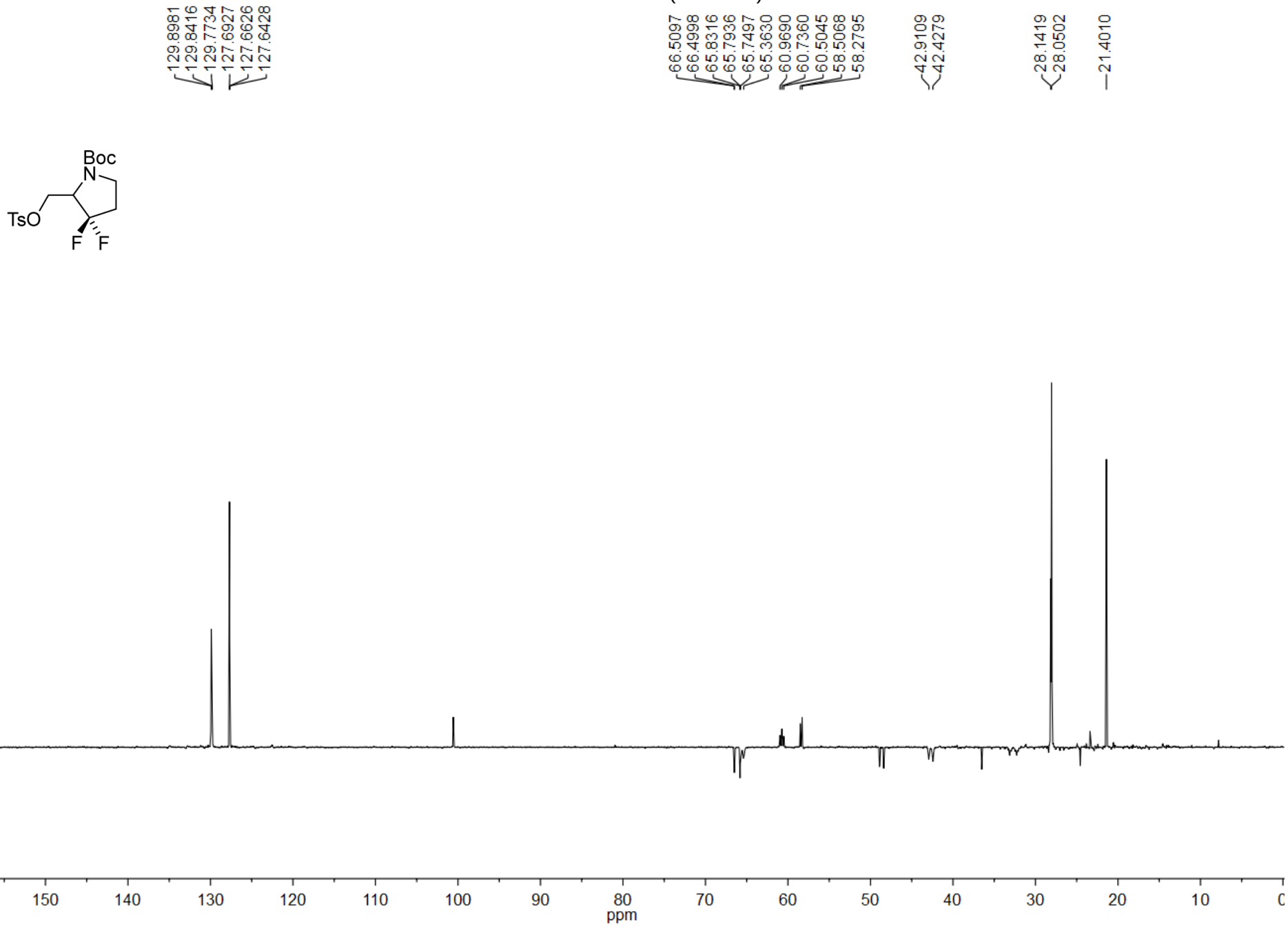

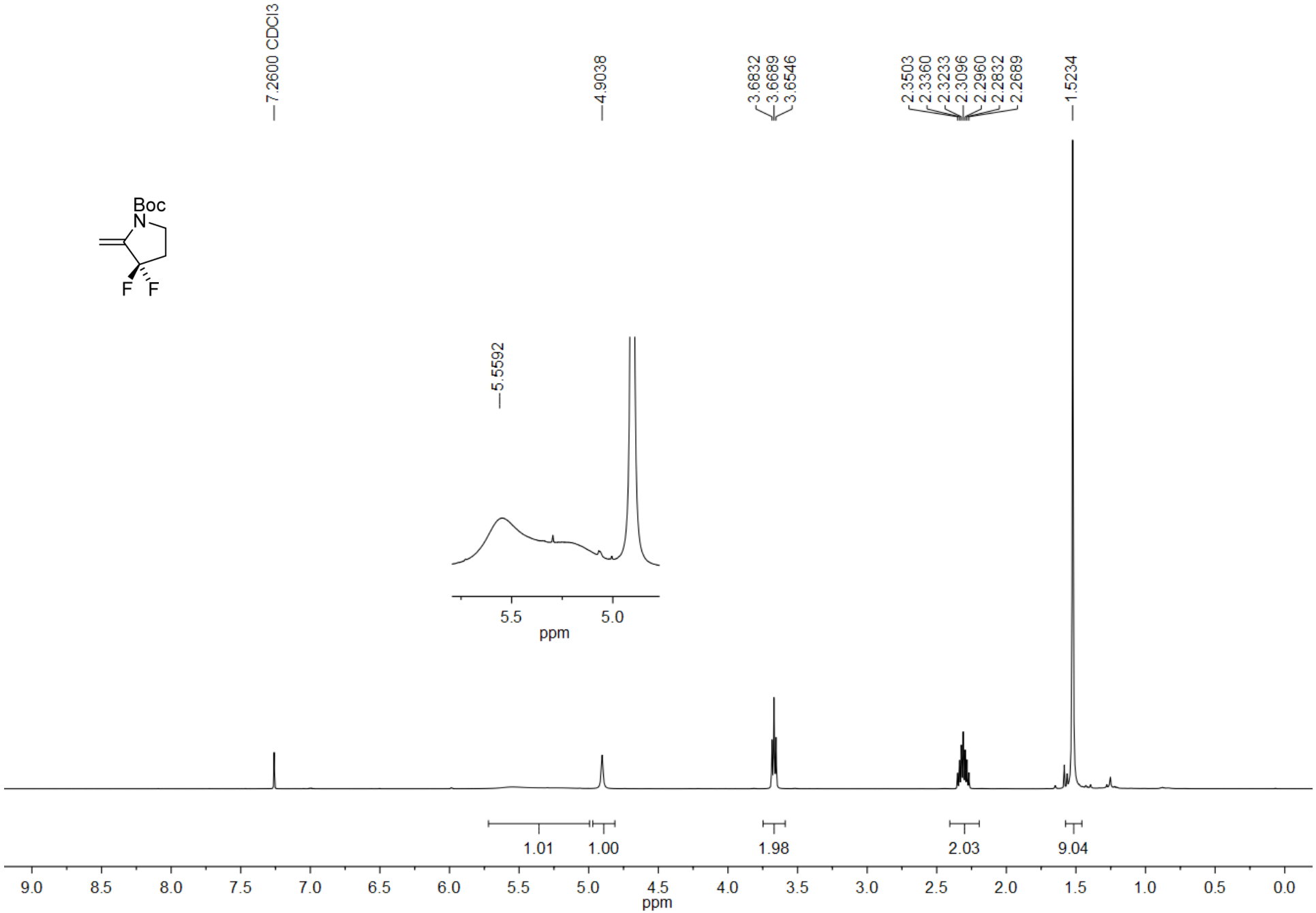
7.2600 CDCl3
4.9038
3.6832
3.6689
3.6546
2.3503
2.3360
2.3233
2.3096
2.2960
2.2832
2.2689
1.5234
Boc
N
F
F
5.5592
5.5
5.0
ppm
1.01
1.00
1.98
2.03
9.04
9.0
8.5
8.0
7.5
7.0
6.5
6.0
5.5
5.0
4.5
4.0
3.5
3.0
2.5
2.0
1.5
1.0
0.5
0.0
ppm

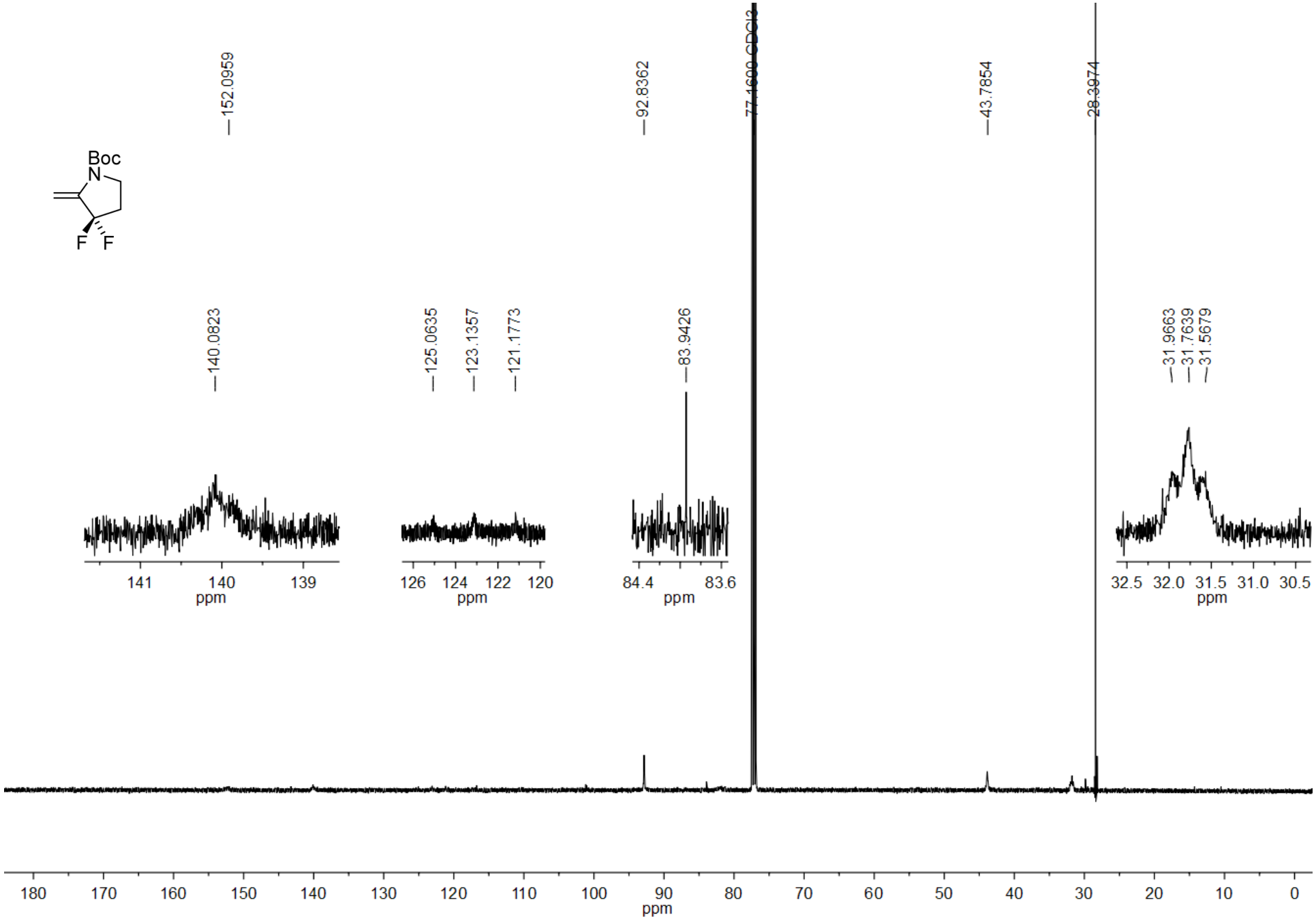
Boc
N
F
F
152.0959
140.0823
125.0635
123.1357
121.1773
92.8362
83.9426
77.4690 CDCl3
43.7854
28.3974
31.9663
31.7639
31.5679
141
140
139
ppm
126
124
122
120
ppm
84.4
83.6
ppm
32.5
32.0
31.5
31.0
30.5
ppm
180
170
160
150
140
130
120
110
100
90
80
70
60
50
40
30
20
10
0
ppm

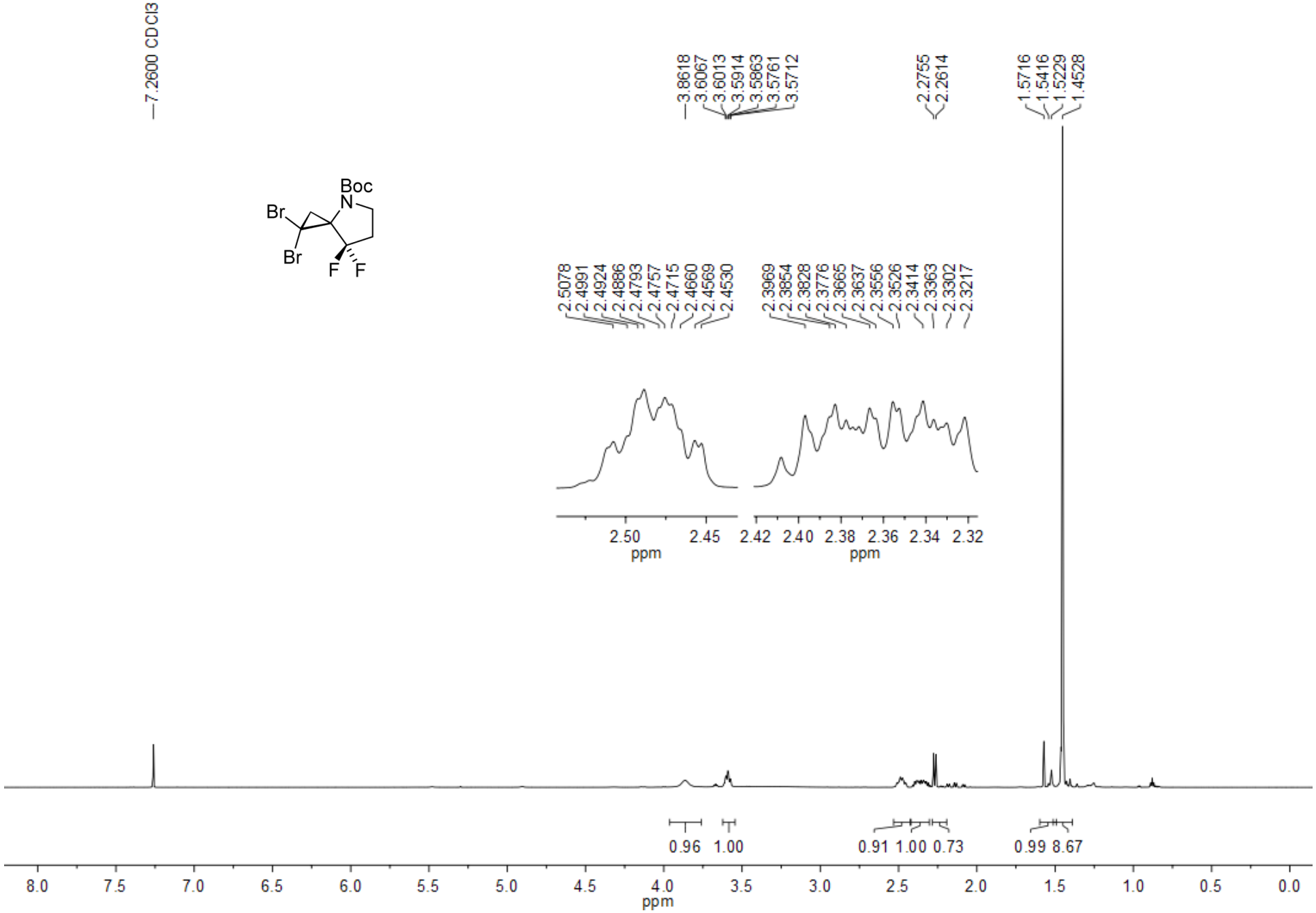
7.2600 CDCl3
3.8618
3.6067
3.6013
3.5914
3.5863
3.5761
3.5712
2.2755
2.2614
1.5716
1.5416
1.5229
1.4528
Boc
N
Br
Br
F
F
2.5078
2.4991
2.4924
2.4886
2.4793
2.4757
2.4715
2.4660
2.4569
2.4530
2.3969
2.3854
2.3828
2.3776
2.3665
2.3637
2.3556
2.3526
2.3414
2.3363
2.3302
2.3217
2.50
2.45
ppm
2.42
2.40
2.38
2.36
2.34
2.32
ppm
0.96
1.00
0.91
1.00
0.73
0.99
8.67
8.0
7.5
7.0
6.5
6.0
5.5
5.0
4.5
4.0
ppm
3.5
3.0
2.5
2.0
1.5
1.0
0.5
0.0

have carbon

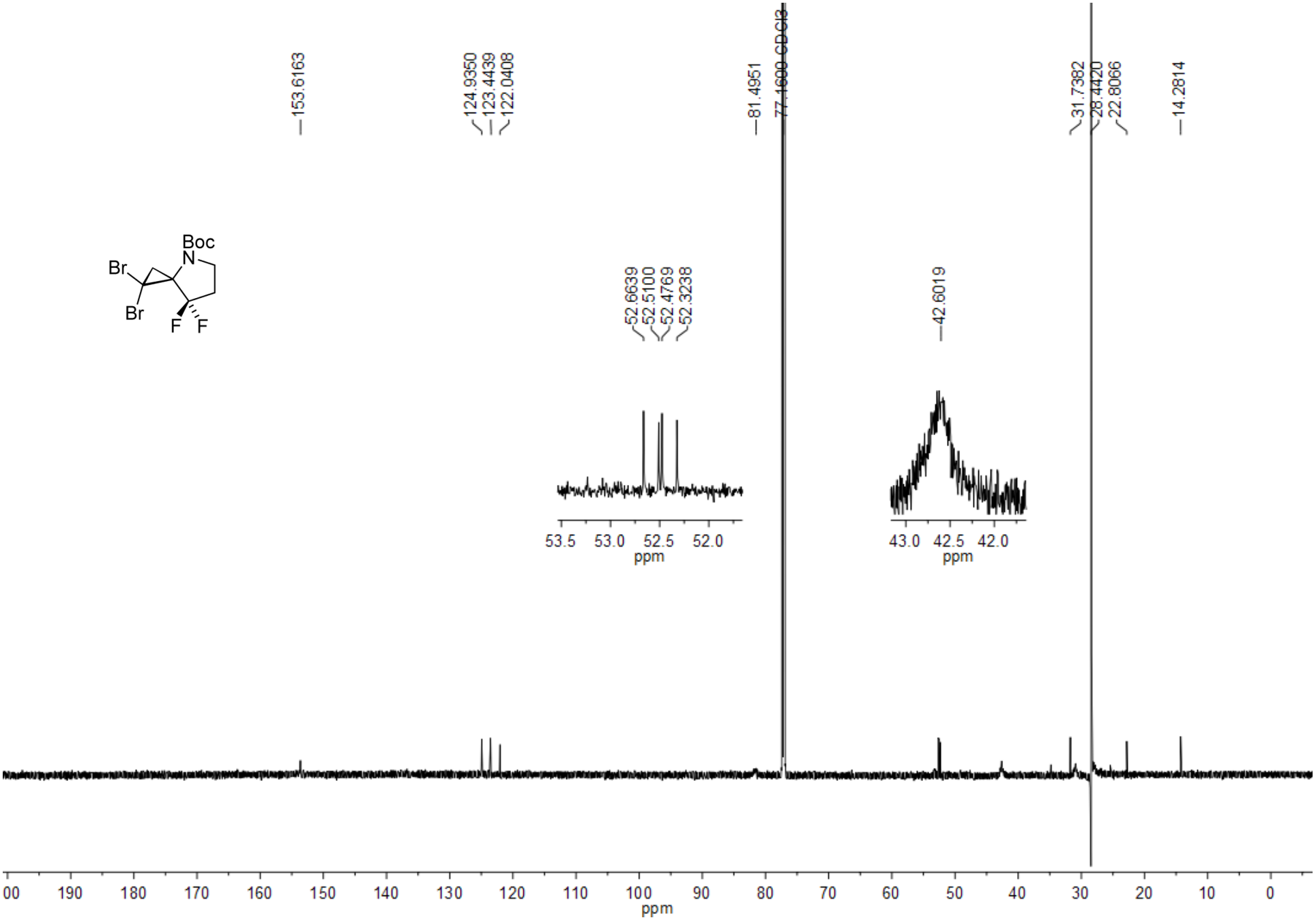
153.6163
124.9350
123.4439
122.0408
81.4951
77.1600 CDCl3
31.7382
28.4420
22.8066
14.2814
52.6639
52.5100
52.4769
52.3238
42.6019
Boc
N
Br
Br
F
F
53.5 53.0 52.5 52.0
ppm
43.0 42.5 42.0
ppm
00 190 180 170 160 150 140 130 120 110 100 90 80 70 60 50 40 30 20 10 0
ppm

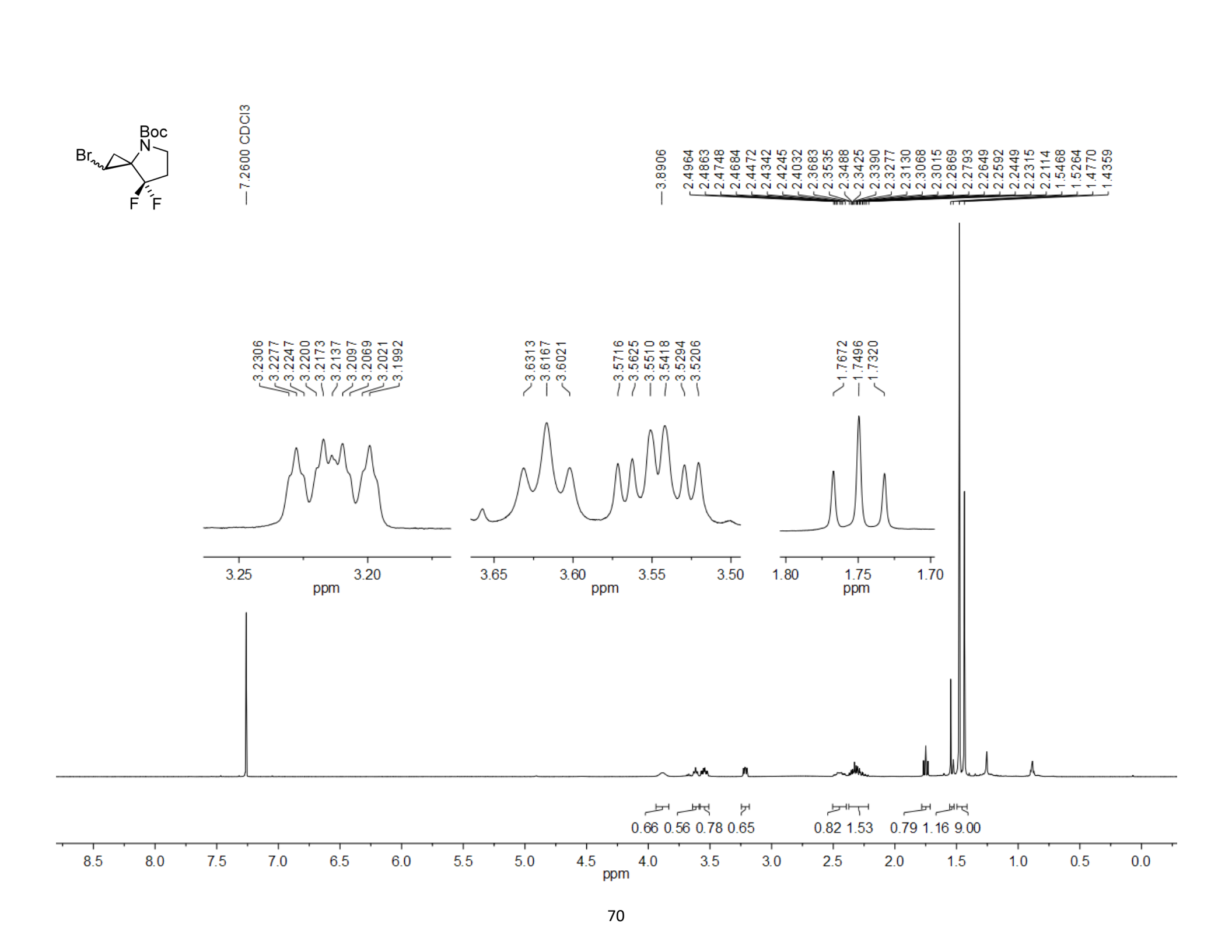
Boc
N
Br
F
F
7.2600 CDCl3
3.8906
2.4964
2.4863
2.4748
2.4684
2.4472
2.4342
2.4245
2.4032
2.3683
2.3535
2.3488
2.3425
2.3390
2.3277
2.3130
2.3068
2.3015
2.2869
2.2793
2.2649
2.2592
2.2449
2.2315
2.2114
1.5468
1.5264
1.4770
1.4359
3.2306
3.2277
3.2247
3.2200
3.2173
3.2137
3.2097
3.2069
3.2021
3.1992
3.6313
3.6167
3.6021
3.5716
3.5625
3.5510
3.5418
3.5294
3.5206
1.7672
1.7496
1.7320
3.25
3.20
3.65
3.60
3.55
3.50
1.80
1.75
1.70
ppm
0.66 0.56 0.78 0.65
0.82 1.53
0.79 1.16 9.00
8.5
8.0
7.5
7.0
6.5
6.0
5.5
5.0
4.5
4.0
3.5
3.0
2.5
2.0
1.5
1.0
0.5
0.0
ppm

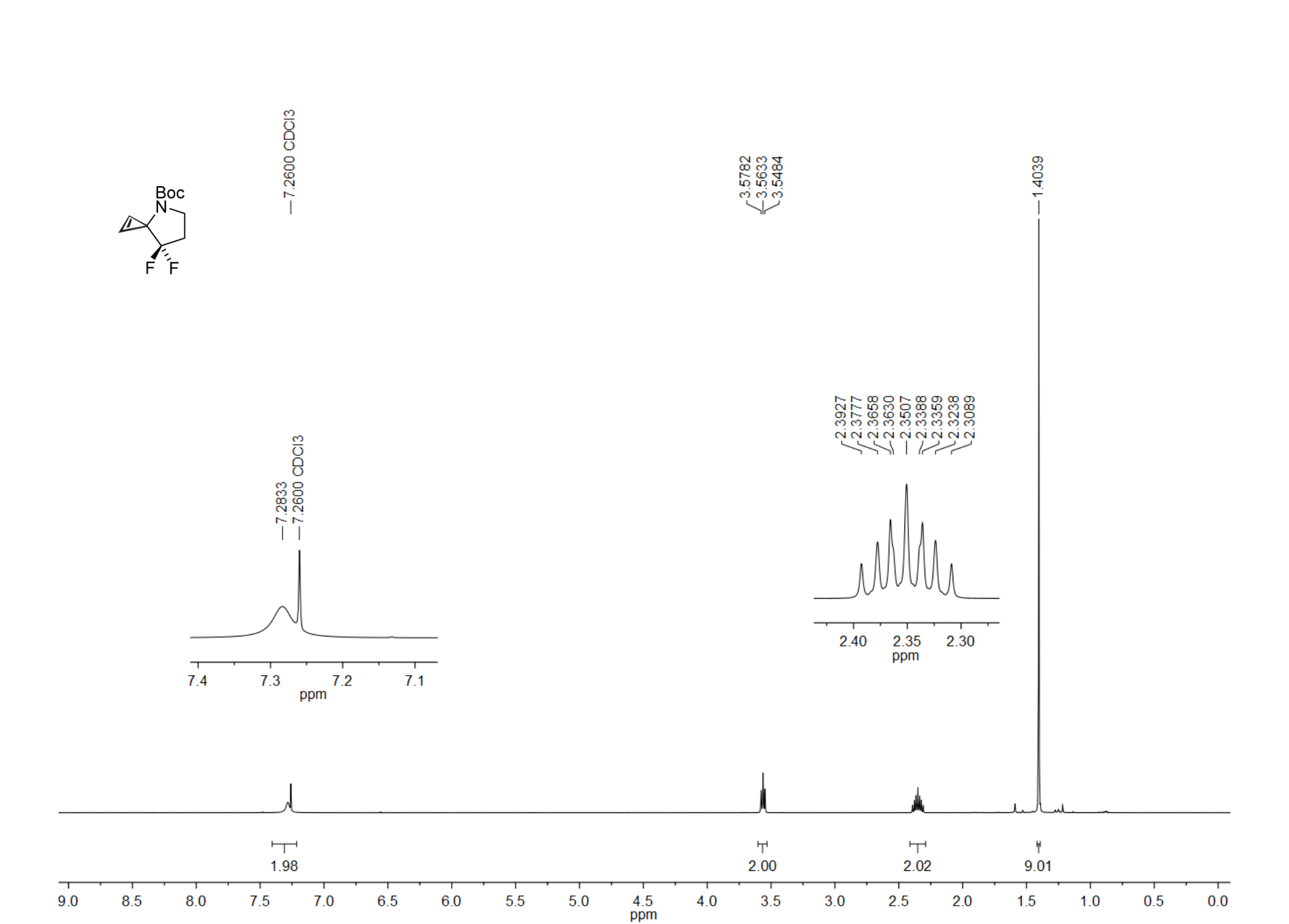
Boc
N
F
F
7.2600 CDCl3
3.5782
3.5633
3.5484
1.4039
2.3927
2.3777
2.3658
2.3630
2.3507
2.3388
2.3359
2.3238
2.3089
7.2833
7.2600 CDCl3
7.4
7.3
7.2
7.1
ppm
2.40
2.35
2.30
ppm
1.98
2.00
2.02
9.01
9.0
8.5
8.0
7.5
7.0
6.5
6.0
5.5
5.0
4.5
4.0
3.5
3.0
2.5
2.0
1.5
1.0
0.5
0.0
ppm

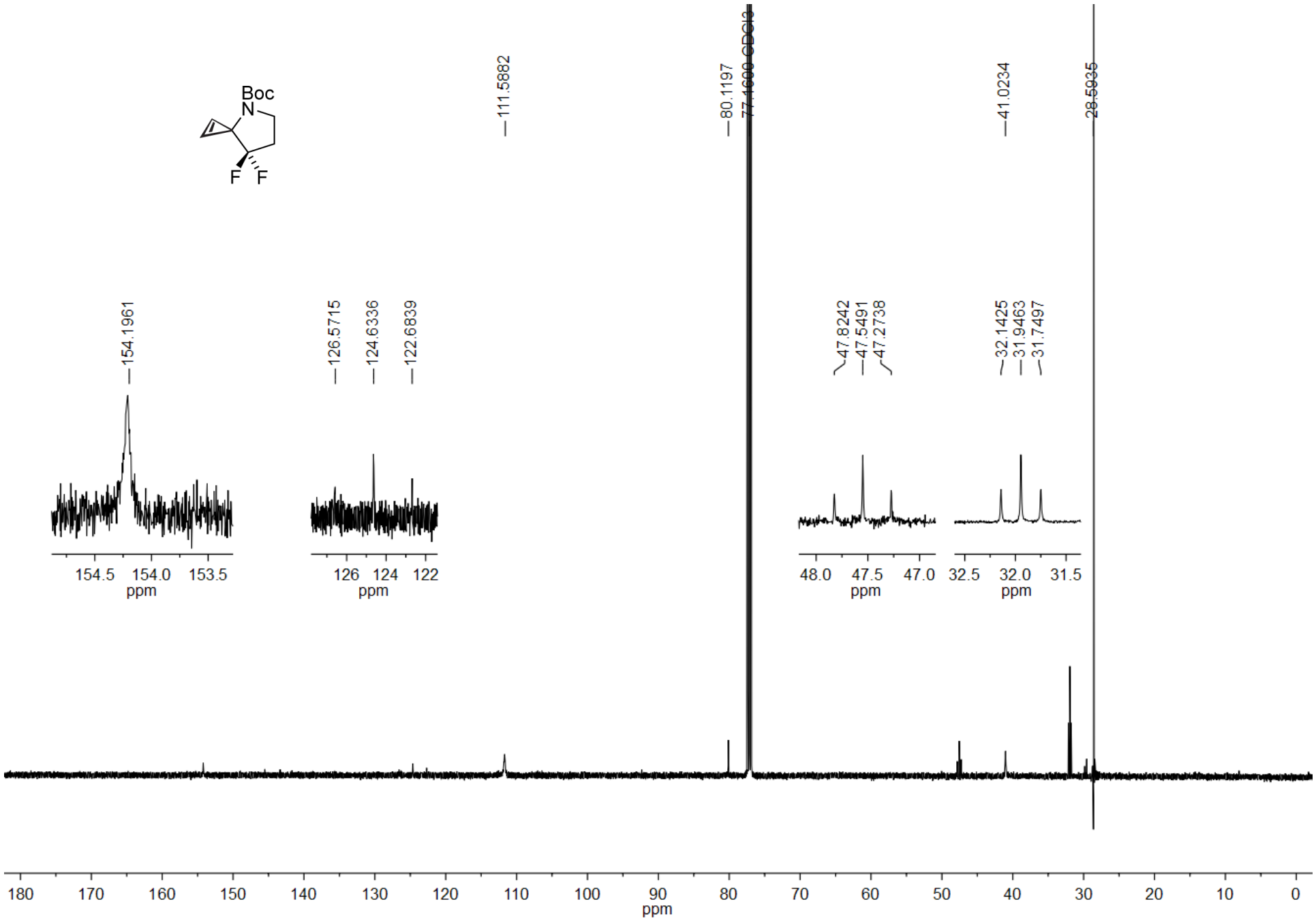
Boc
N
F
F
111.5882
80.1197
77.1600
CDCl3
41.0234
28.5935
154.1961
126.5715
124.6336
122.6839
47.8242
47.5491
47.2738
32.1425
31.9463
31.7497
154.5 154.0 153.5
ppm
126 124 122
ppm
48.0 47.5 47.0
ppm
32.5 32.0 31.5
ppm
180 170 160 150 140 130 120 110 100 90 80 70 60 50 40 30 20 10 0
ppm

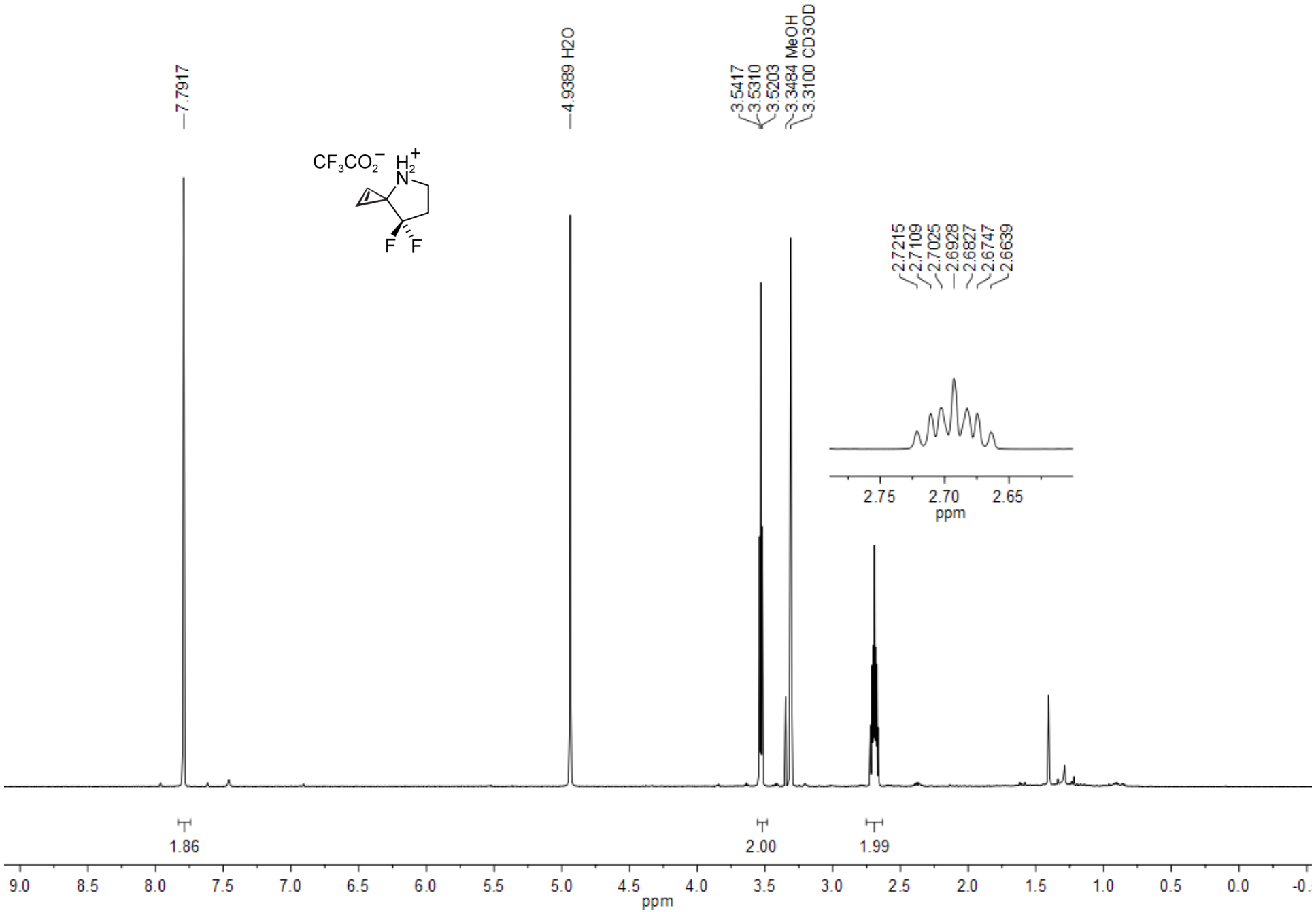
7.7917
4.9389 H2O
3.5417
3.5310
3.5203
3.3484 MeOH
3.3100 CD3OD
2.7215
2.7109
2.7025
2.6928
2.6827
2.6747
2.6639
CF3CO2−
H2+
N
F
F
2.75
2.70
2.65
ppm
1.86
2.00
1.99
9.0
8.5
8.0
7.5
7.0
6.5
6.0
5.5
5.0
4.5
4.0
3.5
3.0
2.5
2.0
1.5
1.0
0.5
0.0
ppm

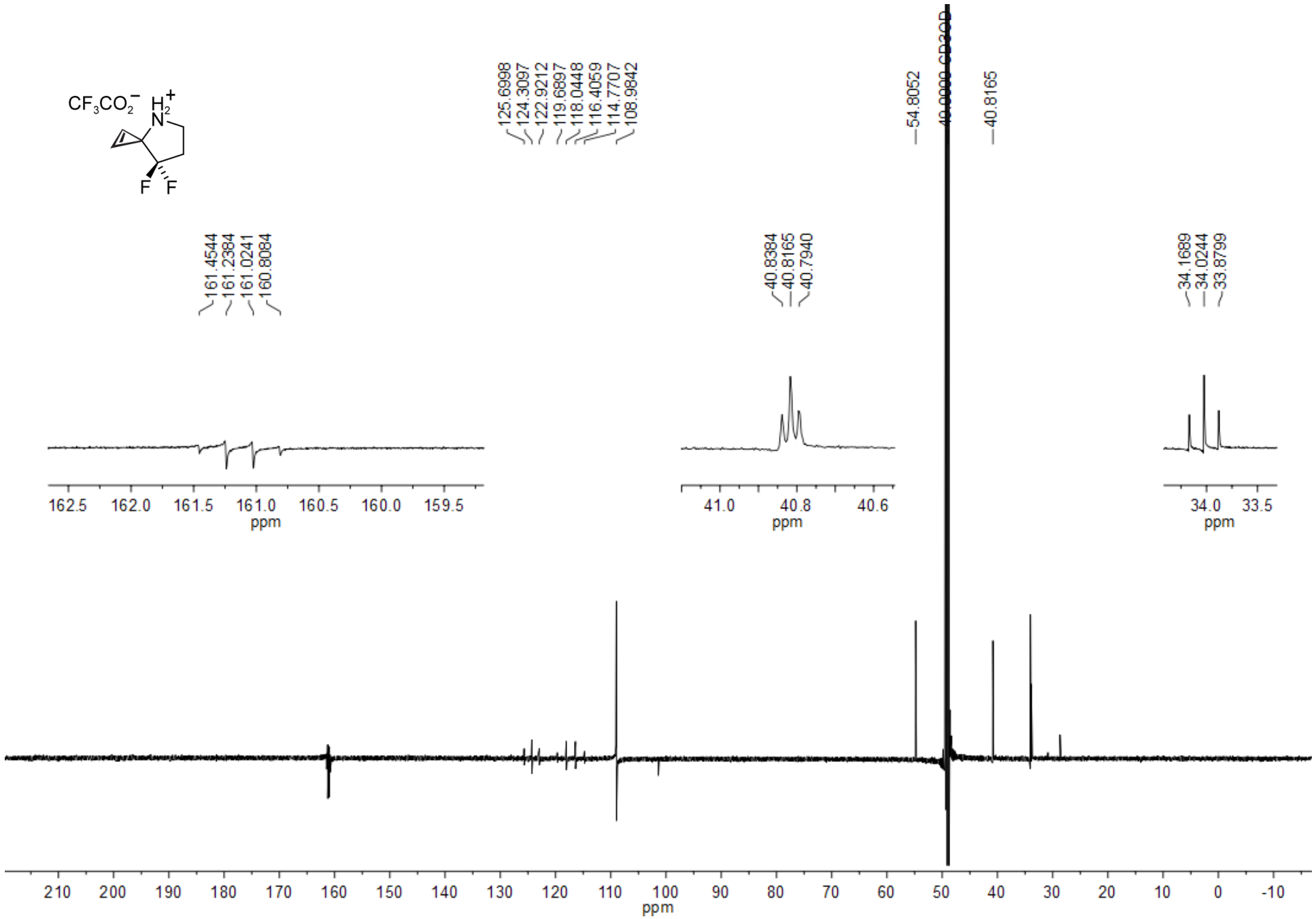
CF3CO2−
H2+
N
F
F
125.6998
124.3097
122.9212
119.6897
118.0448
116.4059
114.7707
108.9842
54.8052
40.8165
161.4544
161.2384
161.0241
160.8084
40.8384
40.8165
40.7940
34.1689
34.0244
33.8799
ppm
ppm
ppm
ppm

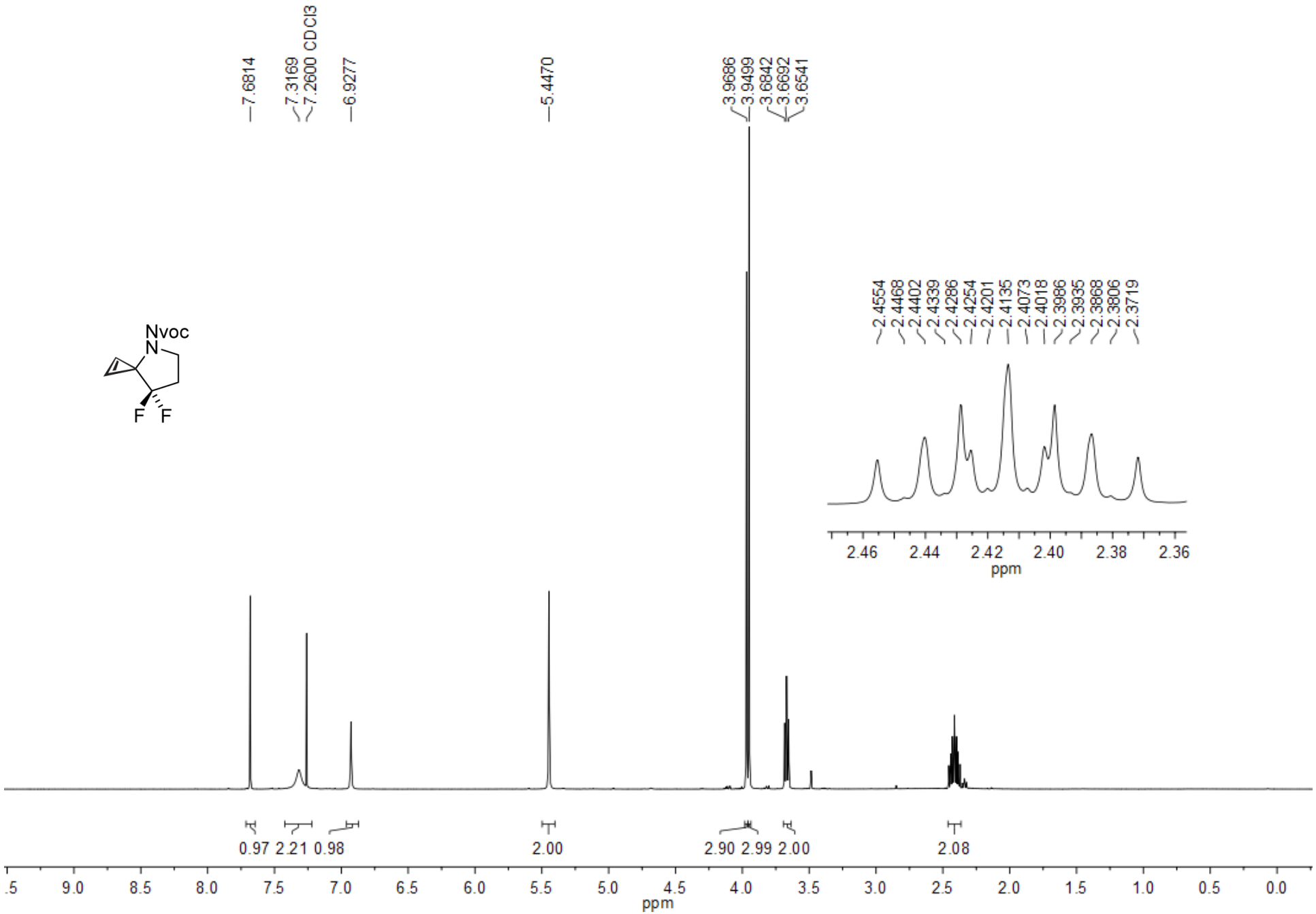
7.6814
7.3169
7.2600 CDCl3
6.9277
5.4470
3.9686
3.9499
3.6842
3.6692
3.6541
Nvoc
N
F
F
2.4554
2.4468
2.4402
2.4339
2.4286
2.4254
2.4201
2.4135
2.4073
2.4018
2.3986
2.3935
2.3868
2.3806
2.3719
2.46
2.44
2.42
2.40
2.38
2.36
ppm
0.97
2.21
0.98
2.00
2.90
2.99
2.00
2.08
9.0
8.5
8.0
7.5
7.0
6.5
6.0
5.5
5.0
4.5
4.0
3.5
3.0
2.5
2.0
1.5
1.0
0.5
0.0
ppm

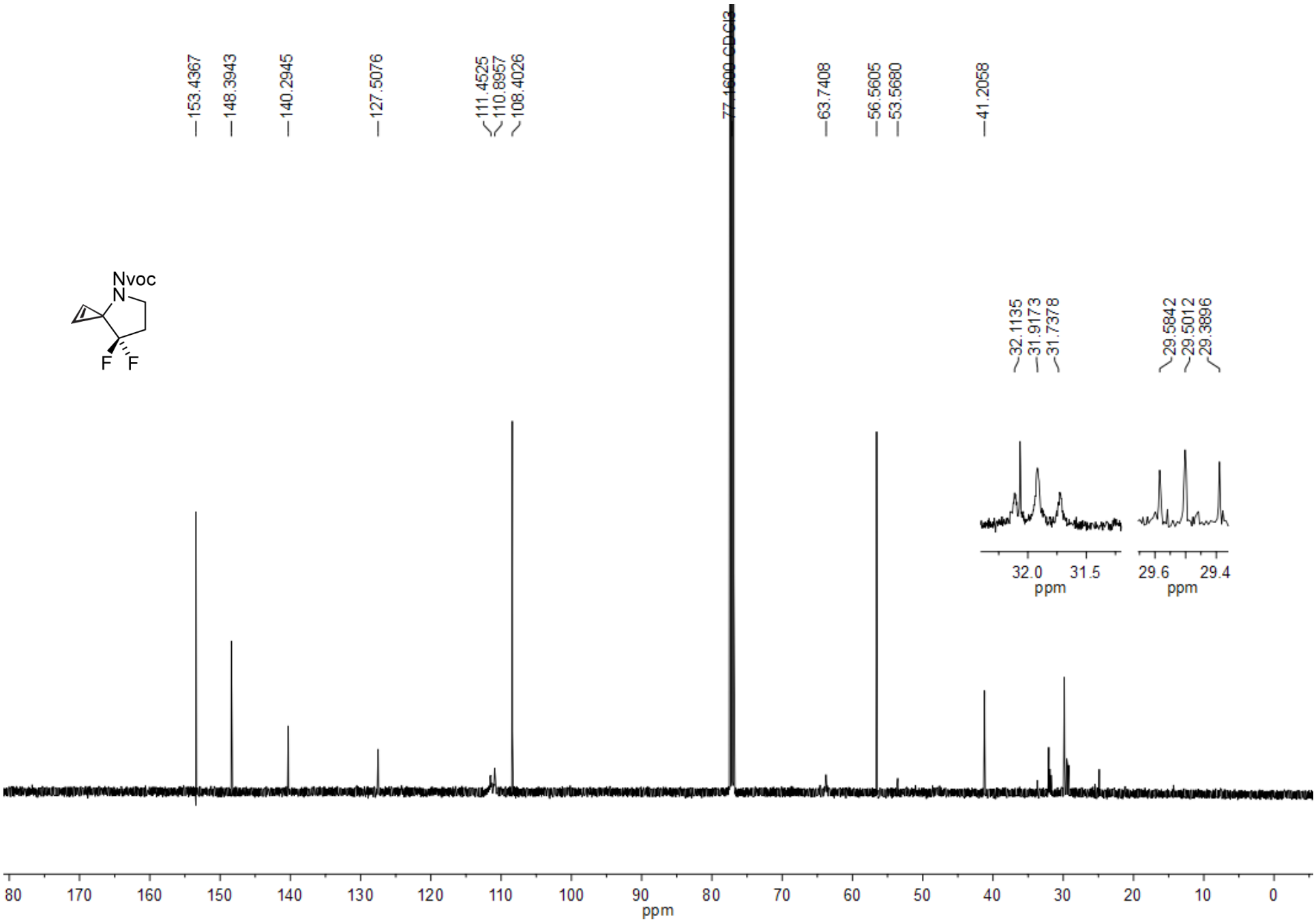
153.4367
148.3943
140.2945
127.5076
111.4525
110.8957
108.4026
77.1600 CDCl3
63.7408
56.5605
53.5680
41.2058
32.1135
31.9173
31.7378
29.5842
29.5012
29.3896
Nvoc
N
F
F
32.0
31.5
ppm
29.6
29.4
ppm
80
170
160
150
140
130
120
110
100
90
80
70
60
50
40
30
20
10
0
ppm

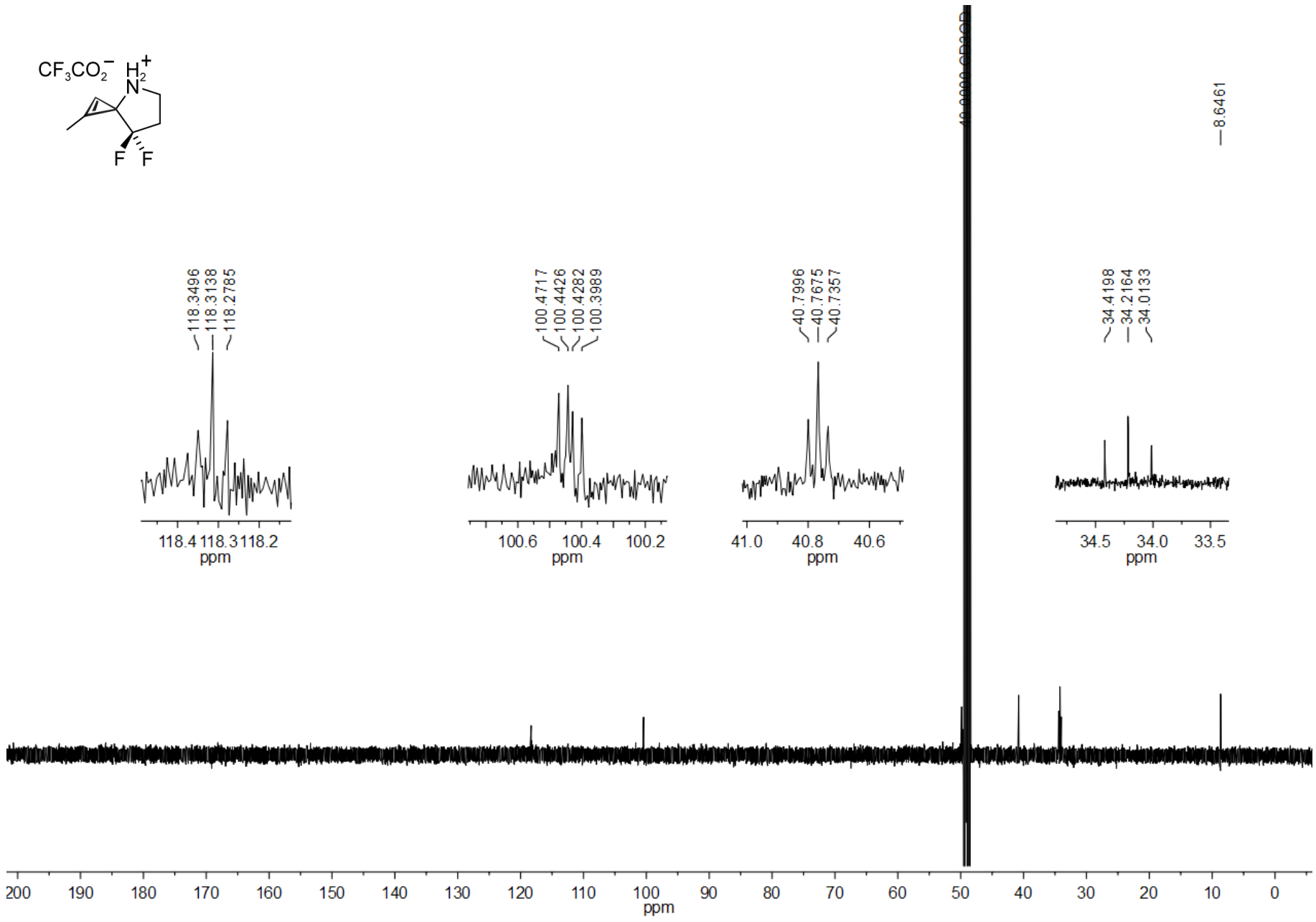
CF3CO2−
H2+
N
F
F
118.3496
118.3138
118.2785
100.4717
100.4426
100.4282
100.3989
40.7996
40.7675
40.7357
34.4198
34.2164
34.0133
8.6461
118.4 118.3 118.2
ppm
100.6 100.4 100.2
ppm
41.0 40.8 40.6
ppm
34.5 34.0 33.5
ppm
200 190 180 170 160 150 140 130 120 110 100 90 80 70 60 50 40 30 20 10 0
ppm

Reference

1. Patterson, D. M., Nazarova, L. A., Xie, B., Kamber, D. N. & Prescher, J. A. Functionalized cyclopropenes as bioorthogonal chemical reporters. *J. Am. Chem. Soc.* **134,** 18638–18643 (2012).

2. Cole, C. M., Devaraj, N. K., Yang, J. & Jolita, S. Angewandte Communications Live-Cell Imaging of Cyclopropene Tags with Fluorogenic Tetrazine Cycloadditions **. 7476–7479 (2012). doi:10.1002/anie.201202122

3. Zhang, X. *et al.* Advances of Molecular Imaging for Monitoring the Anatomical and Functional Architecture of the Olfactory System. *ACS Chem. Neurosci.* **7,** 4–14 (2016).

4. Yu, D., Baird, G. S., Tsien, R. Y. & Davis, R. L. Detection of Calcium Transients in Drosophila Mushroom Body Neurons with Camgaroo Reporters. **23,** 64–72 (2003).

5. Two-Photon Calcium Imaging Reveals an Odor-Evoked Map of Activity in the Fly Brain. *Cell* **112,** 271–282 (2003).

6. Friedrich, R. W. & Korsching, S. I. Chemotopic, combinatorial, and noncombinatorial odorant representations in the olfactory bulb revealed using a voltage-sensitive axon tracer. *J. Neurosci.* **18,** 9977–9988 (1998).

7. Miller, E. W. *et al.* Optically monitoring voltage in neurons by photo- induced electron transfer through molecular wires. *Proc. Natl. Acad. Sci. U. S. A.* **109,** 2114–2119 (2011).

8. Beier, T. *et al.* Correction for Beier et al., Anterograde or retrograde transsynaptic labeling of CNS neurons with vesicular stomatitis virus vectors. *Proc. Natl. Acad. Sci.* **109,** 9219–

9219 (2012).

9. Wall, N. R., Wickersham, I. R., Cetin, A., La, M. De & Callaway, E. M. Monosynaptic circuit tracing in vivo through Cre-dependent targeting and complementation of modi fi ed rabies virus. **107,** (2010).

10. Kriks, S. *et al.* Dopamine neurons derived from human ES cells efficiently engraft in animal models of Parkinson's disease. *Nature* **480,** 547–551 (2011).

11. Tye, K. M. & Deisseroth, K. Optogenetic investigation of neural circuits underlying brain disease in animal models. *Nat. Rev. Neurosci.* **13,** 251–266 (2012).

12. Wen, L. *et al.* Visualization of monoaminergic neurons and neurotoxicity of MPTP in live transgenic zebrafish. *Dev. Biol.* **314,** 84–92 (2008).

13. Gubernator, N. G. *et al.* Fluorescent False Neurotransmitters Visualize Dopamine Release from Individual Presynaptic Terminals. *Science (80-.).* **324,** 1441–1444 (2009).

14. Badalà, F., Nouri-mahdavi, K. & Raoof, D. A. NIH Public Access. *Computer (Long. Beach. Calif).* **144,** 724–732 (2008).

15. Still, W. C., Kahn, M. & Mitra, A. Rapid chromatographic technique for preparative separations with moderate resolution. *J. Org. Chem.* **43,** 2923–2925 (1978).

16. Wakamatsu, K. *et al.* Reduction of the nitro group to amine by hydroiodic acid to synthesize o-aminophenol derivatives as putative degradative markers of neuromelanin. *Molecules* **19,** 8039–8050 (2014).

17. Yang, J., Liang, Y., Šečkutė, J., Houk, K. N. & Devaraj, N. K. Synthesis and reactivity

comparisons of 1-methyl-3-substituted cyclopropene mini-tags for tetrazine bioorthogonal reactions. *Chemistry* **20,** 3365–3375 (2014).

18. Yu, Z. & Lin, Q. Design of spiro[2.3]hex-1-ene, a genetically encodable double-strained alkene for superfast photoclick chemistry. *J. Am. Chem. Soc.* **136,** 4153–4156 (2014).

19. Grenier, V., Walker, A. S. & Miller, E. W. A Small-Molecule Photoactivatable Optical Sensor of Transmembrane Potential. *J. Am. Chem. Soc.* **137,** 10894–10897 (2015).